3-14-2007

An Evaluation of High Velocity Wear

Gregory J. Cameron

AN EVALUATION OF
HIGH VELOCITY WEAR

THESIS

Gregory J. Cameron, Captain, USAF

AFIT/GAE/ENY/07-M06

DEPARTMENT OF THE AIR FORCE
AIR UNIVERSITY

AIR FORCE INSTITUTE OF TECHNOLOGY

Wright-Patterson Air Force Base, Ohio

APPROVED FOR PUBLIC RELEASE; DISTRIBUTION UNLIMITED

The views expressed in this thesis are those of the author and do not reflect the official policy or position of the United States Air Force, Department of Defense, or the U.S. Government.

**AN EVALUATION OF
HIGH VELOCITY WEAR**

THESIS

Presented to the Faculty

Department of Aeronautics and Astronautics

Graduate School of Engineering and Management

Air Force Institute of Technology

Air University

Air Education and Training Command

In Partial Fulfillment of the Requirements for the

Degree of Master of Science in Aeronautical Engineering

Gregory J. Cameron, BS

Captain, USAF

March 2007

AFIT/GAE/ENY/07-M06

AN EVALUATION OF
HIGH VELOCITY WEAR

Gregory J. Cameron, BS

Captain, USAF

Approved:

/SIGNED/   14 Mar 07

_____   _____
Dr. Anthony N. Palazotto (Chair)   Date

/SIGNED/   14 Mar 07

_____   _____
Dr. William P. Baker (Member)   Date

/SIGNED/   1 Mar 07

_____   _____
Dr. Robert A. Brockman (Member)   Date

/SIGNED/   1 Mar 07

_____   _____
Dr. Theodore Nicholas (Member)   Date

Abstract

The Holloman High Speed Test Track (HHSTT) is a rocket-powered sled track facility used for testing a variety of hypervelocity aerospace applications. The current speed record is 6,453 miles per hour. While this seems fast there are customers at the track that have requirements demanding even faster speeds. Significant research has been conducted in the area of rail gouging as it relates to the test track, and efforts are under way to reduce and even eliminate this phenomenon. Any steps taken in this effort may eliminate catastrophic sled failures caused by gouging, however wear is another damaging issue that needs to be understood. This research evaluates wear in two fashions. First, data from the Dynamic Analysis and Design System (DADS) software, used by the HHSTT to model sled loading and vibration, is evaluated in a theoretical model originating from "high-speed" pin-on-disk experimentation. The second method evaluates wear by conducting a series of simulations in which temperature, rail geometry in the form of an asperity, speed and rail coating are varied. These short duration simulations are performed with CTH, a hydrocode designed for analyzing hypervelocity impact problems. A validated CTH model, used in previous gouging research, was used to estimate wear by examining local areas of failure and melting. DADS provides forces related to frictional heating and vertical velocity information that will be incorporated as input into CTH.

Acknowledgements

I would like to, first of all, thank the Lord Jesus for keeping my family together through this very busy period in my life. With him, all things are possible.

Secondly, my wife has worked many more hours than I have to manage the household in my absence. And for that I am forever grateful to her. She deserves to have her name on this work along with mine.

My children have been more than patient with my absenteeism. As I have spent day and night, working and thinking about working on this document, I pray that they will learn to balance their education and love God with their minds as well as their hearts and souls.

I want to sincerely thank Dr. Anthony Palazotto for his encouragement and his undying energy to see this work through to completion. His approachability, availability, experience and dedication cannot be matched.

Dr William Baker provided valuable insight that cannot go unrecognized. I spent much time listening as he and Dr. Palazotto debated about this work.

Additional thanks is extended to Dr. Michael Hooser, George Ayers and their associates at Holloman for quickly responding to my many inquiries about the track.

Finally, without the support of our sponsor, Dr. John Schmisseur at the Air Force Office of Scientific Research, this work would not have been possible.

May God Bless You,

Greg J. Cameron

Table of Contents

List of Figures

ix

List of Tables

List of Symbols

Symbol	Explanation
A	Zerilli-Armstrong Coefficient
A_0	Arrhenius Constant (kg^2/m^4 s or lb^2/in^4 s)
A_n	Nominal Contact Area (cm^2 or in^2)
C	Volume oxidization per mass gained (m^3/kg or in^3/lb)
F_N	Normal Force (N or lbf)
F_f	Friction Force (N or lbf)
$\tilde{F}$	Dimensionless Force
H	Hardness (N/m^2 or psi)
K	Kelvin – Unit of Temperature
K	Thermal Conductivity (W/cm K or lbf/s R)
L	Latent Heat of Melting (J/m^3 or psi)
P	Pressure (N/m^2 or psi)
Pv	Pressure x Velocity (GPA m/s or psi ft/s)
$\tilde{P}\tilde{v}$	Dimensionless Pressure x Velocity
Q_0	Activation Energy for Oxidation (J/mol or lbf in/mol)
R	Rankine – Unit of Temperature
R	Gas Constant (8.314 J/mol K or 40.881 lbf in/mol R)
S	Mathematical Constant
T	Temperature (K or R)
T_m	Melt Temperature (K or R)

T^* .... Equivalent Temperature equal to aH/K (K or R)

T_f .... Flash Temperature (K or R)

T_0 .... Pin/Shoe Temperature (K or R)

V .... Volume of Wear (mm^3 or in^3)

V_m .... Volume Rate of Melting (m^3/s or in^3/s)

Z_c .... Critical Thickness of Oxide Film (cm or in)

a .... Thermal Diffusivity (m^2/s or in^2/s)

c_1, c_2, c_3, c_4, c_5 .... Zerilli-Armstrong Coefficients

c_p .... Specific Heat (J/g K or in^2/s^2 R)

d .... Sliding Distance (m or ft)

dT/dy .... Temperature Gradient into the Shoe (K/cm or R/in)

f_v .... Volume Fraction of Voids

f^*_A .... Critical Area Fraction of Inclusions

k_A .... Dimensionless Wear Coefficient

l_b .... Linear Diffusion Distance (cm or in)

m .... mass (kg or lb)

q .... Friction Heat (W or lbf in/s)

q'' .... Flux (W/m^2 or lbf/in s)

r_0 .... Pin/Shoe Radius (cm or in)

t .... time (s)

v .... Horizontal Velocity (m/s or ft/s)

v_v .... Vertical Velocity (m/s or ft/s)

$\tilde{v}$ .... Dimensionless Velocity

xii

w .... Wear Rate (mm^3/m or in^3/ft)

w_{k_A} .... Mechanical Wear Rate (mm^3/m or in^3/ft)

w_{melt} .... Melt Wear Rate (mm^3/m or in^3/ft)

$\tilde{w}$ .... Dimensionless Wear (mm^3/mm^2 m or in^3/in^2 ft)

y .... Positive Direction into the Shoe (cm or in)

α .... Heat Distribution Coefficient

β .... Dimensionless Parameter equal to l_b/r_0

ε .... Strain

$\dot{\varepsilon}$ .... Strain Rate (1/s)

Δt .... Change in time (s)

Δy .... Change in Position in the Shoe (cm or in)

γ_0 .... Plastic Shear Strain per Pass

γ^* .... Critical Shear Strain

μ .... Coefficient of Friction

θ .... Face Angle in Ploughing or Inclination Angle

ρ .... Density (g/cm^3 or lb/in^3)

σ .... Stress (N/m^2 or psi)

List of Abbreviations

Abbreviation	Explanation
AFIT	Air Force Institute of Technology
CTH	"In 1969 a major report on hydro code was published by Sandia. The report was titled "CHARTD" which stood for "Coupled Hydrodynamics and Radiation Transport Diffusion." This work was extended and the result was called "CSQ" which stood for "CHARTD Squared" which really represents adding the second dimension, not the process of squaring. Then came the 80s when the addition of another computational dimension, i.e., CTH or "CHARTD-to-the-Three Halves Power" was created; thus, CTH stands for "Coupled Hydrodynamics and Radiation Transport Diffusion Performed in One, Two, or Three Dimensions." [22:3]
DADS	Dynamic Analysis and Design System
HHSTT	Holloman High Speed Test Track
HUP	Hypersonic Upgrade Program

AN EVALUATION OF

HIGH VELOCITY WEAR

I. Introduction

Holloman High Speed Test Track

The Holloman High Speed Test Track (HHSTT) located at Holloman Air Force Base in Alamogordo, New Mexico is the world's premier rocket sled test facility that began testing aerospace applications in 1950. Rocket powered sleds are propelled down a track of almost 51,000 feet on heavy-duty crane rails (171 lb/yrd) performing tests investigating hypersonic environments, aircraft ejection seats and munitions and aerodynamic related effects. The track provides cost, safety, efficiency and observability advantages over flight-testing while it also offers a more realistic approach to laboratory-based tests. The fastest sled on record reached a speed of 6,453 miles per hour in April of 2003 on a newly developed dual rail sled system. As technology and interest expand, customers are expressing interest in achieving even faster speeds. In an effort to provide consistent, reliable and payload safe environments, the track engineers are forced to study and understand the effects of these hypersonic speeds.

The sled is connected to the rails by four "shoes" or "slippers" that wrap around the railhead and act as a guide for the sled (Figure 1) as it is propelled down the track. The rails are constructed of 1080 steel. A typical shoe is made of a high strength steel alloy, VascoMax 300, and is dimensionally 20.32 cm (8 inches) in length, by 10.16 cm (4

1

inches) wide and 2.54 cm (1 in) in thickness. The shoes are designed to have a nominal

0.3175 cm (0.125 in) gap between the shoe and the rail. Sleds are constructed with one

or more rocket motors depending on the size of the payload and speed requirements.

Frequently pusher sleds, carrying additional motors that act in stages to propel the sled

system down the track, are used.
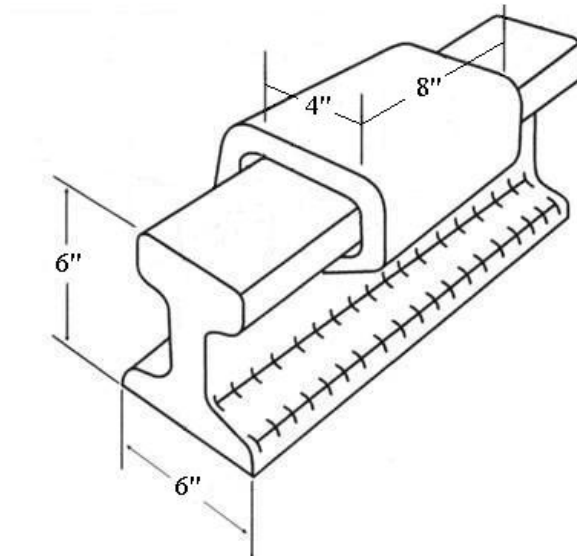
Figure 1 - Typical Shoe/Rail Configuration

As the sled velocity increases, aerodynamic forces and heating become

significant. At supersonic speeds, the leading edges of the shoes are exposed to elevated

temperatures as they are behind a strong shock wave. Aerodynamic lift assists in causing

the sled to oscillate or "bounce" as it moves down the track. In effect, the sled is

constantly transitioning from making contact with the top surface of the rail to the shoe

keeping it from flying off of the rail by contacting the underside of the rail. This

"bouncing" is not only caused by aerodynamic forces but also by the rail irregularities.

These irregularities are a result of inherent manufacturing and alignment tolerances of the

2

rails. As a result the gap between the shoe and the rail is constantly changing. As the sled speed increases, this changing gap causes severe vibrations to occur that only intensify with speed [12:6]. In an effort to reduce the harshness of the environment so that higher speeds could be attainable, a new dual rail system was developed under the Hypersonic Upgrade Program (HUP) [11]. Figure 2 shows the configuration of a dual rail sled of which this research focuses.

Figure 2 - Dual Rail Sled with Pusher Motors

Background

The Air Force Institute of Technology (AFIT) has been studying the HHSTT for several years, focusing all of the efforts on rail gouging. Gouging can be characterized as mixing in a fluid-like behavior of two materials under sliding contact that experience plastic deformation at high strain rates. Laird provides a complete definition of gouging in his work [17:6]. Cinnamon's research on gouging concluded that "a new rail alignment criteria...should mitigate future incidences of hypervelocity gouging" [7:10-11]. If this proves to be true, and gouging is eliminated, the next problem that is of

3

concern to the engineers at Holloman is that of wear. In the problem of wear, the focus changes from looking at the rail to examining the behavior of the shoe as it slides along the rail.

Wear

In 1976, it was estimated that over $24 billion was spent on replacing worn items on automobiles alone [21:7-8]. Many things in addition to automobiles are affected by the wear phenomenon. Wear is not only a financial matter; it often raises safety concerns in such applications as vehicular brakes. Although wear is generally seen in a negative light, it also has some useful purposes such as grinding, sanding and polishing or even the simple exercise of writing with a pencil. The phenomenon of wear warrants a comprehensive understanding; unfortunately wear is very complex and multifaceted.

Wear fits under a larger umbrella of science called tribology. Generally speaking, tribology is the study of the behavior of materials and associated particles in contact as they undergo relative motion. Friction and lubrication, along with wear, are the major fields included in study of tribology. Wear, according to I.M. Hutchings, is defined as "the loss of material from a surface, transfer of material from one surface to another or movement of material within a single surface" [13:1]. For the purposes of this research, wear will be defined as the loss of material due to failure and or melting.

Significant time, money and effort have been spent on the study of wear, and to this day it is still not completely understood. Bowden and Tabor summarize the mystifying behavior of wear in the following paragraph:

"There are no simple laws of wear as there are for friction. On the whole, hard solids wear less than soft, though polyethylene wears less than steel. The wear generally increases with the distance rubbed, though this may not be true if appreciable back transfer occurs. The wear generally increases with load, though this may not be true if more severe running conditions produce appropriate structural changes in the surface layer." – [5:148]

The complexity of wear may be attributed to the ever-changing environment in which two materials interact. The process of wear changes the surface geometry of the materials. Increasing temperatures due to frictional heating and plasticity cause material strength properties and hardness to change, and if enough heat is generated, a material phase change may occur. This dynamic environment significantly impacts the type and amount of wear that occurs.   Because of this, no two systems are identical. As Kato suggests, "wear is not a material property, it is a systems response." [16:9]

Wear can be characterized as a mechanical, chemical or thermal process. Mechanical wear, defined as deformation and/or fracturing of the surface, can be represented by abrasion, adhesion, fatigue and plastic flow. Chemical wear, also referred to as tribochemical or corrosive wear, is characterized by a growing "chemical reaction film" which is "accelerated mechanically by friction" [16:11]. Thermal wear is best represented by surface melting caused by heat generated from friction, however brittle material wear resulting from thermal shocking is also included in thermal wear [16:11].

The following paragraphs include a brief discussion on the concepts of wear on the microstructural level and how it is affected by the environment in which it takes place. This discussion is entirely relevant to sliding speeds below 100 m/s. It is because wear is less common and certainly less understood at speeds higher than 100 m/s that warrants this research. Therefore the conclusion of this chapter provides an engineering

approach for determining wear for speeds that are of interest to the HHSTT, that is speeds on the order of 3000 m/s.

Adhesion - Dry Sliding Wear

Dry sliding wear consists of two surfaces moving relative to each other without the presence of particles, either loose or attached to one or both of the surfaces and without a lubricant film. This type of wear can be thought of as adhesion because it is heavily dependent on the attraction of the mating materials. Abrasive wear on the other hand is classified as sliding wear with particles, which will be discussed briefly in the next section.

As two materials come together, only the peaks of their surface asperities contact, resulting in highly localized stresses. Figure 3 is a depiction of a ground steel surface, shown here to demonstrate the level of contact that two similar mating surfaces undergo.
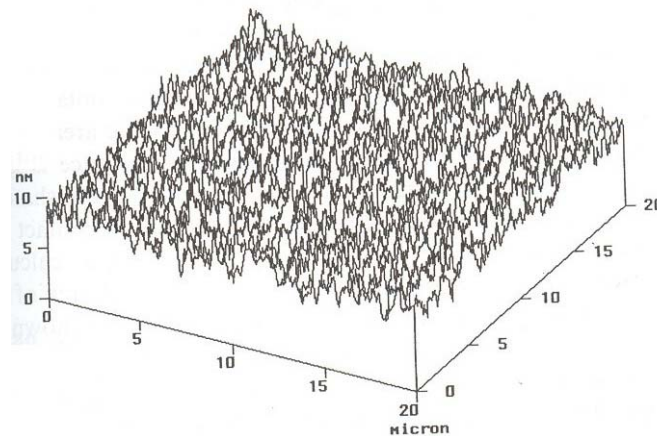
Figure 3 - Typical Surface Illustrating Asperities [4:149]

Wear comes about as pieces of these asperities are deformed or removed. The mechanism that brings about the eventual particle removal is not completely understood. Many theories have been suggested; all of them are focused on the combination of

www.manaraa.com

normal stress bought about by loading; shear stress brought about by transverse motion and friction; and temperature that increases with both load and velocity. Some theories suggest that particles break off as a result of plastic, plate-like movement ending in fracture of the attached end as in Figure 4a, while others suggest that layers fracture independently due to shear instead of breaking off in a stack (Figure 4b).
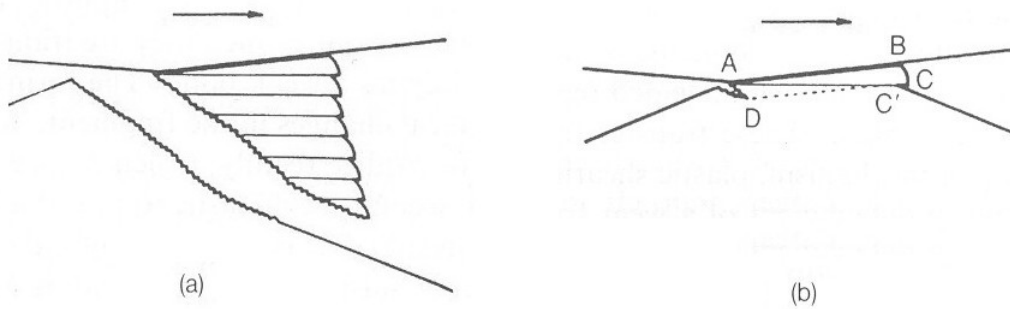
Figure 4 - Adhesive Wear - Plasticity Resulting in Plate-Like Debris [14:99]

Some propose that smaller wear particles transfer from one surface to another from adhesion. These particles build up over time and eventually separate as debris as in Figure 5.
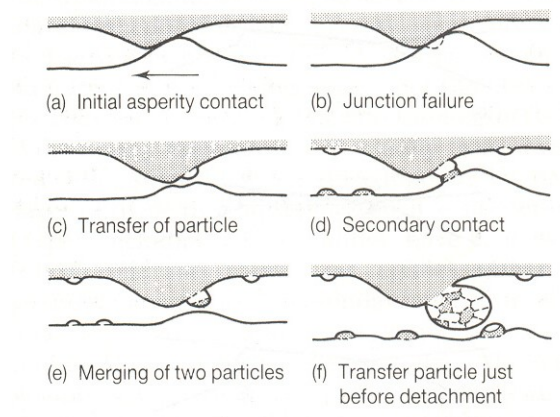
Figure 5 - Smaller Particle Debris Form as a Result of Adhesion [14:100]

7

There are also those that propose cracks generate below and parallel to the surface eventually resulting in the delamination of a particle. All of these theories deal with the asperities reaching the yield point, deforming plastically and eventually fracturing. Examination of worn materials has confirmed that transfer layers, laminate debris and subsurface cracking exist, validating all of the theories, however the exact process remains uncertain [14:92-103].

Abrasion

The previous section focused on wear without particles. Abrasion occurs in one of two forms: particles attached on one of the mating surfaces (Figure 6a) or particles existing unattached between the two mating surfaces (Figure 6b).
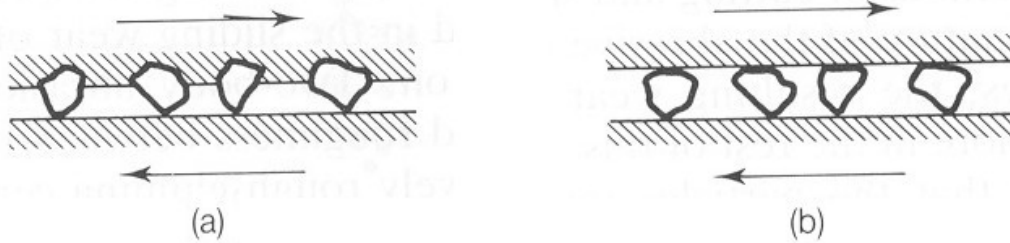
Figure 6 - Two Forms of Abrasion [14:133]

If wear debris is generated from adhesion, as described above, and not ejected from the interface, the result is abrasion. The existence of abrasive particles in the form of wear debris has been shown to increase the coefficient of friction between the two surfaces. The coefficient of friction is a function of the debris particle size, which is dependent on the hardness of the materials [9:137]. The mode of abrasion is mostly dependent on the shape of the abrasive particle.

8
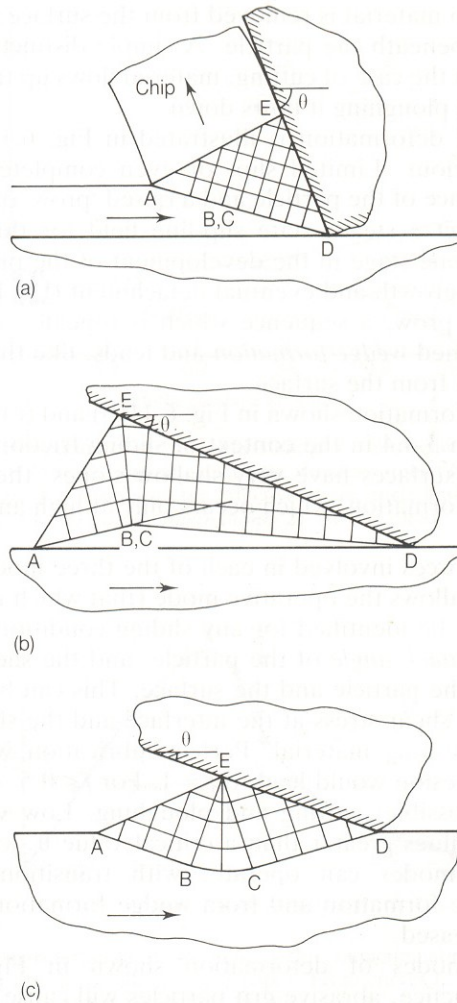
Figure 7 - Three Modes of Abrasion [14:147]

Figure 7 depicts the three modes as cutting (a), ploughing (c) , and the intermediate mode
called wedge formation (b). Cutting is analogous to that of a single point cutting tool
which results in the removal of a chip. Ploughing is like a rolling wave, however this
mode does not result in debris particles whereas the wedge-forming mode does. These
modes mostly depend on the face angle, θ, of the abrasive particle [14:147-148].

Melt

This mechanism of wear is encountered when the interface temperature reaches that equal to one or both of the melting temperatures of the mating materials. This is a result of the frictional heat generated from sliding which is a function of load and velocity. It is generally accepted, in theory, that as a molten layer develops, the coefficient of friction decreases due to the hydrodynamic layer, similar to lubrication. For metals with low melting points like bismuth, experimental evidence exists for the wear rate to increase when melting occurs [23:610], however melt wear models are not conclusive across the board.

Oxidation

This mechanism of wear has to do with the rapid build-up of oxide layers. During the process of oxidation, a chemical reaction occurs between the base metal and the surrounding oxygen, resulting in the formation of oxides of that base metal. Oxides in general, are harder, more brittle and have a lower shear strength than the base metal. These considerations can increase the wear rate if multiple passes occur. These oxide layers are built up and then broken down when they reach a critical thickness. Lower temperatures from slower sliding speeds cause oxides to build up only on the asperities, whereas higher temperatures from higher speeds and loads cause a more general oxide layer to form [14:103-105].

10

Wear Maps

As materials experience repeated contact during the wearing process, the microstructure, micro-surface geometry and material chemistry change as seen in the previous sections. These changes bring about different wear mechanisms that dominate during the wearing process. In order to track this dynamic process in terms of wear, the idea of a wear a map was developed. A wear map is a graphical representation used to indicate operational boundaries such as load and speed for different wear mechanisms and/or rates. Bayer [2:383] also mentions a transition diagram as a form of wear map. These diagrams are generated from empirical data by plotting experimental wear quantities against two operating parameters to designate different wear regimes. A wear map or transition diagram for steel in a pin-on-disk configuration can be seen in Figure 8 as a function of normalized pressure and normalized velocity. These quantities will be defined in the next chapter (see equations (5) and (6)).
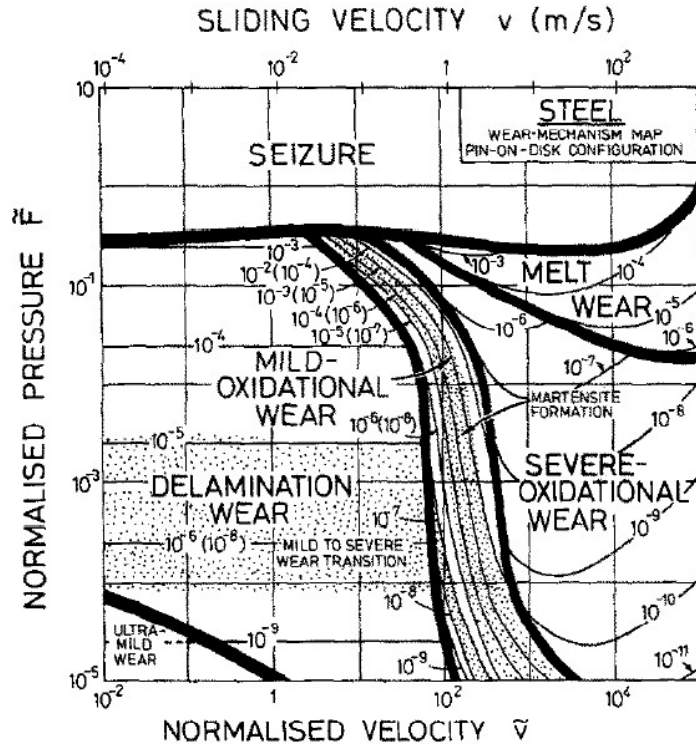
Figure 8 - Wear Map for Metals [18:21]

In the attempt to determine the total wear of a surface, it will be necessary to account for the wear from all of the mechanisms.

Engineering Solution to Wear

As previously discussed, experimental wear maps show where certain wear mechanisms will dominate in terms of some operational parameters. It is therefore desirable, in the absence of experimental data, to be able predict and quantify wear and its mechanisms for a given wear scenario. This can be done by analytically developing a wear model from a specific system and applying it generically to others.

Wear is generally expressed in the form of a rate, volume of material removed per distance slid. The wear rate, as alluded to in the last section, does not remain constant throughout the life of the system. Typically there is a "break-in" period where the wear

12

rate is high, and then it tapers off with time as the mating surfaces are smoothed. In the case of the Holloman sled, the wear rate may never reach a steady state value due to the constant acceleration and intermittent contact with the rail. The volume of wear can be expressed as

$$V = k_A \frac{F_N d}{H} \tag{1}$$

where H is the material hardness in units of pressure, F_N is the normal load, d is the sliding distance and k_A is the dimensionless wear coefficient. The wear rate can be expressed as

$$w = \frac{V}{d} \tag{2}$$

or as a dimensionless quantity, $\tilde{w}$

$$\tilde{w} = \frac{V}{A_n d} \tag{3}$$

with A_n being the nominal area of contact. Substituting equation (1) into equation (2) results in the most rudimentary form of a wear model.

$$w = k_A \frac{F_N}{H} \tag{4}$$

This equation is known as Archard's wear equation, and k_A is known as Archard's wear coefficient, named after a British scientist who was one of the first to derive the relationship between wear and load in 1953. Archard developed this equation based on the probability of an asperity in contact producing a wear particle. He took no specific consideration for the wear mechanism [14:83-84]. Others have derived a wear equation identical to equation (4) by beginning with the assumptions of adhesive wear as well as

13

abrasive wear [16:11-12]. Considering that almost all wear scenarios involve these two mechanisms, equation (4) can be generally applied as an estimation of wear. In that light, k_A is left to take on a large range of values depending on the type of wear under consideration.

Problem Statement and Objectives

As the Holloman High Speed Test Track continues to push the speed boundaries, the problem of wear becomes a significant issue. Wear in general is complex and not completely understood; even less is known about wear at speeds above 500 m/s. With Holloman hoping to soon achieve 3,000 m/s, this problem becomes uniquely interesting. The HHSTT hopes to be able to predict the shoe wear so that it does not completely wear through during a test and gouge the rail or worse, cause a catastrophic sled failure, as the shoe would loose its ability to keep the sled on the track. Sled failures are not only costly to the track in terms of maintenance and repair; they are costly to the customer as well. The objectives of this research are to:

- Relate low speed wear experiments to higher velocity applications using parameters such as pressure and velocity.
- Evaluate high velocity wear using CTH considering the effects of temperature, rail geometry, velocity and coatings.

Methodology Preview

This research consists of the development of two models, an analytical model and a numerical model. The numerical model is created in CTH while the analytical model is

developed from the work of Lim and Ashby [18] and applied to the data provided by the Dynamic Analysis and Design System (DADS).

CTH, a hydrocode that was developed by Sandia National Labs for modeling high-energy impact, has been used to successfully model the problem of rail gouging at Holloman. CTH was originally chosen to model gouging because of its ability to model high pressure interaction between materials leading to large deformations and the propagation of shock waves. This was also used to estimate shoe wear considering the sled contacting the rail and generating areas of higher pressure. While gouging is characterized by the flow and mixing of the shoe and rail materials, wear is characterized by localized melting, failure and debris generation. CTH will be used to quantify wear by looking at the temperature and failure zones in the shoe, as well as material loss, if any exists.

Computer generated sled parameters such as force and velocity as functions of time are available through a sled as modeled in DADS. The particular DADS file that was used for this research was a dual rail sled with a mass of 841 kg (1854 lb); it is partially listed in Appendix D. The model was based on an actual sled run from October 2000, designated Mission 80X-A1, but was modified to travel farther and faster. The model traveled a distance of over 3.65 km (12,000 ft) reaching a maximum speed of approximately 3 km/s (10,000 ft/s) in 2.5 seconds. A wear rate can be generated for each contact the sled makes with the rail and then integrated over the distance to determine the wear volume and therefore thickness. The DADS also provides a method for calculating frictional heating that will be used to calculate a temperature distribution in the shoe.

CTH is used to run a series of simulations at certain velocities to determine the effects that temperature, rail coatings, and rail discontinuities in the form of an asperities, have on wear. The temperature input is the result of the DADS heat transfer solution just mentioned. Because CTH runs for very short time intervals, on the order of 10 microseconds, only selected scenarios can be examined. The goal is to eventually characterize the entire sled run by a broad range of scenarios and statistically calculate the total wear. The two methods for evaluating wear can be used to check each other, however it will not be until actual test track wear data is gathered for comparison that the two methods will be validated.

II. Methodology

Pin-On-Disk

       Pin-on-disk experiments have been used for many years to simulate wear in the laboratory. These tests can vary in geometric setup; for example, the pin can be applied to the edge of the disk instead of the face. Bayer [2] dedicates several chapters to the discussion of wear testing and techniques. This research focuses on the setup illustrated in Figure 9. A pin of known material properties and geometry, namely density, hardness, length, and diameter, is placed against a disk with constant angular velocity for some defined period. From that period and angular velocity, the sliding distance can be determined. When simulating a linear sliding scenario in one direction, such as the Holloman sled, or a projectile traveling down a gun barrel, the pin can be moved in a radial direction away from the center of the disk to allow it not to pass over the same path on the disk more than once. This radial rate would also be used to calculate the sliding distance. The force applied to the pin in the normal direction is measured as well as the frictional force exerted on the pin. The frictional force can be determined by calculating the bending moment in the pin from a strain gage located on the front or back of the pin.
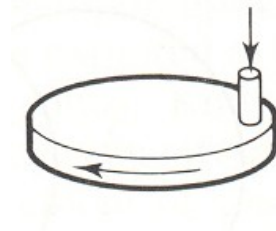
Figure 9 - Pin-on-Disk Experimental Setup [14:79]

Sled vs. Pin-on-Disk

The speed of the sled alone makes the HHSTT unique. There are no other tests or experiments that can be used as an equivalent comparison when considering only velocity. The fastest experimental data available reaches only 549 m/s (1800 ft/s). On the other hand, the pin-on-disk experimentation can achieve incredible pressures, 78 MPa (11,000 psi) for example, by only applying a 246 N (55 lbf) load to a 2 mm (0.08 in) diameter pin. If one would consider the shoe, having an area of 206.5 cm^2 (32 in^2), large pressures are not achievable because of the large contact area. It would require a load of 1.57 x 10^6 N (352 kips) to produce the same pressure as the pin-on-disk. If one considers the product of pressure and velocity, an adequate comparison can be made between the pin-on-disk and the shoe/rail system. A disk spinning at a constant rate of 45.7 m/s (150 ft/s) with the same 246 N force applied to the pin will produce a *Pv* value of 3.57 GPa m/s (1.7 x 10^6 psi ft/s). In order to achieve the same *Pv* value for the sled/shoe system, a load of 48.3 kN (10,860 lbf) would need to be applied on the shoe traveling at a velocity of 1,524 m/s (5000 ft/s). For this case, both the load and the speed are easily achieved by the HHSTT. The *Pv* quantity appears frequently when studying wear because normal force, surface area and velocity contribute to the wear behavior. As will be shown later, the range of *Pv* for the pin-on-disk is 0 to 70 GPa m/s and that of the shoe/rail is 0 to 35 GPa m/s. Experimental pin-on-disk testing and models have been sufficiently developed such that their application to the Holloman shoe, by way of DADS, may be valid considering initial assumptions. A list of these assumptions follows:

- For simplification, one corner of the four-shoe sled will be considered. The mass applied on each corner is assumed to be one quarter of the total mass of the sled,

18

throughout the entire run. This assumption eliminates the effects of pitching and rolling of the sled.

- The contact between the shoe and rail is uniformly distributed over the entire shoe area, 206.5 cm^2 (32 in^2).

- Contact other than the top of the rail with the bottom of the shoe is irrelevant to this research.

- The understanding of wear at low speeds can be applied to wear at high speeds.

Lim and Ashby [18]

In 1987 two researchers, Lim and Ashby, contending that the mechanisms of wear change during the wearing process, attempted to define a wear map in order to track and characterize the changing wear mechanisms and ultimately compute the total wear. An example of a Lim and Ashby wear map was shown in Figure 8, where the different wear mechanisms are displayed in regions as functions of normalized pressure and velocity. Their work was based on experimental data that was collected from various sources. Most of the data resulted from pin-on-disk experimentation such as that published by Montgomery in 1975 [19]. With that in mind, it is important to note that Lim and Ashby developed their wear models around the pin-on-disk geometry of Figure 9.

Lim and Ashby almost exclusively expressed wear in terms of normalized quantities as defined earlier in equation (3). It is important to note that equation (3) is non-dimensional but has the units of volume of wear per area of contact, per distance slid, which becomes important when trying to determine a wear thickness or volume.

19

They also used normalized force and normalized velocity terms. Normalized force is defined as

$$\tilde{F} = \frac{F_N}{A_n H} \tag{5}$$

and normalized velocity as

$$\tilde{v} = \frac{v r_o}{a} \tag{6}$$

where v is the velocity, r_o is the radius of the contact area (for the pin-on-disk scenario) and a (m^2/s) is the thermal diffusivity.

By plotting the experimental data, they were able to surmise that the data naturally fell into categories of wear mechanisms. They then formulated a theoretical model for each mechanism to match the experimental data. They suggest that wear occurs in three main mechanisms, melt, oxidation-dominated, and plasticity-dominated wear [18:3]. This research focuses on their melt and plastic wear models.

Melt Wear

The model for melt wear was based on part of the energy generated by friction being used to heat the entire pin while another part is focused on melting the pin at the interface. This fraction is defined by the variable α. Lim and Ashby used an expression for α based on transient conditions in the disk. Assumptions are made later for α to be constant at ½. The flux, q'', in W/m^2 due to frictional heating is defined as

$$q'' = \frac{\mu F_N v}{A_n} \tag{7}$$

20

where μ is the coefficient of friction. Some of that flux goes into heating the pin and some to melting the pin, as

$$\alpha q'' = -K\frac{dT}{dy} + L\frac{V_m}{A_n} \tag{8}$$

The first term is taken from the heat conduction equation, which will be examined later. K is the thermal conductivity (W/m K) and dT/dy is the temperature gradient into the shoe. The second term is for the portion of the heat that melts the pin, where L is the latent heat of melting (J/m^3) and V_m is the volume rate of melting (m^3/s). Substituting equation (7) into equation (8) gives

$$\frac{\alpha\mu F_N v}{A_n} = \frac{K(T_m - T_0)}{l_b} + L\frac{V_m}{A_n} \tag{9}$$

where l_b is the equivalent linear diffusion distance. Lim and Ashby assume that all of the melted metal is removed as wear, therefore the equation for melt wear rate is

$$\widetilde{w} = \frac{V_m}{vA_n} \tag{10}$$

Equation (9) can be solved for V_m and substituting it into equation (10) results in the following equation for melt wear [18:12].

$$\widetilde{w} = \left(\frac{T_m - T_0}{T^*}\right)\frac{H}{L}\frac{1}{\beta\widetilde{v}}\left[\alpha\mu\widetilde{F}\widetilde{v}\frac{T^*\beta}{(T_m - T_0)} - 1\right] \tag{11}$$

where

T_m = melt temperature

T_o = sink temperature

T^* = aH / K ; equivalent temperature of the metal

β = l_b / r_0 ; dimensionless parameter for bulk heating

21

Plastic Wear / Mechanical Wear

As mentioned earlier, the most widely known wear model is Archard's law in the form of equation (4). By combining equations (1), (3) and (5), Archard's law can be written in dimensionless form as

$$\widetilde{w} = k_A \widetilde{F} \tag{12}$$

Lim and Ashby arrived at this solution for what they term plastic wear by suggesting that voids nucleating around material inclusions beneath the surface generate wear particles as plastic shear strain accumulates beyond a critical value γ^* for speeds below 0.1 m/s. In this case k_A is defined by

$$k_A = \frac{2\gamma_0 f_v}{f_A^*} \tag{13}$$

with γ_0 being the plastic shear strain generated each time that an asperity undergoes deformation, f_v is the volume fraction of inclusions and f_A^* is the critical area fraction of voids. By taking γ_0 to be 1%, f_v to be 10^{-3} and f_A^* to be 0.5, $k_A = 4 \times 10^{-5}$, a value consistent with experimental results. Lim and Ashby distinguish between mild and severe plastic wear by changing k_A from 5×10^{-5} to 5×10^{-3} respectively, when the normalized load, $\widetilde{F}$, equals 3×10^{-4} [18:18-19]. Authors such as Hutchings and Rabinowicz however, do not explicitly limit equation (12) to plastic wear. They suggest that this equation can be applied to wear in general [21:155-167; 13:4-5]. For this reason, wear calculated from equation (12) in this research will be referred to as mechanical wear.

Oxidation Dominated Wear

The equation for mild oxidation-dominated wear as presented by Lim and Ashby is shown below in equation (14). The development of this equation is beyond the scope but is discussed in Lim and Ashby's work [18:14].

$$\tilde{w} = \left(\frac{C^2 A_0 r_0}{Z_c a} \right) \exp\left[-\frac{Q_0}{R T_f} \right] \frac{\tilde{F}}{\tilde{v}} \tag{14}$$

where

$\quad C$ = volume oxidized iron per mass gained (m^3/kg)

$\quad A_0$ = Arrhenius constant for oxidation (kg^2/m^4 s)

$\quad Z_c$ = critical thickness for oxide film

$\quad Q_0$ = activation energy for oxidation (J/mol)

$\quad R$ = gas constant (8.314 J/mol K)

$\quad T_f$ = flash temperature

With some basic information about a wear scenario, namely velocity, pressure, coefficient of friction, geometric configuration and material properties, these models can be aptly applied. However, due to their complexity, they were first applied to the data published by Montgomery in 1975, which listed experimentally determined wear rates. This way, the calculated values in the above equations should be close to the experimental data. This allowed for validation before using the DADS sled data.

Montgomery Report [19]

In 1975 Montgomery published a paper on simulated wear inside a cannon muzzle by using the pin-on-disk experiment. The tests were conducted by the U.S. Army

23

in the 1940s and 50s but were classified at the time. Montgomery's paper emphasized the use of the product of pressure and velocity, or *Pv*, for use in analyzing the wear results. The highest speed tested in the Army's work was only 549 m/s (1,800 ft/s), significantly lower than what is seen at Holloman. However the significance of the Montgomery data is that it provides 53 unique records of data characterized by velocity, pressure and sliding distance with corresponding wear values. When considering the Holloman sled, the contacts of the sled with the rail never occur at the same speed and never slide for the same distance. This fact makes Montgomery's publication very relevant due to its wide variety of speed, load and distance slid. Based on the previous discussion of the use of the *Pv* quantity, Montgomery's data will be used in this fashion to qualify the models that will be applied to the DADS data.

Montgomery concluded that the wear seen in the Army's study was categorized as melt wear because the materials tested had different melt temperatures, and the materials with the lower melt temperatures showed greater wear amounts [19:297-298]. Lim and Ashby therefore used the Montgomery data to validate their melt wear model. This model will be shown later in the results section in Figure 27.

DADS

The Dynamic Analysis and Design System, or DADS, is a commercial-off-the-shelf software package used to solve the equations of motion for multi-body mechanisms. The HHSTT purchased DADS to help predict sled loading. Understanding the vibrations experienced by a sled was necessary to reduce sled failures, and design optimal sleds that could protect sensitive payloads at higher speeds. DADS had to be modified in order to

24

model the HHSTT environment. In addition to the aerodynamic effects seen in Figure 11, the most significant modification is in regard to the roughness or waviness along the track's 15.5 km (50,800 feet). In reality, what causes the sled to "bounce" down the track are the track irregularities on the top surface as well ever changing gap between the sides of the shoe and the rail in the width dimension. These irregularities are mostly a result of inherent manufacturing and rail alignment tolerances. As pointed out by Cinnamon, the current specification for rail flatness is no more than 0.0635 cm of rail height change in a 132 cm length and no more than 0.19 cm change in a 2.54 cm length at the rail seams [7:9-14,15]. Figure 10 illustrates some of the conditions that might exist along the rail or at a seam yet still be within the current HHSTT tolerance. Rail conditions such as these, in effect, are part of what causes the sled to vibrate. The influence of an asperity like the ones shown below on wear will be examined later.
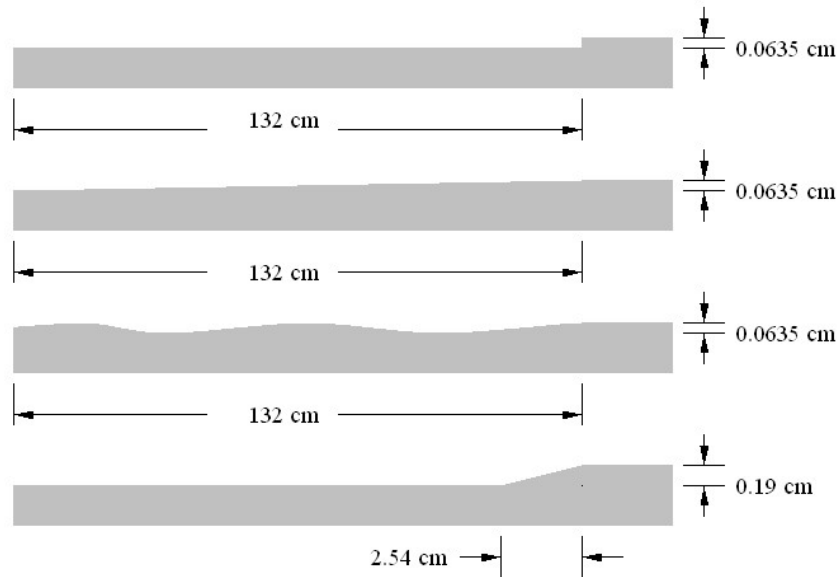
Figure 10 - Examples of Possible Rail Asperities

After these rail irregularities were incorporated, the model produced results that correlated with measured dynamics from three separate sled runs. This rail geometry data is acquired and input into the DADS model every time the Holloman survey team physically inspects and measures the height and width of the rails at 66 cm (26 in) intervals along the length [10]. As a result of this process, the engineers at Holloman have great confidence that DADS accurately predicts the dynamic environment. [12].

Figure 11 - Nike Sled Used in Mission 80X-A1 [1]

Courtesy of the HHSTT, Figure 11 shows a picture of Mission 80X-A1, a Nike sled from October 2000, an actual test that was part of the Hypersonic Upgrade Program (HUP). The DADS model used in this research is based on this sled configuration.
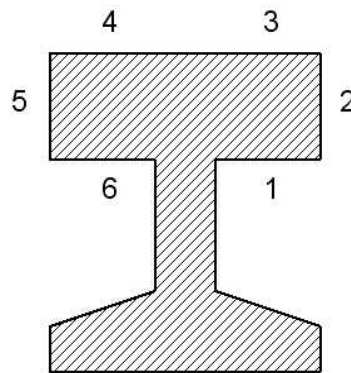
Figure 12 - Cross Section of Rail Showing DADS Contact Locations [1]

DADS reports normal forces at locations 1 through 6 in the rail cross-section shown in Figure 12 for each shoe. Locations 2 and 5 are the subject of future work for

the HHSTT to include the effects of wind on yawing. DADS also reports vertical and
down rail velocities for the sled at each of the four shoes. This research will focus only
on forces acting on locations 3 and 4 for the right rear shoe. The values for these two
locations will be averaged in order to eliminate the rolling motion of the sled and
estimate the average force exerted over the entire area of the shoe. Finally, the particular
DADS file used in this research (partially listed in Appendix D) reports all of this data as
a function of time for every 0.0001 seconds, or 100 microseconds. This becomes
important later in the subsequent discussions of heat transfer and wear.
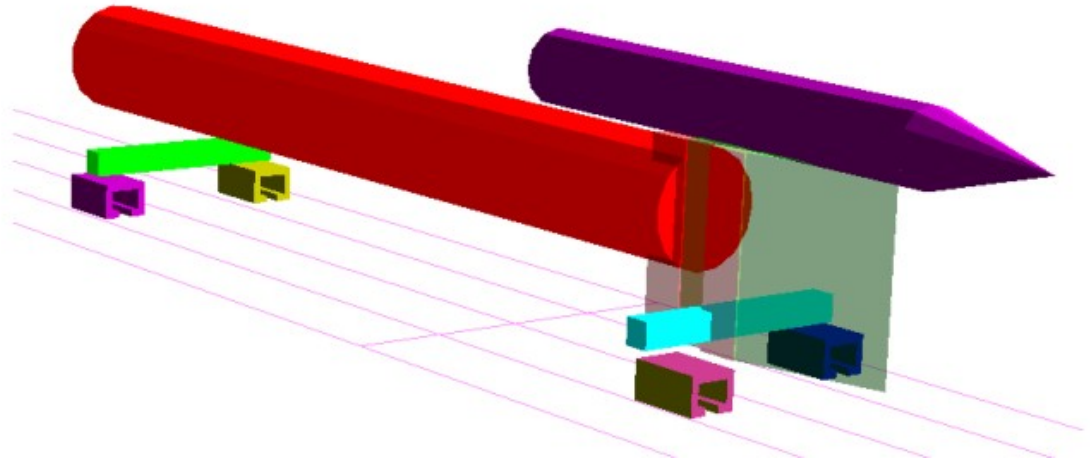
Figure 13 - DADS Model for Mission 80X-A1 Hybrid

Mission 80X-A1* Data Characteristics

Before proceeding further, it is worth looking at the DADS data for the hybrid
Mission 80X-A1 that was discussed in chapter I. This actual sled only achieved a
velocity of 762 m/s (2500 ft/s). The model was increased for the purposes of studying
high velocities. Figure 14 depicts distance, velocity and acceleration down the track as
well as vertical force and velocity all as a function of time.

27
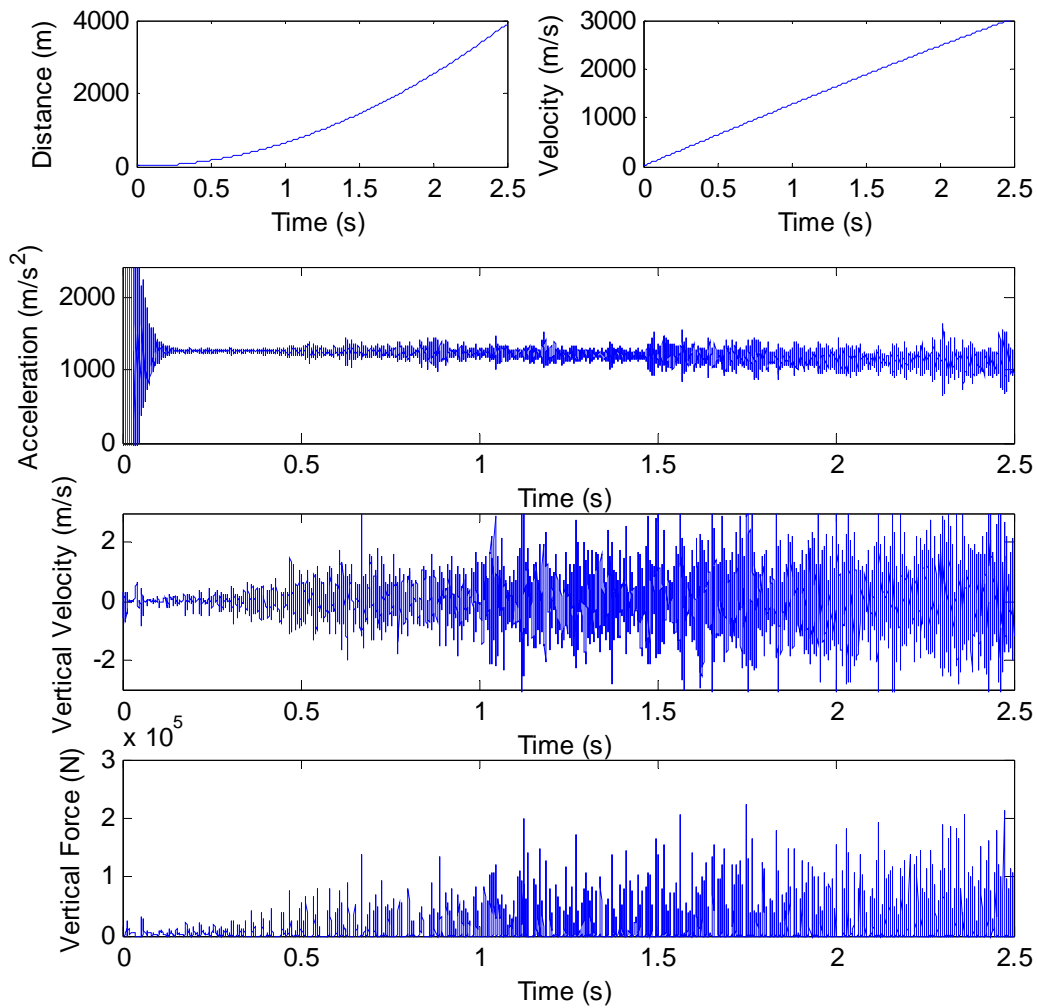
Figure 14 - Characteristics of DADS Data

The distance traveled by the sled model increases parabolically with time, with the velocity verifying this by its linear increase with time, and the acceleration is approximately constant at 1219 m/s^2 (4000 ft/s^2). With the velocity being supplied by DADS, the distance was found by integrating the velocity with respect to time using the trapezoid rule. Recall that the wear rate spoken about in equation (2) was in terms of volume of wear per distance slid; the distance therefore is used in calculating the wear volume. The acceleration was found by $(v_i - v_{i-1})/\Delta t$. Taking a closer look at the vertical

velocity and vertical force in Figure 15 shows how the sled actually comes off of the rail (where the force goes to zero).
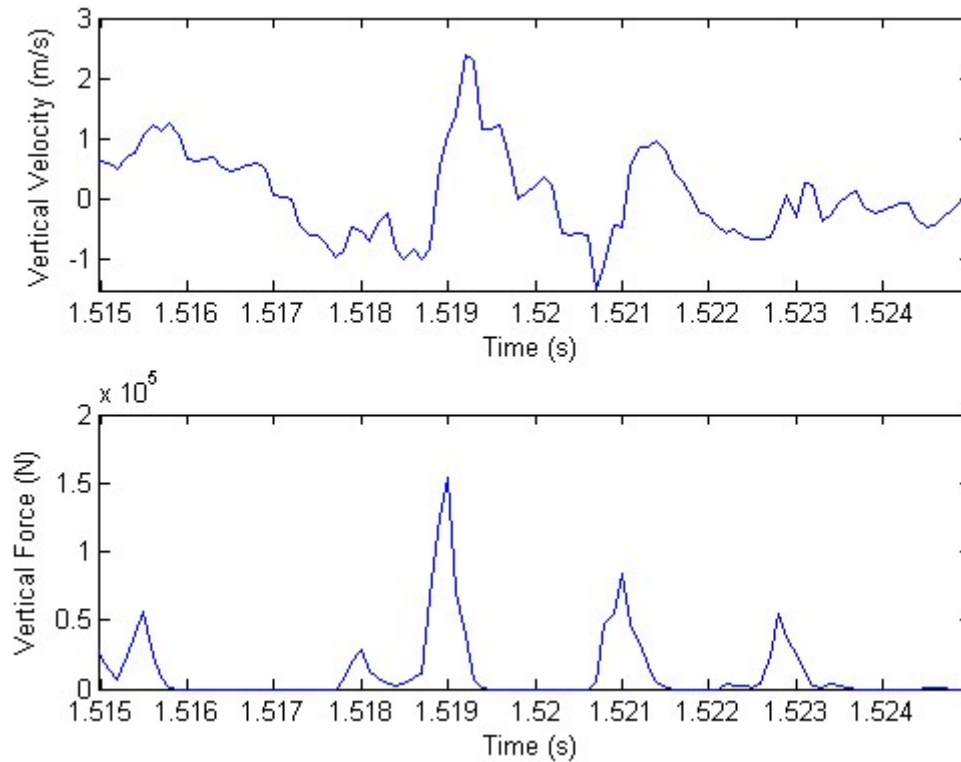
Figure 15 - DADS Vertical Velocity and Vertical Force for 1.515 – 1.525 s

CTH

Developed by Sandia National Laboratories, CTH is a hydrocode that was designed to simulate large deformation and shock physics of multi-material, multi-dimensional models. CTH focuses on the conservation of energy and momentum equations along with equations of state and a constitutive model. CTH uses finite differencing and finite volume methods to solve these equations by expressing them in Lagrangian coordinates for the material reference frames and Eulerian coordinates for the spatial frames. For a more detailed discussion on CTH solution methods see Cinnamon's

29

work in the section on Hypervelocity Impact Solution Procedure [7:1-3]. Both Laird [17]
and Szmerekovsky [24] also give details on the CTH algorithm.

Montgomery and Lim and Ashby

As previously discussed, the Lim and Ashby models were selected because of
their development and use of experimental data. The Montgomery pin-on-disk
experiments provide the sufficient data to evaluate the Lim and Ashby wear equations. A
portion of the experimental pin-on-disk data from Montgomery is in Table 1, while the
complete data can be seen in Appendix E.

Table 1 - Excerpt from Montgomery Pin-on-Disk Experimentation [19]

Velocity $(ft\,s^{-1})$	Bearing pressure $(lb\,in^{-2})$	PV $(\times 10^{-6})$	f	fPV $(\times 10^{-6})$	Sliding distance (ft)	Wt. loss (mg)	Length loss (mil)	Wear rate $(\times 10^{7}$ $in^{3}\,ft^{-1})$
150	11 300	1.7	0.26	0.44	5.7	15.0	25	200
600	11 900	7.1	0.27	1.92	7.2	0.6	3	6

The third column of Table 1 is the *Pv* value discussed earlier. In addition to
measuring the normal force, Montgomery also measured the friction force on the pins by
using strain gages on the pin holder, which was also discussed earlier. This allowed for
the calculation of the coefficient of friction, μ, from the equation $F_f = \mu F_N$. This value is
located in column four labeled '*f*'. The far right column is the experimental wear in
(in^3/ft) presumably obtained by measuring the weight loss and dividing by the density
and sliding distance. The diameter of the pin used in these experiments was 0.203 cm
(0.080 inches). This data was subjected to the Lim and Ashby equations for melt, plastic
(both mild and severe), and oxidation dominated wear and plotted along with the
experimental value for wear. These results can be seen in Figure 16. Note that oxidation

30

wear does not appear on the chart because the results from the equation were not realistic; they were extremely large. Additionally, Lim and Ashby did not use the Montgomery data to validate their oxidation-dominated model like they did for the melt wear model. This may suggest that oxidation wear does not occur at the speeds considered in Montgomery's data.

Before proceeding with discussing the results of applying the Lim and Ashby equations to the Montgomery data, it is necessary to expand on the α term used by Lim and Ashby in equation (11) to characterize the heat distribution split between the pin and the disk. This is important, because a slightly different assumption will be made later when looking at the shoe and rail for determining the temperature profile. Lim and Ashby declared α to be

$$\alpha = \frac{1}{2 + l_b \left(\pi v / 8 a r_0 \right)^{1/2}} = \frac{1}{2 + \beta \left(\pi \tilde{v} / 8 \right)^{1/2}} \tag{15}$$

This is a valid expression if

$$\beta = \frac{l_b}{r_0} \tag{16}$$

They suggest that "β is a dimensionless number of general order 1", but use $\beta = 6$ [19:7] (recalling that r_0 is the pin radius, 1.016 mm (0.040 inches) in Montgomery's work). Other important values are listed in Table 2. However l_b, the "equivalent linear diffusion distance", is not so easily known. If one should solve for it in equation (16), using $\beta = 6$, l_b would equal 6.096 mm (0.24 inches), and applying either expression from equation (15) into the melt wear model, equation (11), yields results with negative values representing growth, not wear. On the other hand, if $l_b = 1.016$ mm (0.04 in), (solved by

using $\beta = 1$, but still using $\beta = 6$ in equation (11)) and the left expression of equation (15) is used in equation (11) to obtain the melt wear values, the melt wear results in what is shown in Figure 16.

Table 2 - Values used for Lim and Ashby Equations for the Pin-on-Disk (Steel)

Value	Description	SI	English
r_0	Pin Radius	1.016 mm	0.040 in
H	Pin Hardness	1.00 GPa	1.45×10^5 psi
a	Thermal Diffusivity	9.1×10^{-6} m^2/s	0.014 in^2/s
K	Thermal Conductivity	0.41 W/cm K	5.12 lbf/s R
T_0	Pin Temperature	297 K	535 R
T_m	Melt Temperature	1800 K	3240 R
T^*	Thermal Quantity	222 K	400 R
L	Latent Heat of Melting	2.1×10^9 J/m^3	3.05×10^5 psi

$T^* = aH/K$
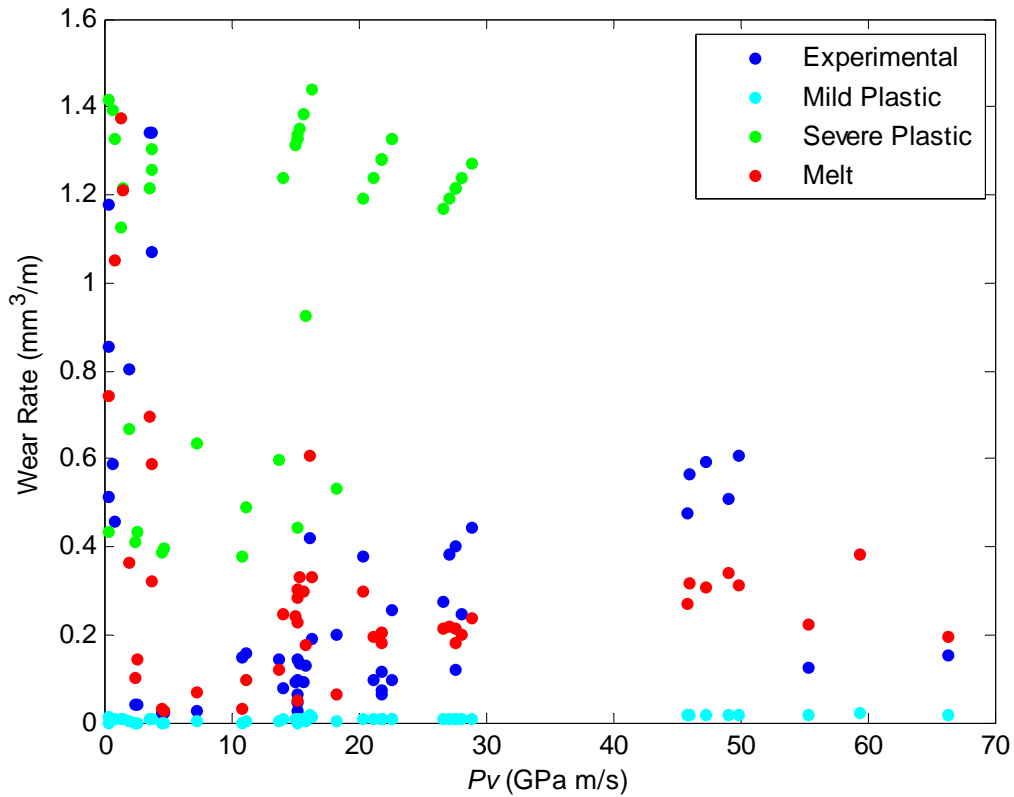
Figure 16 - Montgomery Experimental Data and Montgomery Data used in Lim and

Ashby Equations

The wear rate is plotted as volume (mm^3) per sliding distance (m) versus the

quantity of pressure multiplied by the velocity (GPa m/s). Two conclusions can be drawn

from Figure 16; first, melt wear is present if the correct expression for α is used in

equation (11), and the correct value of β and l_b are chosen. And second, the plastic

(mechanical) wear model, as defined earlier, can be a viable solution in defining wear

which is simply a function of the non-dimensional normal force multiplied by the

constant k_A, as shown in equation (12).

33

Further developing the second conclusion, k_A being somewhat arbitrary, can be solved for using the empirical data given by Montgomery in the following manner to provide a mechanical wear function for all values of Pv within the experimental range.

$$k_A = \frac{w_{Montgomery}H}{A_n P_{Montgomery}} \tag{17}$$

Here, $w_{Montgomery}$ and $P_{Montgomery}$ are the experimental wear rate and pressure respectively from Montgomery. These values of k_A are shown in Figure 17 as "k_A". Notice that some values of k_A at low Pv values are out of the suggested range of 5×10^{-5} to 5×10^{-3} given by Lim and Ashby in the section on plastic (mechanical) wear. These values were manually adjusted to the range limit of 5×10^{-3} suggested by Lim and Ashby. These numbers are represented in Figure 17 as "k_A adjusted". Finally, these adjusted values were averaged over three arbitrary ranges of Pv, which can be seen in Figure 17 as the series "k_A averaged".

34
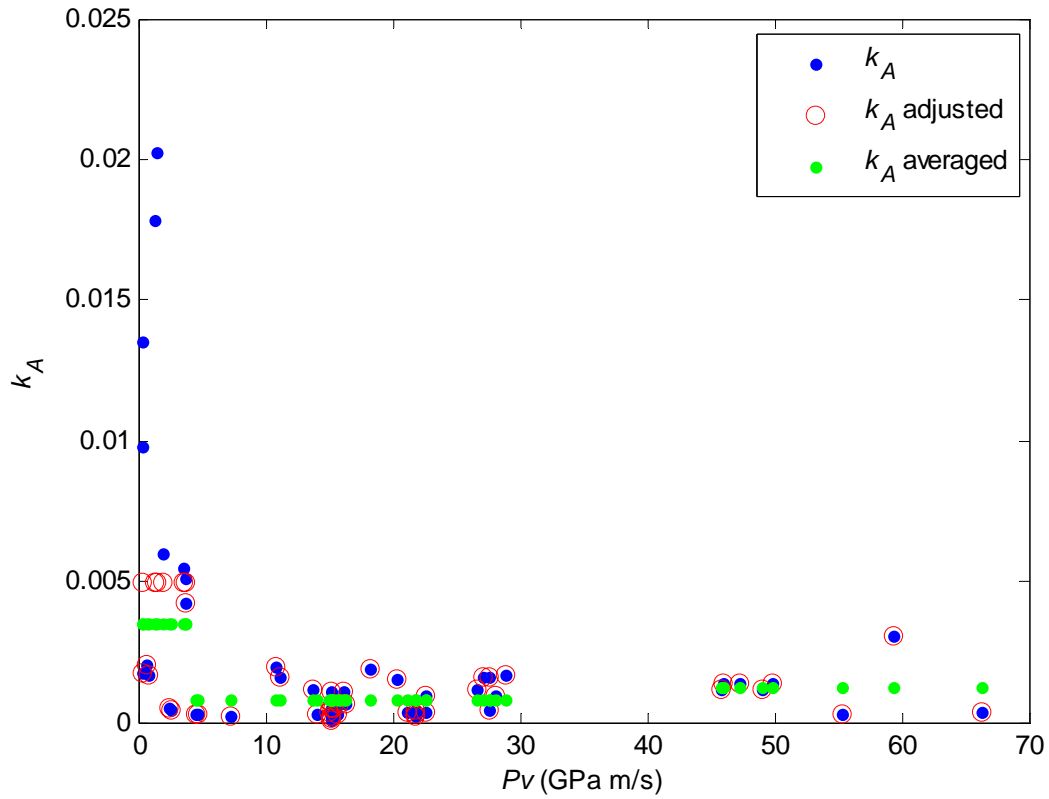
Figure 17 - Adjusted k$_A$ Values for Montgomery Data

This final set of k_A values for the three different Pv ranges, shown in Table 3, were then used to calculate the theoretical wear as defined by equation (4). Figure 18 shows how this method correlates with the experimental data.

Table 3 - Values for k$_A$ Across *Pv* Range

Pv (GPa m/s)	k_A (-)
< 4.2	3.53 x 10^{-3}
4.2-31.5	8.16 x 10^{-4}
> 31.5	1.30 x 10^{-3}

35
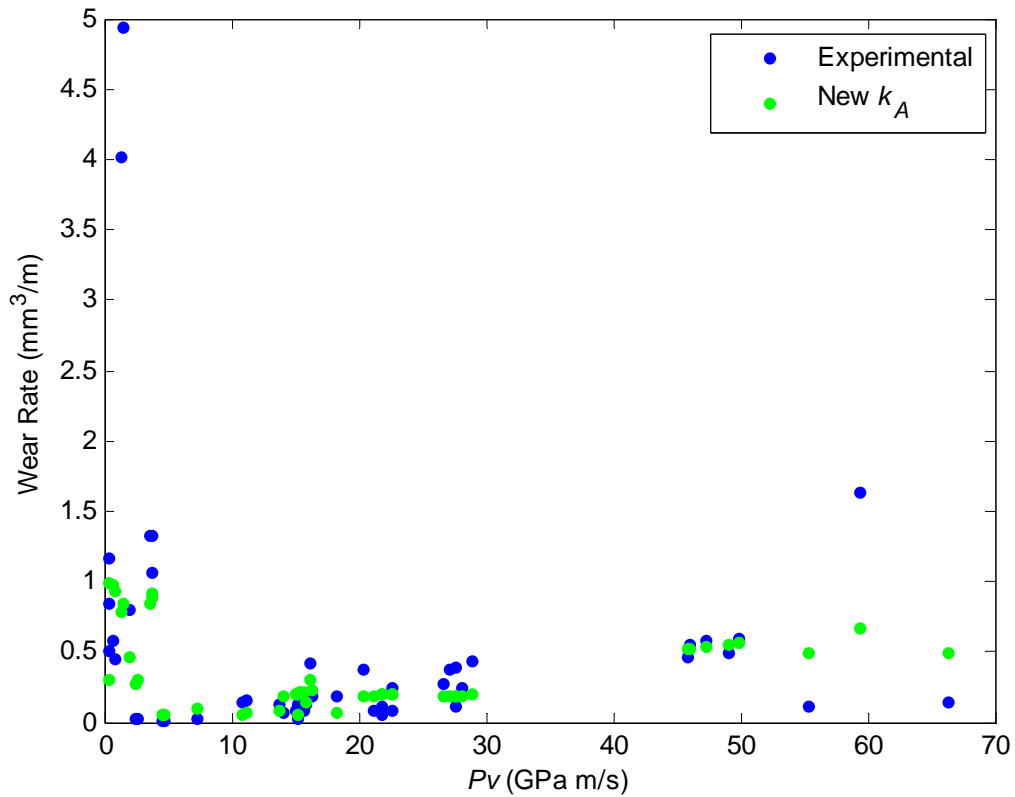
Figure 18 - Montgomery Experimental Data with Calculated Wear

Using Equation (17) and Adjusted k_A Values from Table 3

The method for finding the appropriate k_A could be modified to use a least squares fit or some curve fit function instead of using an average in three different arbitrary regions. For the current effort, the values in Table 3 will be used to calculate wear for the Holloman sled. This leads to the next step, the application of these wear models, equation (11) and equation (12) to the DADS data to calculate wear.

DADS and Lim and Ashby

Just as Table 2 defined some necessary values for steel in the pin-on-disk experimentation, Table 4 provides the same data for VascoMax as related to the HHSTT.

36

Table 4 - Values used for Lim and Ashby Equations for the HHSTT (VascoMax)

Value	Description	SI	English
r_0	Equivalent Radius	50.80 mm	2.0 in
A_n	Shoe Area	206.45 cm^2	32.0 in^2
H_V	Shoe Hardness	1.00 GPa	1.45 x 10^5 psi
a_V	Thermal Diffusivity	4.5 x 10^{-6} m^2/s	0.007 in^2/s
K_V	Thermal Conductivity	0.31 W/cm K	3.85 lbf/s R
c_{pV}	Specific Heat	0.858 J/g K	7.39 x 10^5 in^2/s^2 R
T_0	Shoe Temperature	297 K	535 R
T_{mV}	Melt Temperature	1685 K	3033 R
T^*_V	Thermal Quantity	146 K	264 R
L_V	Latent Heat for Melting	2.1 x 10^9 J/m^3	3.05 x 10^5 psi

Subscript *V* denotes VascoMax

The thermal conductivity, thermal diffusivity and specific heat for Vascomax were taken from Laird's work where he assumed constant properties at a temperature of 700 K [17:84]. The material hardness and latent heat of melting are the same as that of steel.

The previous section concluded that equation (11), with a properly chosen value for l_b and equation (12), with the appropriate k_A value, would provide analytical results for predicting melt and mechanical wear respectively for the shoe. In order to use equation (11), however, the coefficient of friction is needed.

Coefficient of Friction

Montgomery measured the coefficient of friction, μ. DADS, unfortunately, does not provide this information. Lim and Ashby used the following equation for their models which is based on a variety of experimental data:

$$\mu = 0.78 - 0.13\log_{10}(\tilde{v})$$ (18)

μ is expressed solely as a function of normalized velocity [18:7]. However, when $\tilde{v}$ reaches 10^6, μ equals zero, and any further increase in $\tilde{v}$ causes μ to become negative. For the Holloman sled, $\tilde{v}$ reaches 10^6 or 88.9 m/s (291.6 ft/s) in the first 0.07 seconds of the run according to equation (6) and Figure 14. Therefore, the coefficient of friction, μ, was determined by using a curve fit from the Montgomery pin-on-disk data, not only as a function of $\tilde{v}$ but $\tilde{P}$ (or $\tilde{F}$) as well. $\tilde{P}\tilde{v}$ is used instead of Pv so that it can be used in a power function without having to deal with the units. Generating a curve fit of the plotted coefficient of friction vs. normalized Pv shows a power function that can also be applied to the DADS data for the range of normalized Pv under examination. Figure 19 shows the Montgomery friction data plotted against $\tilde{P}\tilde{v}$ along with two curves, the higher curve is representative of the function shown, while the lower curve has been modified so that the coefficient of friction will asymptotically approach 0.02 for the range of normalized Pv shown (0 – 8000). In a separate paper, Montgomery recognized that experimental pin-on-disk data for the coefficient of friction was an order of magnitude higher than the actual value. His work suggested that the true value of the coefficient of friction approaches 0.02 as Pv increases [20:242].
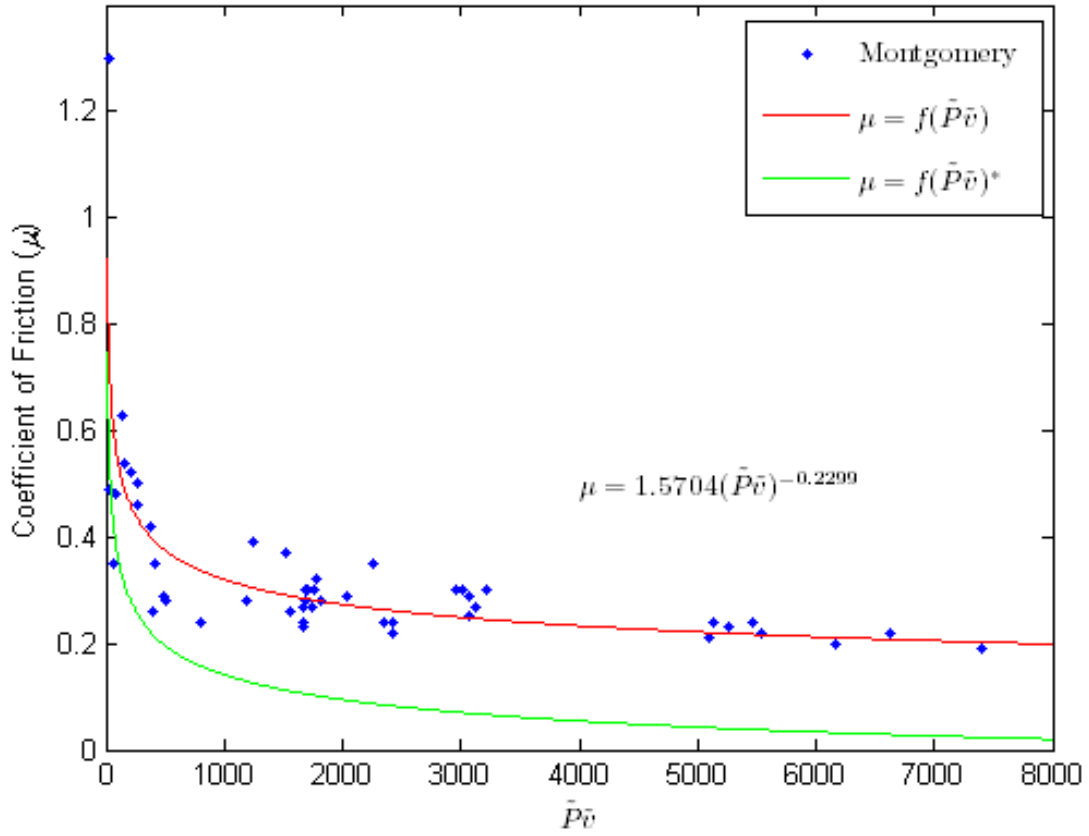
Figure 19 - Function for Coefficient of Friction vs $\tilde{P}\tilde{v}$ Based on Montgomery Data

The modified power function was simply determined by subtracting a constant

from the actual curve. The constant was calculated by taking the minimum value (for the

$\tilde{P}\tilde{v}$ range of 0 - 8000) on the actual curve and subtracting 0.02.

$$\mu = 1.5704(\tilde{P}\tilde{v})^{-0.2299} - S$$

where (19)

$$S = \min\left\{1.5704(\tilde{P}\tilde{v})^{-0.2299}\right\} - 0.02$$

Equation (19) was then used to calculate the coefficient of friction for the DADS data.

The results are displayed in Figure 20. These values will be used in subsequent

calculations for melt wear as well as frictional heat generation.
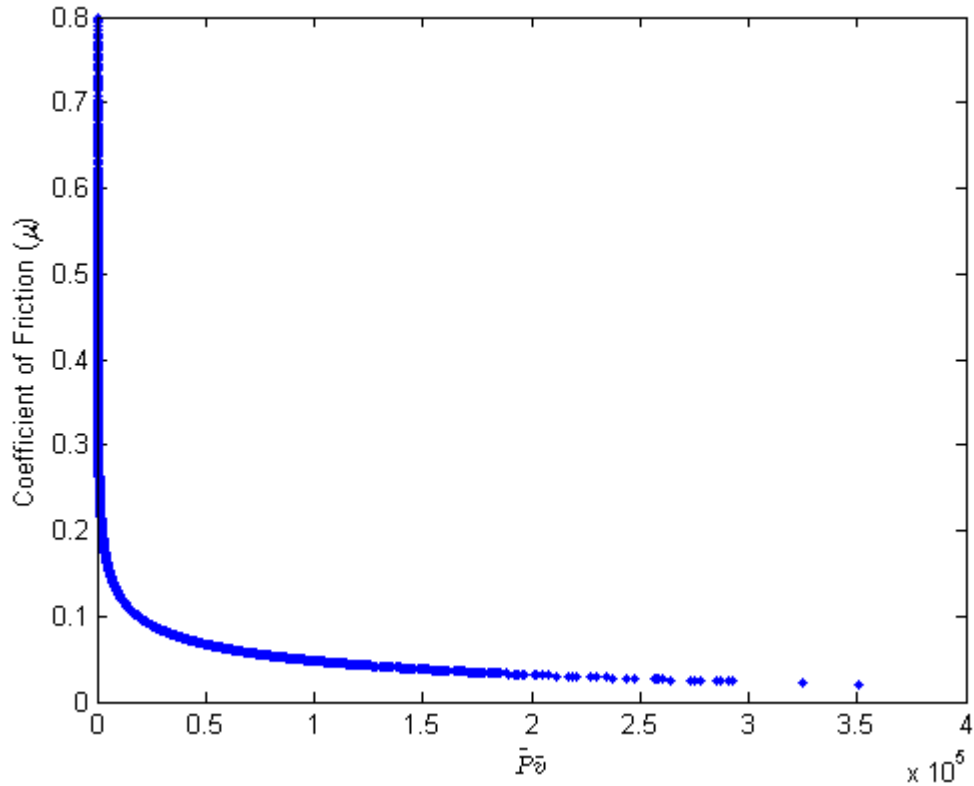
Figure 20 - Coefficient of Friction vs. Normalized *Pv* for DADS Data

Calculation of Wear for DADS

In order to calculate wear from equation (12) for the DADS data, $\tilde{F}$ was calculated

from equation (5), and *Pv* was calculated by dividing the normal force by the nominal

area of the shoe, A_n, assuming uniform contact, and multiplying by the velocity.

Knowing the *Pv* term, k_A for each time step can be taken from Table 3 and be used to

calculate the wear for that time step. Similarly, equation (11) will provide the melt wear

quantities, but first α needs to be calculated from the left-hand expression in equation

(15). The value of l_b was chosen as 1.016 cm (0.04 in), and $\beta = 6$, similar to the Lim and

Ashby model that produced the melt wear results shown in Figure 16.

40

This leads to two quantities, wear due to melting from equation (11) and wear as a function of k_A from equation (12), both as a function of time, or for that matter a function of Pv or distance. For the remainder of this research, these quantities will be referred to as w_{k_A} (mechanical) and w_{melt}. Figure 21 shows w_{k_A} and w_{melt} as a function of distance. The second plot of Figure 21 is a close-up look over a distance of 50 m centered at the 600 m mark. This illustrates the "bouncing" effect of the sled. When the wear rates goes to zero, the sled is not in contact with the rail. By taking the area under these curves (using the trapezoid rule for integration), it is possible to determine the total wear volume and a wear thickness in the shoe due to each mechanism. These results will be discussed in Chapter III.

41
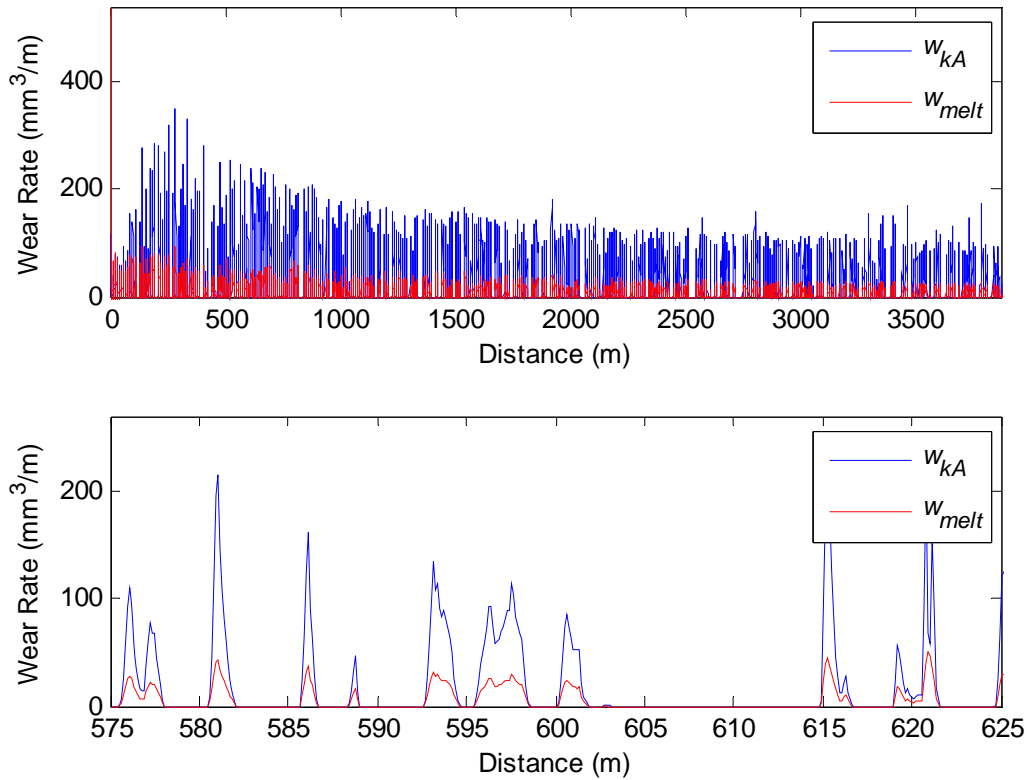
Figure 21 - Wear Rates for DADS Data for Entire Sled Run and for 575 – 625 m

Heat Transfer

The DADS supplied normal force is used to calculate the amount of heat transfer that takes place in the shoe due to the frictional heating at the boundary of the shoe and rail interface. This method was first performed by Laird in his work on gouging [17:83-89]. For the purposes of this research, a one-dimensional heat transfer analysis was considered sufficient. Later research should consider the two-dimensional effects as well as other heat sources such as the stagnation temperatures at the front of the shoe resulting

42

from the hypersonic flow. Frictional heating can be expressed as a function of time, in terms of power by the following equation:

$$q(t) = \mu(t)F_N(t)v(t) \tag{20}$$

The assumption is made that because the thermal conductivities of the1080 steel rail and the VacoMax 300 shoe, an alloy of steel, are very similar, 50% of the heat generated by friction is transferred to the rail while the remaining 50% is transferred to the shoe. Finally the heat transfer into the shoe in terms of flux (W/m^2) can be determined for each time step of the DADS data by using the following expression:

$$q''(t) = \frac{1}{2}\frac{q(t)}{A_n} \tag{21}$$

The ½ represents the heat transfer split between the rail and shoe. Laird, in his work, solved a heat equation with a constant temperature boundary condition at the rail/shoe interface determined from the total energy generated by frictional heating over the entire run using the average normal force value.

43
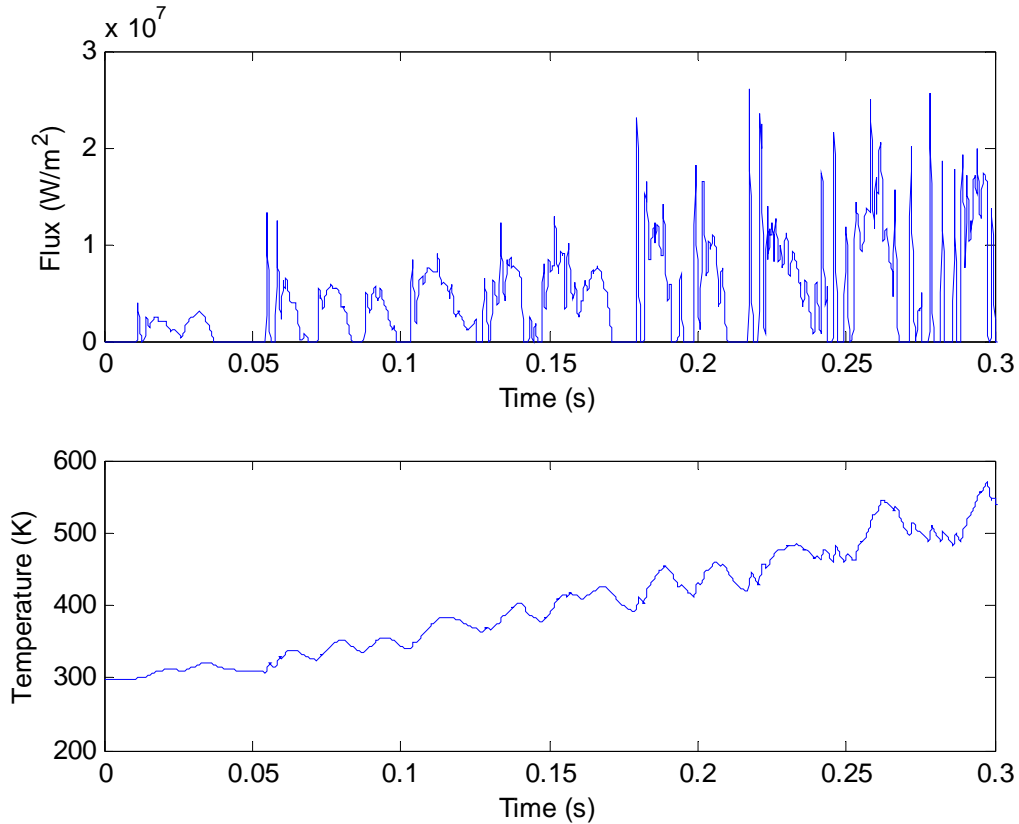
Figure 22 - Flux and Temperature vs Time for the First 0.3 Seconds

In this case, the flux, *q"(t)*, will be used as the boundary condition for each time step in the solution. The flux as a function of time, for the first 0.3 seconds of the run is displayed in Figure 22 along with the corresponding temperature.

The temperature through the thickness of the shoe as a function of time is determined by solving the heat equation in one dimension:

$$\frac{\partial T}{\partial t} = a_V \left(\frac{\partial^2 T}{\partial y^2} \right) \qquad\qquad t > 0, \; y > 0 \qquad\qquad (22)$$

where *y* is the positive direction into the shoe. The one-dimensional solution was thought to be sufficient for determining the temperature profile in the shoe especially for the sled traveling at slower speeds. A more accurate, two-dimensional approach should be

44

investigated at higher sled speeds. The a_V term in equation (22) is the thermal diffusivity defined by

$$a_V = \frac{K_V}{\rho c_{p_V}} \tag{23}$$

K_V is the thermal conductivity, ρ is the density and c_{pV} is the specific heat of VascoMax.

A finite differencing method was used to solve this one-dimensional heat equation explicitly using a forward difference on time and central difference on space by

$$T_i^{n+1} = T_i^n + a_V \frac{\Delta t}{\Delta y^2}\left(T_{i+1}^n - 2T_i^n + T_{i-1}^n\right) \tag{24}$$

i represents the spatial coordinate, and n represents time. If a second order approximation is used for the boundary, the flux condition

$$\frac{dT}{dy} = -\frac{q''(t)}{K_V} \tag{25}$$

can be represented for each time step as

$$T_0 = T_2 + 2\Delta y \frac{q''(t)}{K_V} \tag{26}$$

Where T_0 is at an imaginary point outside the boundary and is used in equation (24) in the T_{i-1} position to calculate the temperature at the boundary. Figure 23 illustrates the flux boundary condition. This indicates that the slope, dT/dy, at the boundary is negative according to the right side of equation (25), and therefore the temperature, moving away from the boundary, is decreasing.

45
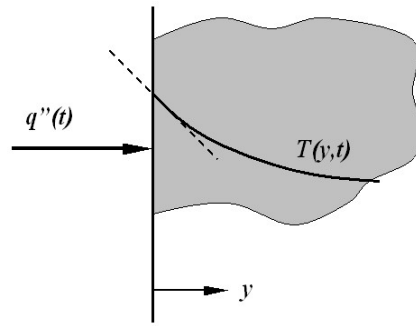
Figure 23 - Heat Diffusion with a Flux Boundary Condition [15:63]

For this explicit method, it is important to check the stability of the solution by

maintaining that the quantity $a_v \Delta t / \Delta y^2$, is less than 0.5 [6:702]. Because the heat equation

is second order in the spatial dimension and first order in time, the solution requires a

second boundary condition, as well as an initial condition. Therefore the boundary

condition in the far field was a shoe temperature equal to ambient, or 297 K. The initial

condition was a uniform ambient temperature throughout the shoe.

The CTH Plane Strain Model

The numerical model being used for high velocity wear was developed by Laird

[17] and improved upon by both Szmerekovsky [24] and later Cinnamon [7].

Szmerekovsky laid the groundwork for the two dimensional plane-strain model by

conducting a mesh convergence study and computing the simulation run-time limit. The

mesh converged at a square cell dimension of 0.002 cm. Using a smaller mesh would

increase total simulation time without significantly improving the results. The reflected

stress wave at the material interface boundary limits the simulation to less than 20

microseconds. A 10 microsecond simulation time is used to ensure there would be no

46

interference from the wave reflection. Cinnamon added the strain rate dependent Zerilli-Armstrong constitutive model for VascoMax 300 and 1080 steel [7:3-11 to 3-12].

$$\sigma = A + (c_1 + c_2 \sqrt{\varepsilon})e^{(-c_3 T + c_4 T \ln \dot{\varepsilon})} + c_5 \varepsilon^n \qquad (27)$$

The plane strain model developed by Szmerekovsky is described in Figure 24. The intention is to model a real world, three-dimensional scenario in a two dimensional plane strain simulation, taking care to maintain the kinetic energy and momentum. The model represents a sled of 841 kg (1854 lbm). The mass is evenly distributed over the four shoes and sliced from 10.16 cm (4 in) to 1 cm (0.394 in) to make it a plane strain model (CTH uses length units of centimeters). Platinum, being the most dense material defined in CTH, $\rho = 21.45$ gm/cm^3, is used for the sled mass having a total height of 46.53 cm (18.32 inches). This calculation is detailed in Appendix C.
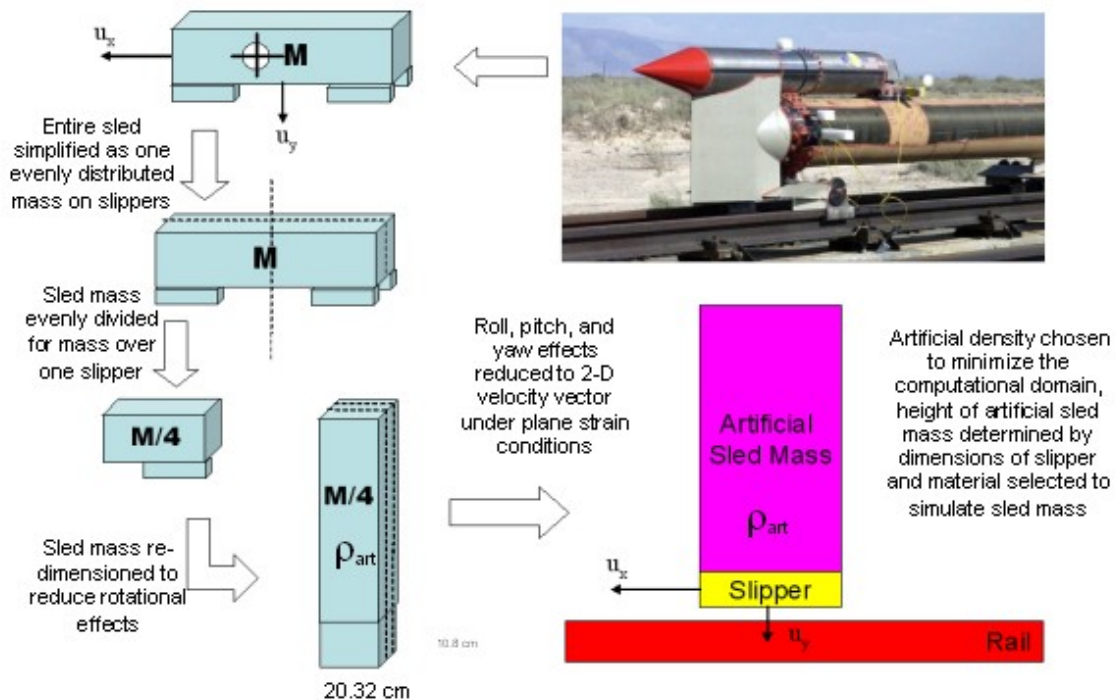
Figure 24 - Plane Strain CTH Model Development [24:5-2]

It is important to note that this method neglects the potential effects of sled roll, pitch and yaw, and the possibility of the weight being unevenly distributed on the sled. These considerations should be researched in future efforts.

Correlating CTH with DADS

In order to use CTH to model what DADS predicts, the attempt was made to associate the DADS normal force with the forces experienced in the CTH model at a particular horizontal velocity. Holloman historically suggested using a vertical velocity of –1 m/s for all cases, because this is roughly the average vertical velocity produced by DADS over an entire sled run. Previous research involving gouging has been run with this –1 m/s vertical velocity. Because CTH does not output force, an attempt was made to determine the downward force in CTH by looking at the rigid body motion over a chosen time interval. Initially this was performed at 100 m/s sled velocity. The rigid body was identified as the concentration of the sled mass that had the same vertical velocity from one time period to the next, suggesting no deformation. The force was determined with Newton's second law by estimating the mass of the rigid body from the dimensions in Figure 25 to obtain the volume, multiplying by density and then multiplying by the change in the vertical velocity over time.
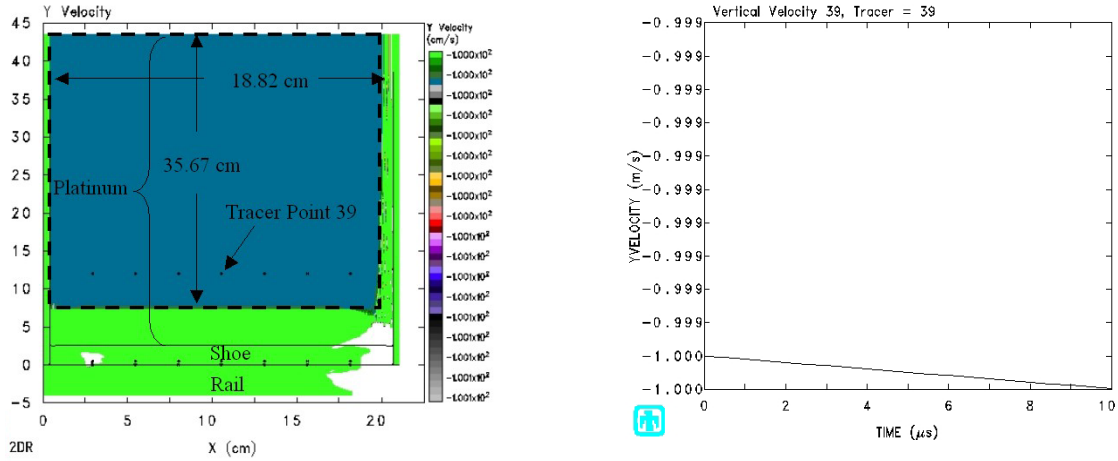
Figure 25 - CTH Vertical Force Prediction Using Δ*v*/Δ*t*

Tracer point 39, which lies within the rigid body, hinted toward the fact that the rigid

body was accelerating downward as indicated by the chart on the right. The scale of the

chart on the left provided a coarse estimation of the velocity. This calculation resulted in

an acceleration of -21.33 m/s^2 and a force of 3,123 N, remarkably close to the 3,363 N

that DADS supplied at this speed for this particular sled file. This technique was also

applied to the sled traveling at 1000 m/s. The results were nearly identical to the 100 m/s

case, suggesting that this technique was inadequate, because DADS produced a much

larger vertical force for the higher speed. Consequently, the acceleration in CTH that the

sled experienced was mostly a product of the acceleration due to gravity. What resulted

from this effort is that the gravity term in CTH was discovered. Previous models did not

take gravity into consideration, however previous models did not simulate the sled at the

relatively low speed of 100 m/s where gravity is more of a factor because the system's

momentum is lower. The 21.33 m/s^2 acceleration in retrospect was well within the error

tolerance of this calculation to sufficiently say it was in fact gravity. The conclusion was

that CTH focuses more on momentum conservation than forces in the sense that forces

49

are neither input nor output parameters whereas velocities are both input and output parameters. The author recognizes that force and velocity are related through the change in momentum over time. Therefore the correlation between CTH and DADS would be sufficiently satisfied if, instead of using –1 m/s vertical velocity the actual DADS produced vertical velocity was used. Recall from Figure 14, that DADS calculates a vertical velocity as well as a horizontal sled velocity as a function of time. The technique would involve choosing the simulation velocity then determining the corresponding vertical velocity.

Defining the Mesh

As mentioned in the section on the plane strain model, the smallest mesh size is 0.002 cm. Considering that computational time is a function of the number of cells and therefore the cell size, it is more efficient to only use the 0.002 cm cell size in areas of interest, namely at the material interfaces. It is also important to maintain an aspect ratio close to unity for all cells. The mesh definition that was used for the final analysis can be seen in Appendix B, CTH Input File, while a typical model can be seen in Figure 26. The figure on the left is depicting the mesh. The figure on the right is material definition at time equals zero. Overlaying the two figures gives an indication of the where the model fits in the mesh. The idea was to use a fine mesh in the places of interest, namely the shoe/rail interface and the leading edge of the shoe. The typical runtime for a simulation using this mesh was roughly eight hours.

50
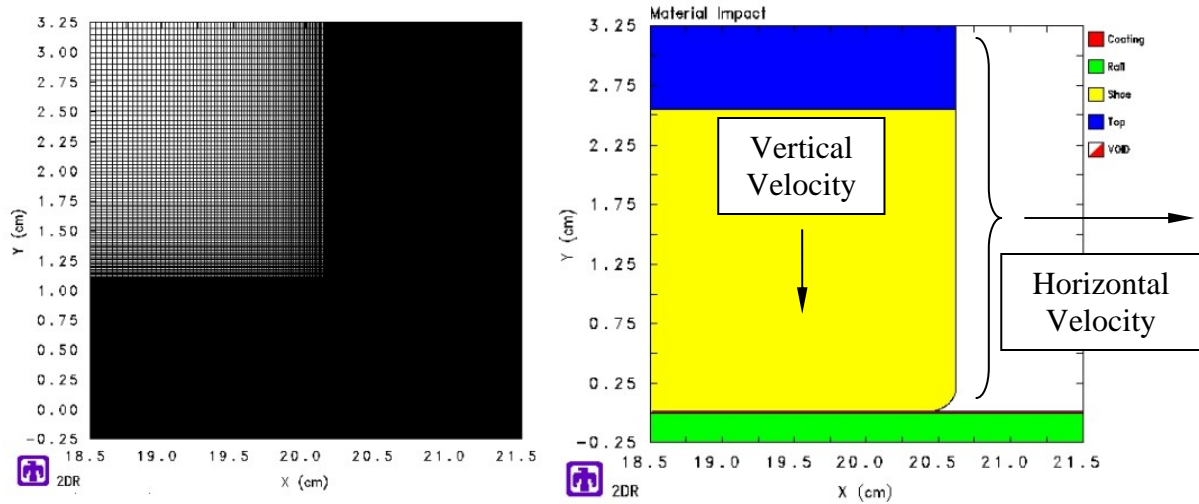
Figure 26 - Representative Mesh

CTH Material Interface

Cinnamon conducted a study to determine which of the three material interface scenarios within CTH would be best for the gouging problem. The three techniques used are no-slide, slide-line and boundary layer approaches. The slide-line technique, which sets the shear strengths to zero to allow sliding to occur, generated instabilities within the solution in that shear stresses developed far away from the interface. The boundary layer method was found to be valid only for two-dimensional axi-symmetric problems using one computational processor to solve the problem compiled by CTH. Therefore the no-slide method was chosen as the best method to model the material interface for the gouging problem [7:6-30]. The same method was used for the wear problem.

The concept of no-slip suggests that no sliding will occur during the simulation. However, CTH handles the problem of sliding under no-slip by requiring the materials to fail under shear. Shearing is brought about by giving the sled and rail different velocities. Initially all materials are considered joined at the beginning of each time step where

51

contact exists. If the case occurs where a cell would have a mixture of one or more materials, the cell strength is governed by the material volume fractions. As it turns out, this is a good representation of friction on the micro-structural scale discussed in Chapter I. This motion can generate plasticity, heat, material fracture and debris, all of which contribute to wear directly or indirectly. In addition, the use of a lower strength, thin layered coating on the rail, such as epoxy, gives the effective sliding boundary condition as will be discussed along with the result in the next section.

Melt Wear

Lim and Ashby state that "Agreement is good" between the experimental data
(they were referring to the Montgomery data) and their wear model. [18:13]. Figure 27
is the graphical representation of their wear model along with the experimental data
plotted in 3D space ($\tilde{v}$, $\tilde{F}$, $\tilde{w}$). The contours are the lines established by the model
(equation (11)) and represent lines of constant wear rate. The numbers next to the
experimental data points are $log_{10}(\tilde{w})$.
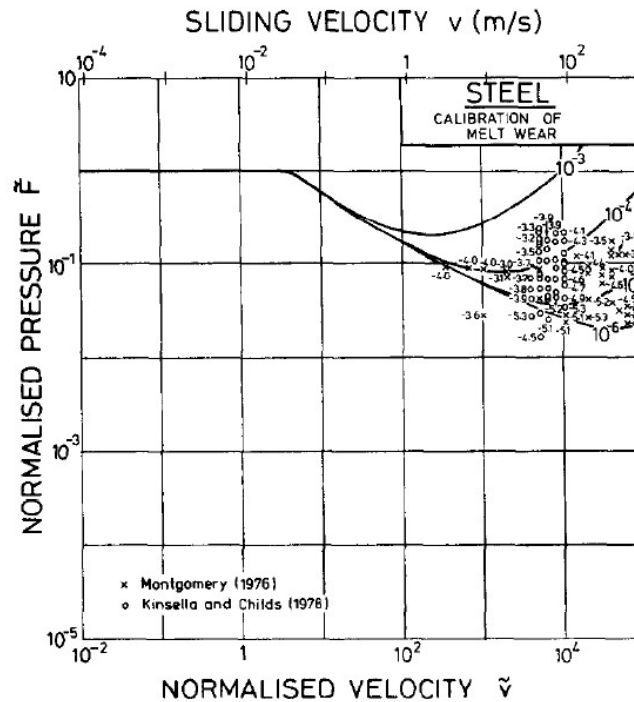
Figure 27 - Lim and Ashby Model for Melt Wear [18:13]

However, a closer look in three dimensions shows that the values for $\tilde{w}$ are close but not within the contours (Figure 28). This would indicate that the model is not entirely accurate.
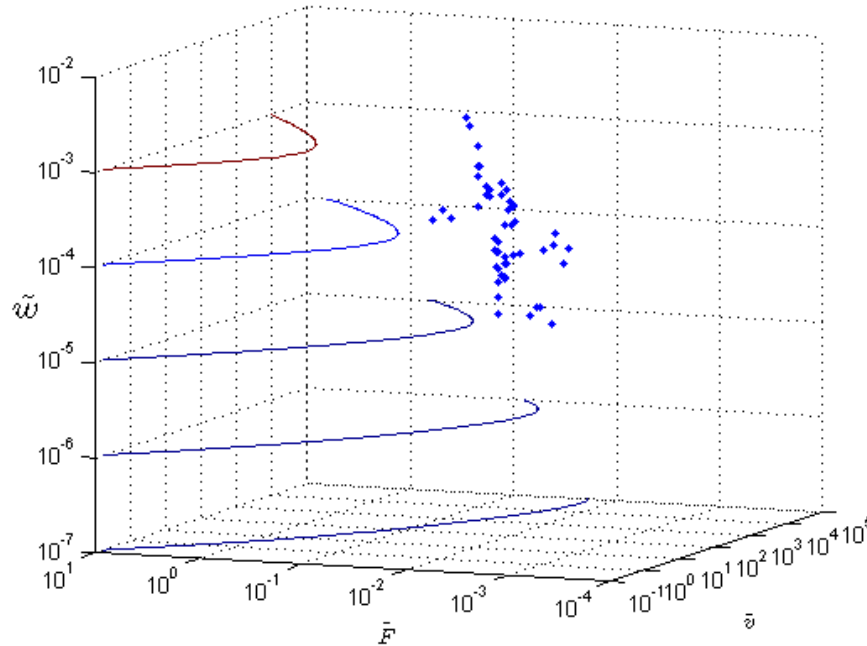
Figure 28 - Three Dimensional View of Lim and Ashby's Melt Wear Model

Accordingly, when the melt wear model was applied to the DADS data as discussed previously, acceptable values for melt wear were achieved using the same values for β and l_b that were used for the Montgomery data, that is $\beta = 6$ and $l_b = 1.016$ mm (0.04 in). The results shown in and Figure 30 are similar, however the DADS data points are not as close to the contour lines as the Montgomery data was. This is because the function used in the model for the coefficient of friction, μ, is different than the function used for the calculation of melt wear using the DADS data (equation (18) versus equation (19)). Also recall that the geometry used to create the model was based on the pin-on-disk scenario with a very small pin diameter whereas the DADS data uses a much larger radius to

54

represent the shoe. However this could simply be an indication that either the model is

invalid or the shoe does not experience melt wear.
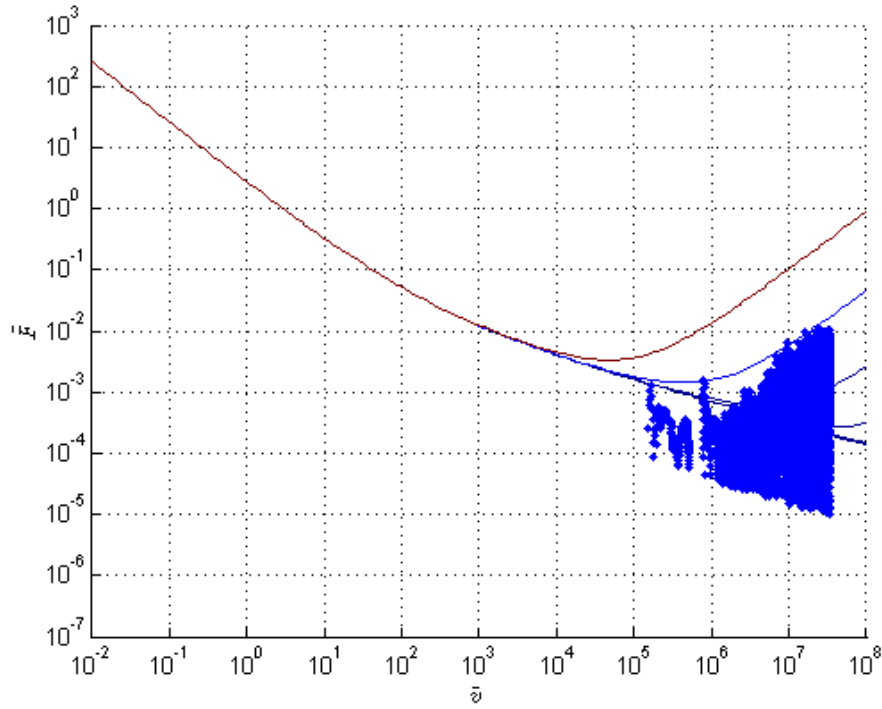
Figure 29 - Melt Wear Results for DADS Data

55
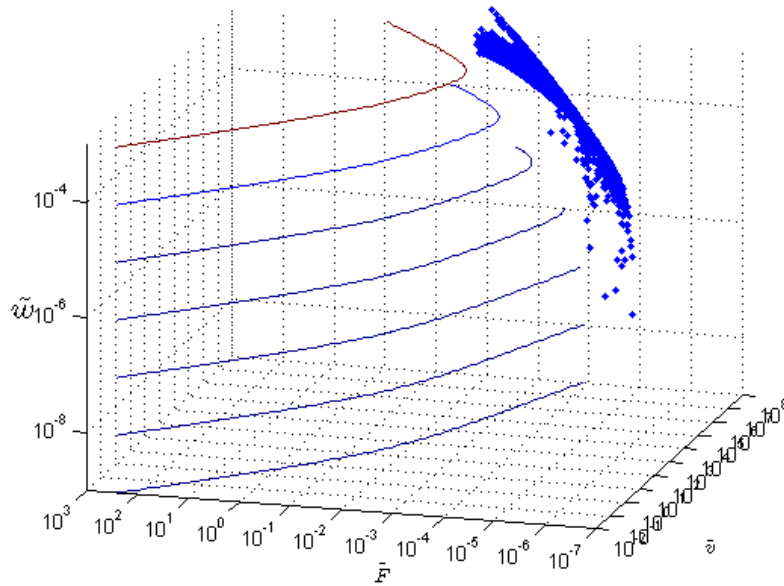
Figure 30 - Three Dimensional View of Melt Wear for DADS Data

Lim and Ashby Equations Predicting Wear

A MATLAB code was constructed to model the shoe wear from the DADS data using the Lim and Ashby equation for wear w_{kA} and w_{melt}. This was detailed in the last chapter. For the numerical modeling in CTH, two velocities were chosen to be analyzed in detail with one additional velocity chosen to get a data point at an even higher velocity. The velocities were somewhat arbitrarily selected based on their relatively low magnitude and corresponding vertical velocity. All of the work that was conducted by Cinnamon with regard to gouging was performed at 3,000 m/s [7]. This research focuses more on how velocity affects the shoe by examining the behavior at 394 m/s and 798 m/s, in combination with several other parameters and one case with a velocity of 1,411 m/s. Table 5 and Figure 31 details the relevant information about the points chosen from the DADS data to be analyzed.

Table 5 - Velocity Points from DADS

	Time (s)	Horizontal Velocity (m/s)	Vertical Velocity (m/s)	Distance Traveled (m)
A	0.31	394	-0.77	61.1
B	0.63	798	-1.98	252.0
C	1.12	1,411	-3.48	796.5
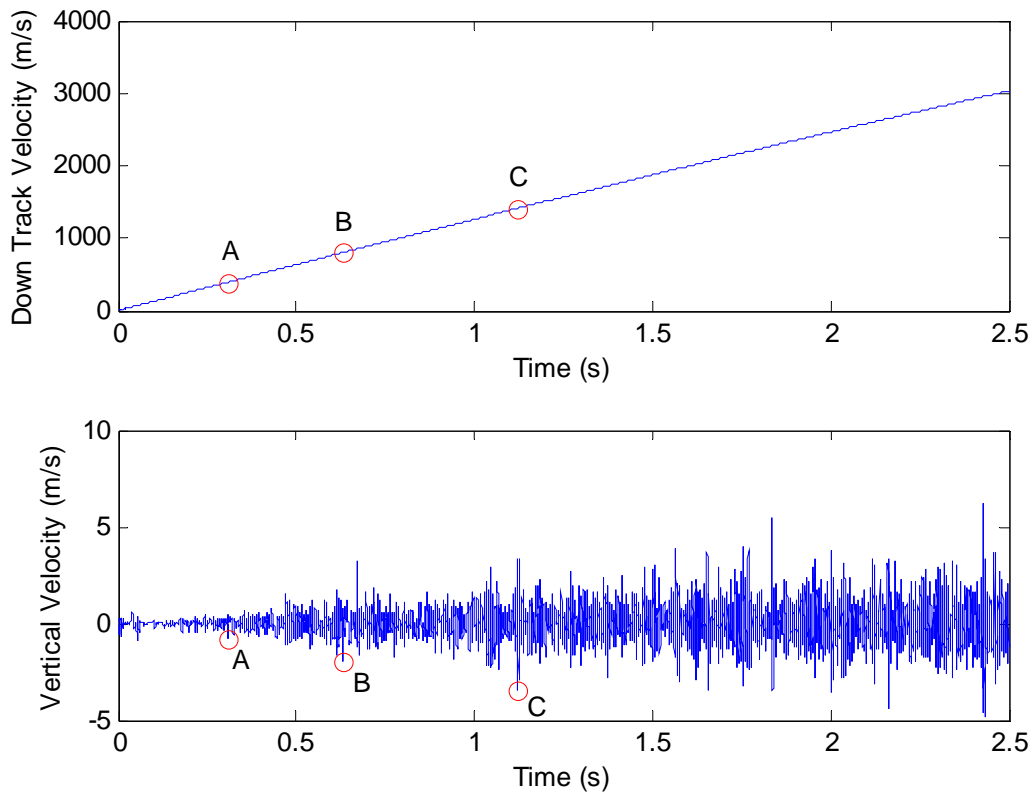
Figure 31 - Plots Indicating Velocities Used in CTH

The next sections, including Table 6, discuss the results from the analytical models with the assumption, as stated earlier, that the shoe makes uniform contact with the rail over the entire 206.5 cm^2 (32 in^2) area. This assumption allows for a simple calculation of wear (or material removal) by dividing the volume of wear by the area. Recall that the volume of wear was determined by integrating the wear rate (mm^3/m) with respect to the distance the sled traveled.

394 m/s

The MATLAB code was designed to calculate the wear up to a specified input velocity. The amount of mechanical wear generated by the sled according to equation

57

(12) up to 394 m/s was 0.0035 cm, and the amount of melt wear was 0.0047 cm after traveling a distance of 61.1 m.

The temperature distribution resulting from the frictional heating that was used to put into CTH is shown in Figure 32. Recall that the flux, $q''(t)$, is a function of time, and the coefficient of friction is a function of force and velocity as stated by equation (19). Depending on the length and duration of the contact, a specific quantity of heat is generated due to friction that accumulates over time. The figure on the left therefore, is the curve that MATLAB generated for the temperature distribution in the shoe at the point when the sled reaches 394 m/s. The indicated points were taken and used to create a temperature profile in CTH. The figure on the right is the representative profile in CTH. The maximum temperature seen by the shoe was calculated to be 567 K, which may seem contrary to Figure 32. Remembering that the flux varies with time and at some instances equals zero, suggests that the time the sled reaches 394 m/s or 0.31 seconds into the run the sled is not in contact with the rail, and heat is not being transferred into the shoe.
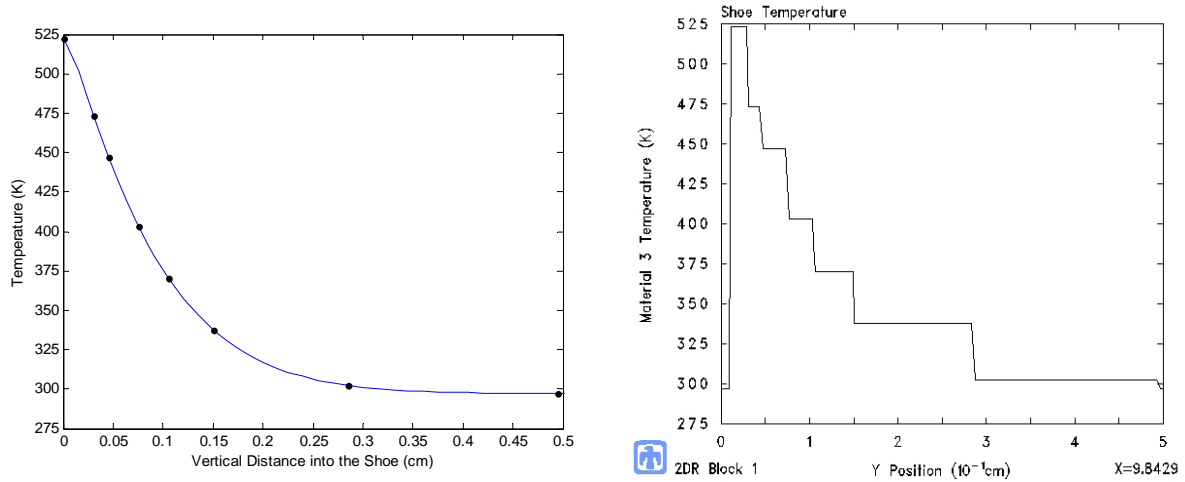
Figure 32 - Temperature Distribution for Heat Generated from Friction for the Sled up to 394 m/s – MATLAB and CTH Curves

798 m/s

Identical to the previous case, the MATLAB code was executed for the sled's travel up to 798 m/s. The resulting reduction in thickness of the shoe due to mechanical wear was 0.0156 cm and 0.0113 cm for melt wear. The maximum temperature reached was 854 K in a distance of 252.0 m. The temperature distribution from frictional heating for this speed is in Figure 33. The MATLAB generated profile is on the left along with the points used in CTH. The CTH profile from those points is shown in the figure on the right.

59
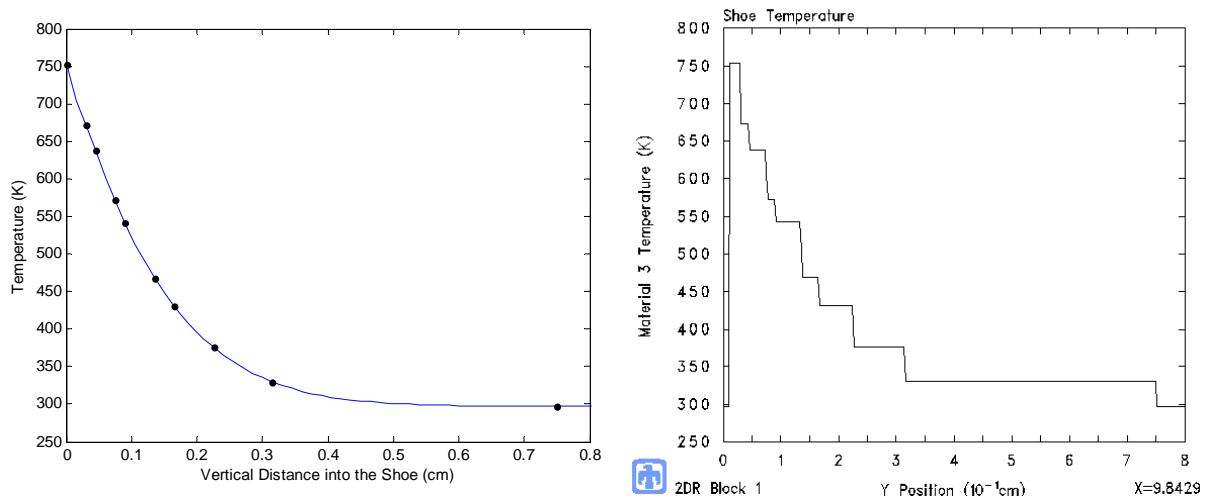
Figure 33 - Temperature Distribution for Heat Generated from Friction for the Sled up to 798 m/s – MATLAB and CTH Curves

1,411 m/s

The analysis at 1,411 m/s was not conducted in as much detail as the slower velocities. The analytically derived melt wear amount of 0.0246 cm and a mechanical wear amount of 0.0576 cm was calculated for a distance traveled of 796.5 m.

One simulation was conducted in CTH at this velocity against an asperity, at ambient initial temperature conditions and without a coating. For this reason a temperature profile was not established to be input into CTH. However, according the heat transfer portion of the MATLAB code, the maximum temperature was 1451 K.

Table 6 is a complete summary of the results for both melt wear and mechanical wear calculated from the analytical model developed in MATLAB. This code can be seen in Appendix A. Notice that the last row of data is for the complete run. This shows a total wear thickness of 0.2731 cm for mechanical wear and 0.0797 cm for melt wear. These values, if superimposed, amount to approximately 0.35 cm of total wear. Although

60

these results may not be completely accurate, they are realistic considering the shoe is 2.54 cm thick.

Table 6 - Analytical Model Results for Melt and Mechanical Wear and Maximum Temperature

	Maximum Temperature (K)	Melt Wear (cm)	Mechanical Wear (cm)
394 m/s	570	0.0047	0.0035
798 m/s	854	0.0113	0.0156
1,411 m/s	1,451	0.0246	0.0576
3,030 m/s	3,925	0.0797	0.2731

In addition, Figure 34 shows how the DADS data looks in terms of wear rate vs. *Pv*. Comparing this figure with Figure 16 from the Montgomery data shows that the wear rates are significantly higher for the DADS data, however all of the DADS data occurs at lower *Pv* values compared to the Montgomery data.
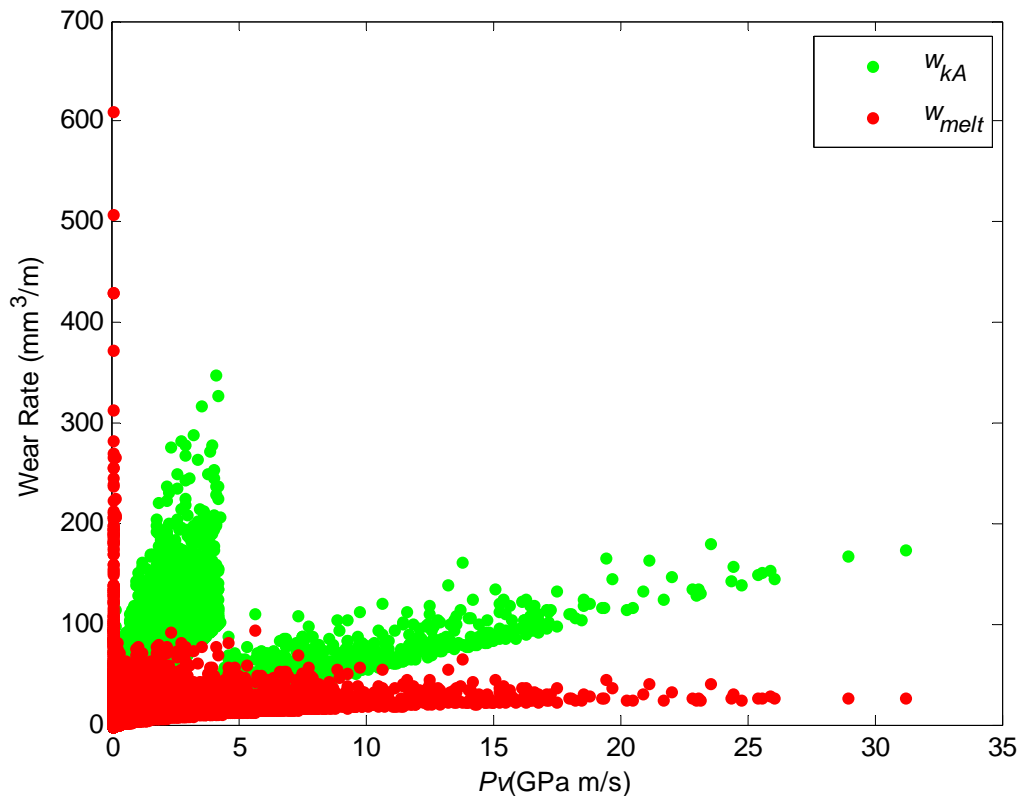
Figure 34 - DADS Melt and Mechanical Wear Rate vs. *Pv*

CTH

In the effort to numerically generate wear results using CTH, several scenarios of the sled/rail system were simulated. Four different parameters with two possible variations each, were simulated in all possible combinations resulting in 16 cases. The parameters are velocity, 394 m/s and 798 m/s as discussed above; a flat rail or a rail with an asperity; a rail with or without a coating; and the rail at ambient temperature and the rail with the profile generated from the MATLAB code. A 0.01 cm coating was customarily used in CTH gouging simulations to more closely approximate the sliding phenomenon that CTH does not adequately model as previously discussed. The use of a coating provided excellent results correlation for past researchers, therefore it has been

62

carried forward for the modeling of wear. In reality, a thin epoxy layer is frequently used at Holloman, therefore using a coating in the model is not impracticable.

It was anticipated that characterizing wear in CTH would be possible in the mechanisms of melt and localized fracture or failure. With this in mind, the CTH results were analyzed by examining the shoe temperature and the maximum principal stress in the shoe. The temperature field is generated during the CTH model execution from plastic deformation in the materials; this is also referred to as plasticity. Melt was determined by comparing the temperature field produced by CTH to the melt temperature of VascoMax 300 which is 1685 K. Localized failure occurs when the maximum principal stress exceeds the fracture strength defined for VascoMax 300. The maximum principle stress is the largest normal stress in a principal direction for any given state of stress. The principal directions, or principal planes, are those for which a given state of stress, including normal and shearing stresses, are transformed to only normal stresses. Cinnamon experimentally determined the fracture strength for VascoMax 300 to be 2.5 GPa (2.5×10^{10} dyne/cm^2) [7:5-13]. CTH conveniently supplies the maximum principal stress as an output parameter.

The following sections will examine the output from CTH for the 16 cases simulated. The procedure was to first visually find the highest temperature or maximum principal stress from the respective contours and then produce a one-dimensional plot of that parameter versus the y dimension, or through the thickness of the shoe, as it passes through that maximum area identified on the contour.

Flat Rail, 394 m/s, Coating

For this case, neither the maximum principal stress nor the temperature exceeded the fracture strength or the melt temperature respectively. The maximum temperature reached in the shoe material was approximately 329 K at 1 microsecond, near the back of the shoe, well short of melt. Figure 35 shows a 2D temperature profile for the rail shoe interface as well as a 1D look at the temperature into the shoe at an x position of 2.38 cm, both of which are for simulation time equal to 1 microsecond.
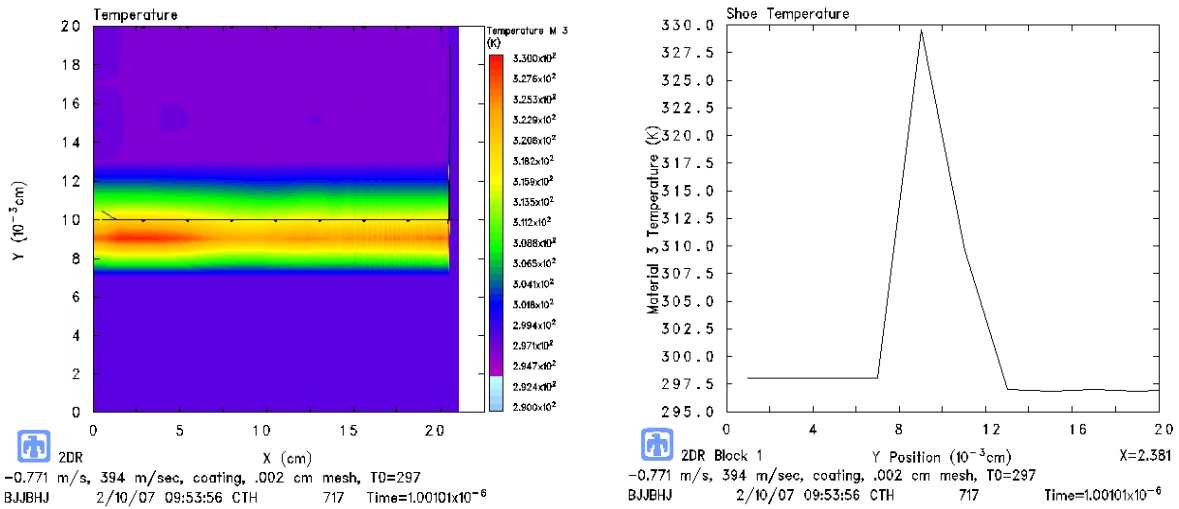
Figure 35 - Temperature for 394 m/s, Coating, Initial Ambient Temperature

Similarly, Figure 36 shows areas of high stress near the front of the shoe; however, the stress in these areas is significantly less than the fracture strength.

64
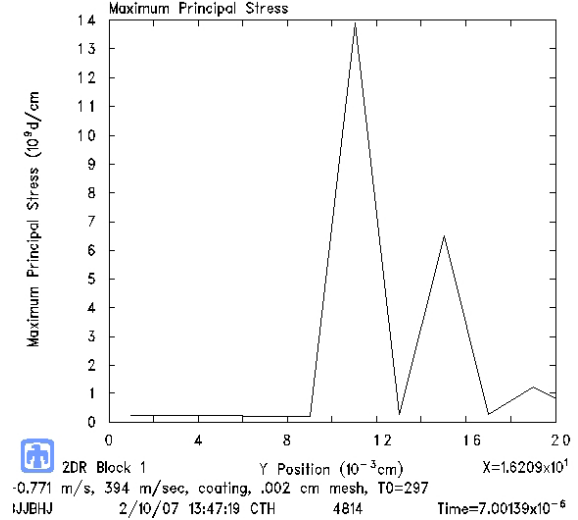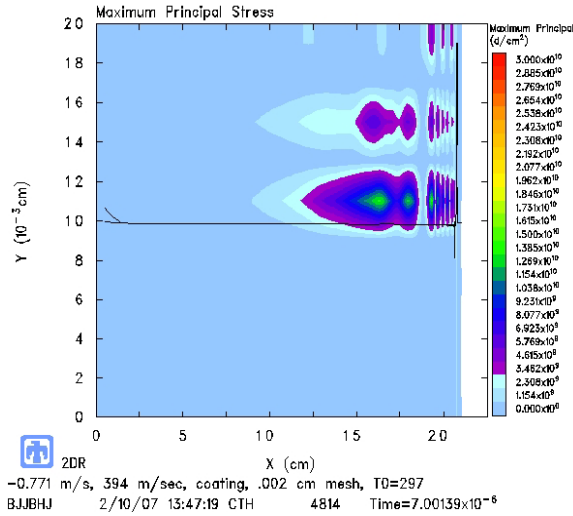
Figure 36 - Maximum Principal Stress for 394 m/s, Coating, Initial Ambient

Temperature

The effect of running the simulation with the temperature profile can be seen in

Figure 37 where the highest temperatures are found toward the middle of the shoe at x =

9.84 cm.
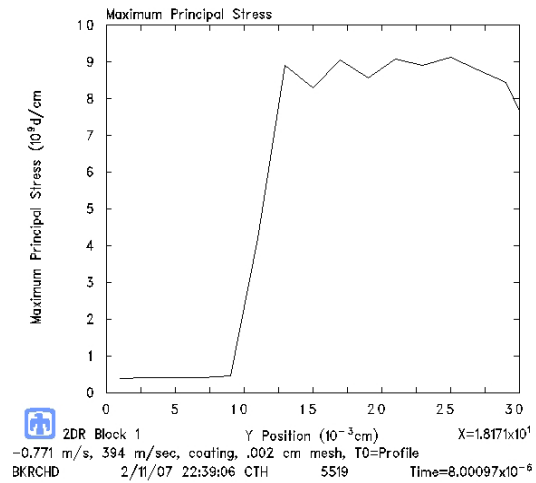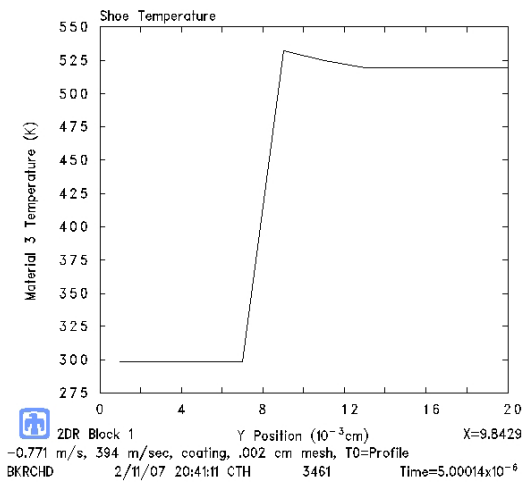
Figure 37 - Temperature and Maximum Principal Stress for 394 m/s, Coating,

Initial Temperature Profile

Recall that the temperature profile input into CTH (Figure 32) had a maximum

temperature of 525 K. As one can see from Figure 37, the effect of plasticity raised the

65

shoe temperature approximately 10 degrees. The maximum principal stress decreased,

yet it became more uniform through the thickness.

Flat Rail, 798 m/s, Coating

As expected, increasing the horizontal velocity, and therefore the vertical velocity

also increased the resultant temperature in addition to moving the area of high

temperature towards the front of the shoe. Figure 38 and Figure 39 shows a higher

temperature initially (at 1 microsecond versus 10 microseconds) of approximately 422 K

and a lower maximum principal stress, yet these values are both still well below what is

necessary to characterize wear.
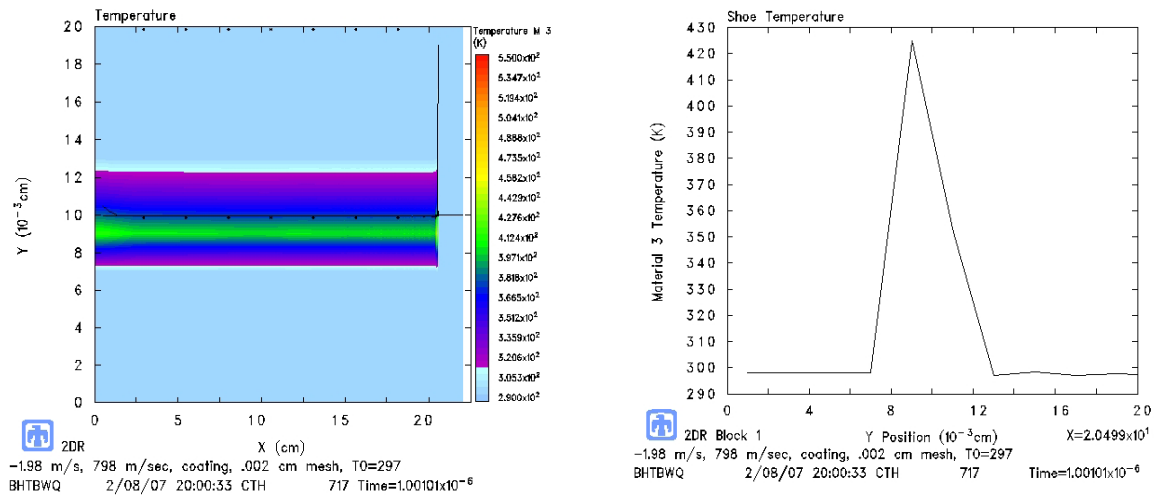
Figure 38 - Temperature for 798 m/s, Coating, Initial Ambient Temperature

66
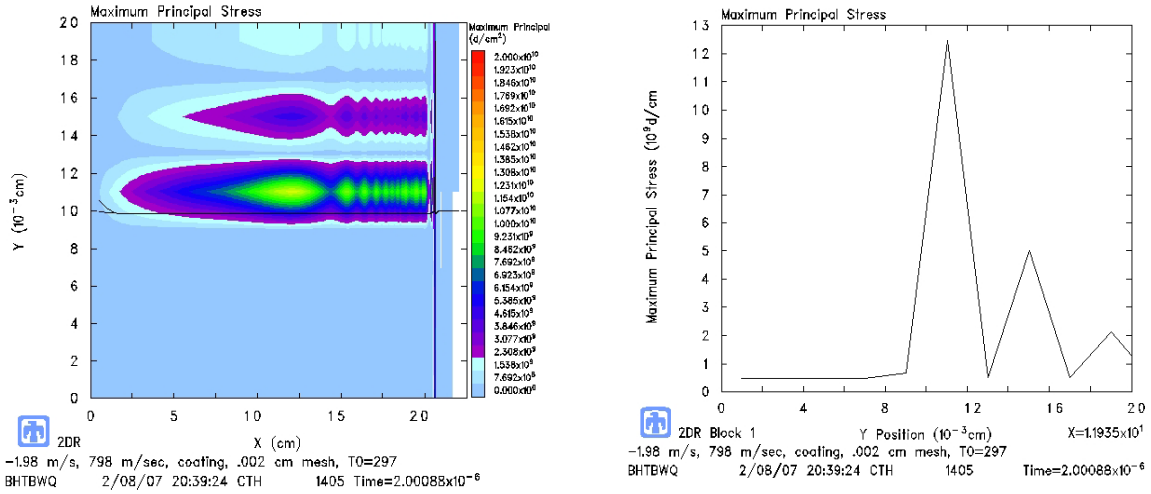
Figure 39 - Maximum Principal Stress for 798 m/s, Coating, Initial Ambient Temperature

The effect of the temperature profile on temperature and maximum principal stress can be seen in Figure 40. Once again the effect of the initial temperature profile (Figure 33) slightly increased the temperature and thickened the portion of the shoe experiencing the highest value of maximum principal stress.
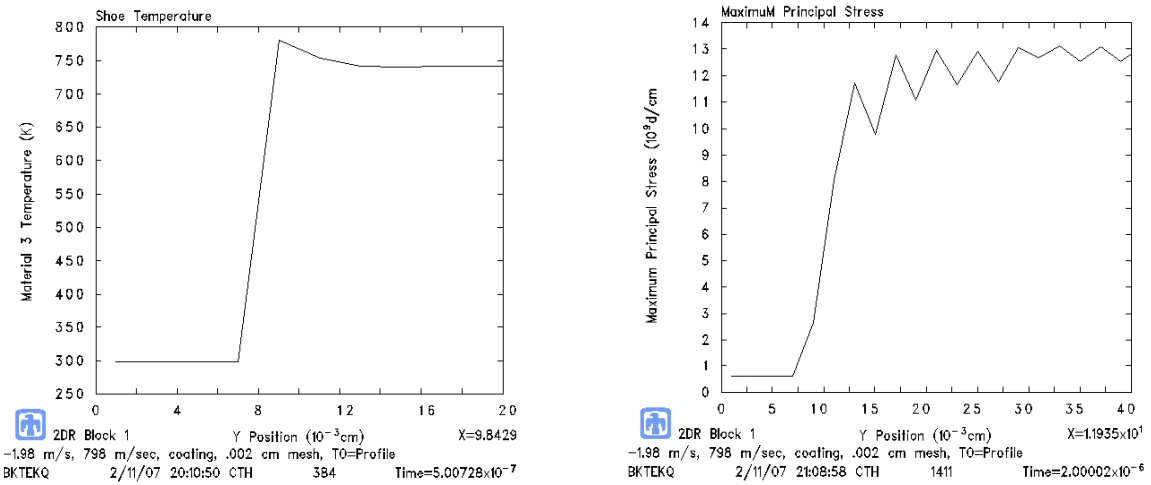
Figure 40 - Temperature and Maximum Principal Stress for 798 m/s, Coating, Initial Temperature Profile

67

Flat Rail, 394 m/s, No Coating

The effects of running a sled directly on the rail, in the absence of a coating, will now be discussed. Figure 41 shows the resulting temperature field and one-dimensional plot of temperature through the thickness of the shoe at the end of 10 microseconds at the x position of 20.5 cm.
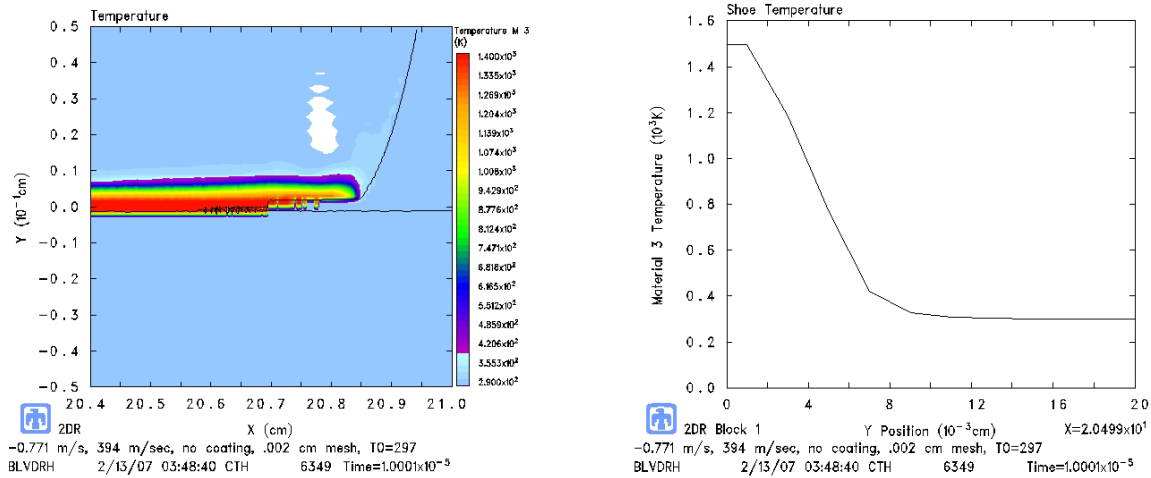
Figure 41 - Temperature for 394 m/s, No Coating, Initial Ambient Temperature

The effect of the initial temperature profile is nearly negligible as depicted in

Figure 42, with the slight distinction between the far field temperature of 550 K versus

300 K

.
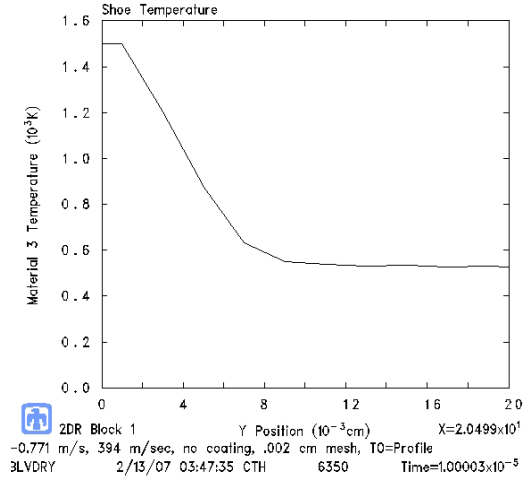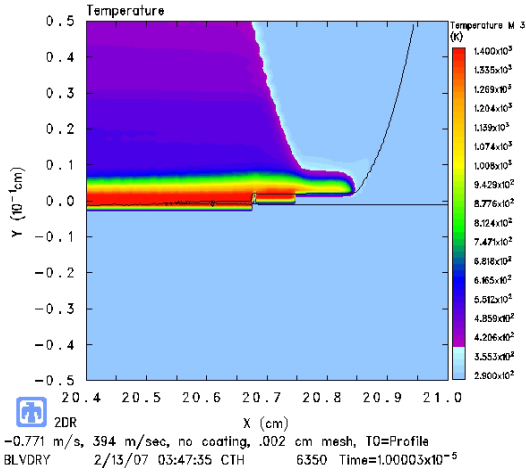
Figure 42 - Temperature for 394 m/s, No Coating, Initial Temperature Profile

Flat Rail, 798 m/s, No Coating

Increasing the velocity to 798 m/s resulted in temperatures that can be seen in

Figure 43. These are nearly identical to the 394 m/s case.
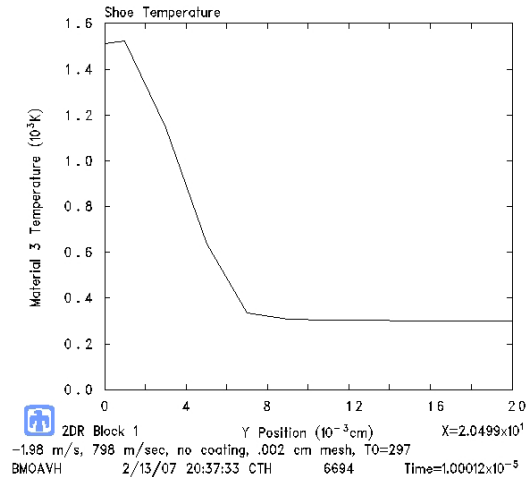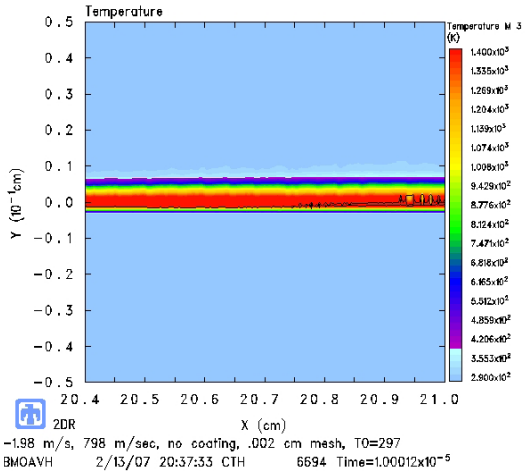
Figure 43 - Temperature for 798 m/s, No Coating, Initial Ambient Temperature

Again the effects of the initial temperature profile resulted in nearly identical results for

the 394 m/s case with an initial temperature profile in that the maximum temperature

increased only slightly.
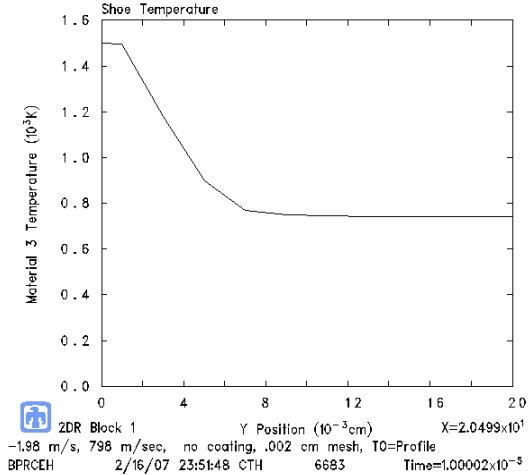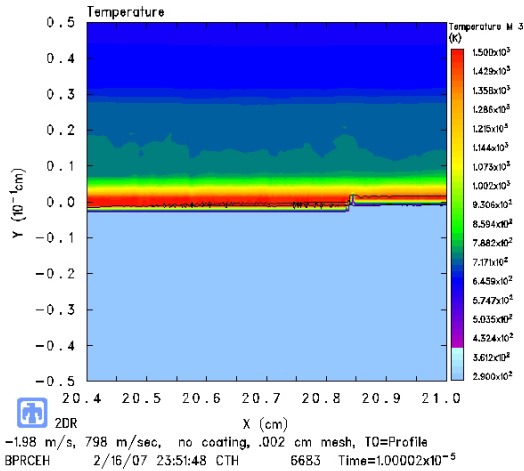
Figure 44 - Temperature for 798 m/s, No Coating, Initial Temperature Profile

Asperity, 394 m/s, Coating

Cinnamon [7:9-32] used an asperity to generate gouging in the rail. Asperities were discussed earlier where it was stated that they exist because of the rail seams and the inherent manufacturing tolerances. His study conducted on asperity geometry (acute face angle and height) was conducted at a sled velocity of 3000 m/s and a vertical velocity of –1 m/s. He concluded that the highest asperity that would not generate a gouge, for this velocity, was 0.03 cm with a face angle of 10 degrees. This particular geometry, well within the current HHSTT rail specifications, was used in this research to initiate wear. Figure 45 shows the asperity geometry.

70
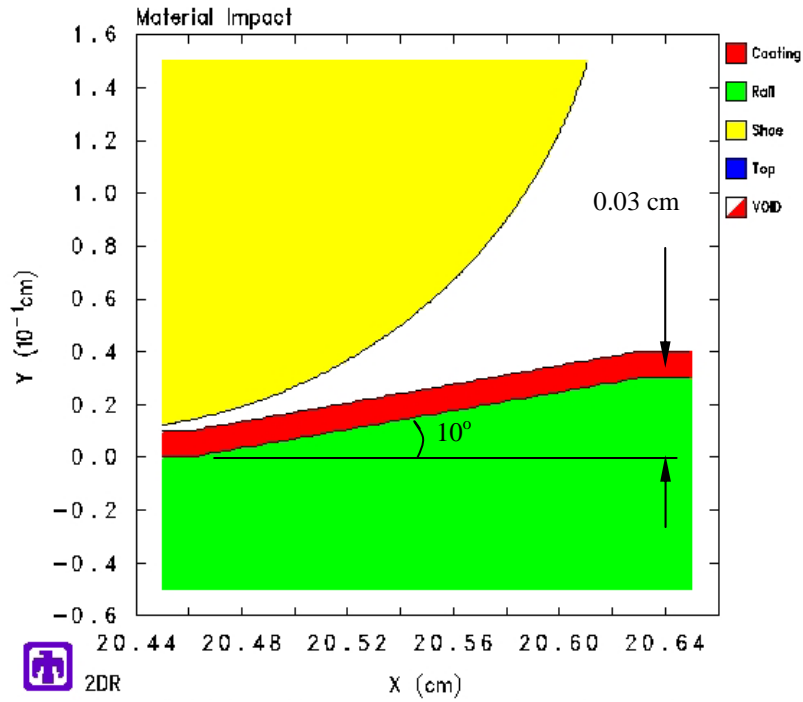
Figure 45 - Asperity Geometry

In the first case with an asperity, the speed of 394 m/s was used with the epoxy

coating. Figure 46 shows a high temperature spot near the x position of 20.75 cm. The

graph on the right indicates that the highest temperature at this position is very nearly

1500 K.
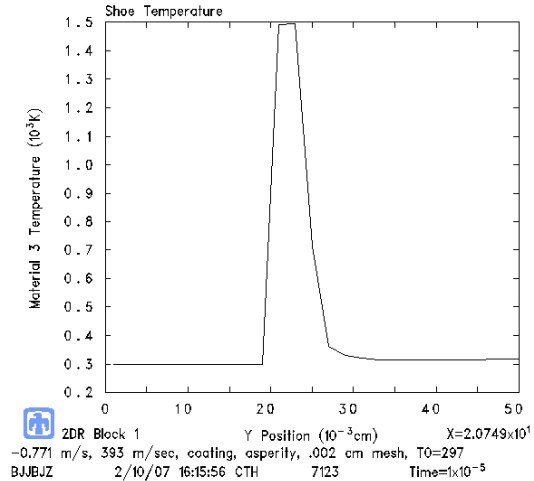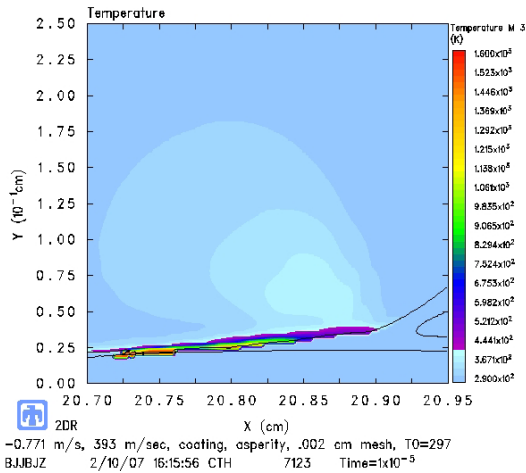
Figure 46 - Temperature for 394 m/s, Asperity, Coating, Initial Ambient Temperature

Figure 47 displays that the maximum principal stress at an x position of 20.72 cm is significantly greater than the fracture strength of VascoMax 300. This, according to the earlier discussion, is an indication of wear. The amount of wear could be considered by taking the thickness of the shoe that is above the fracture strength and subtracting off the height of the asperity and the coating (0.04 cm); in this case it would be approximately 0.08 cm.
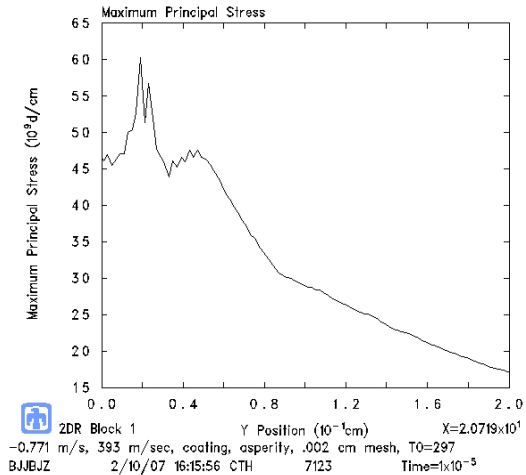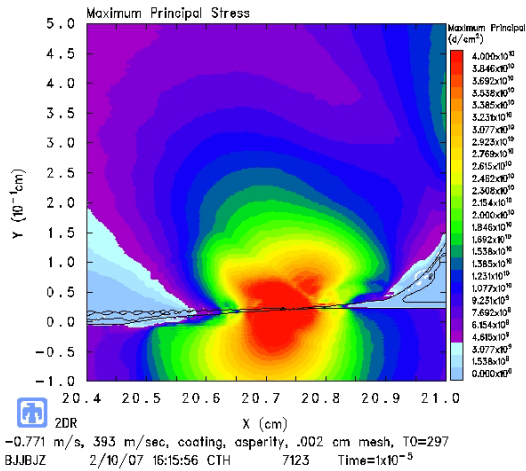
Figure 47 - Maximum Principal Stress for 394 m/s, Asperity, Coating, Initial Ambient Temperature

The effects of applying the initial temperature profile due to frictional heating in this case appear to be negligible. A quick comparison of Figure 46 with Figure 48 and Figure 47 with Figure 49 indicates that the maximum temperatures and maximum principal stresses are nearly equivalent.
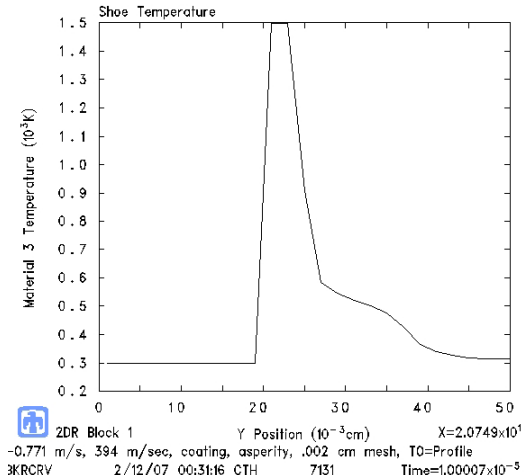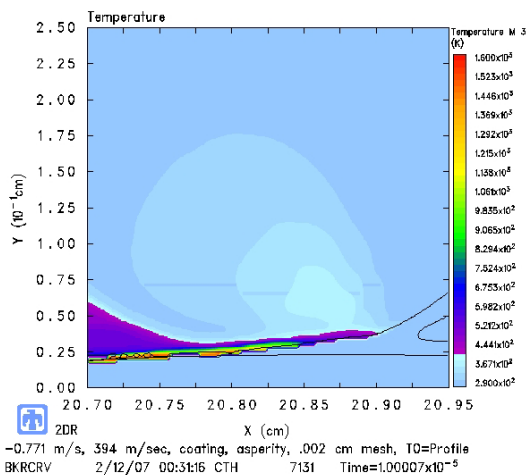
Figure 48 - Temperature for 394 m/s, Asperity, Coating, Initial Temperature Profile
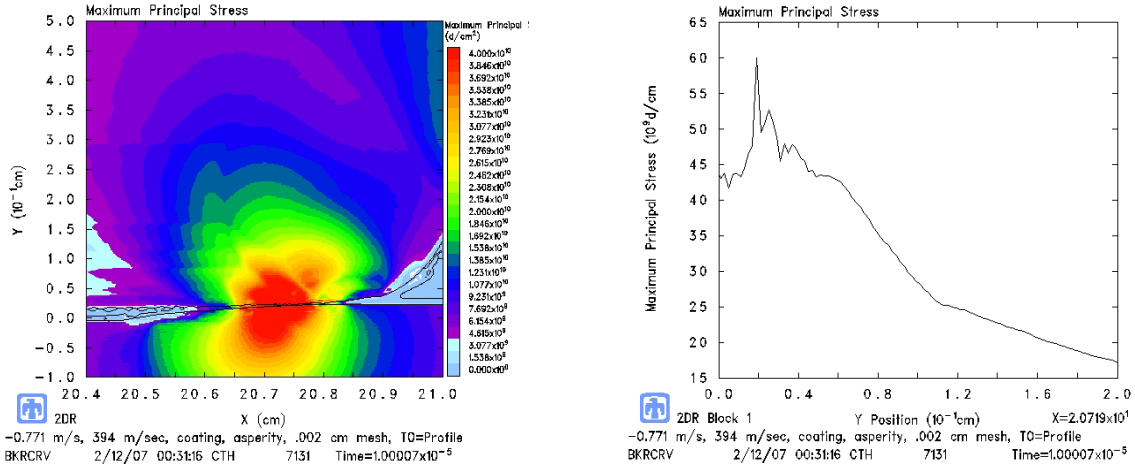
Figure 49 - Maximum Principal for 394 m/s, Asperity, Coating, Initial Temperature

Profile

Asperity, 798 m/s, Coating

This case is identical to the previous case with the exception of an increase in vertical and horizontal velocities. The vertical velocity was increased to –1.98 m/s and the horizontal velocity to 798 m/s in accordance with the DADS point selected earlier in Figure 31. As Figure 50 indicates the temperature nearly reaches 1580 K.
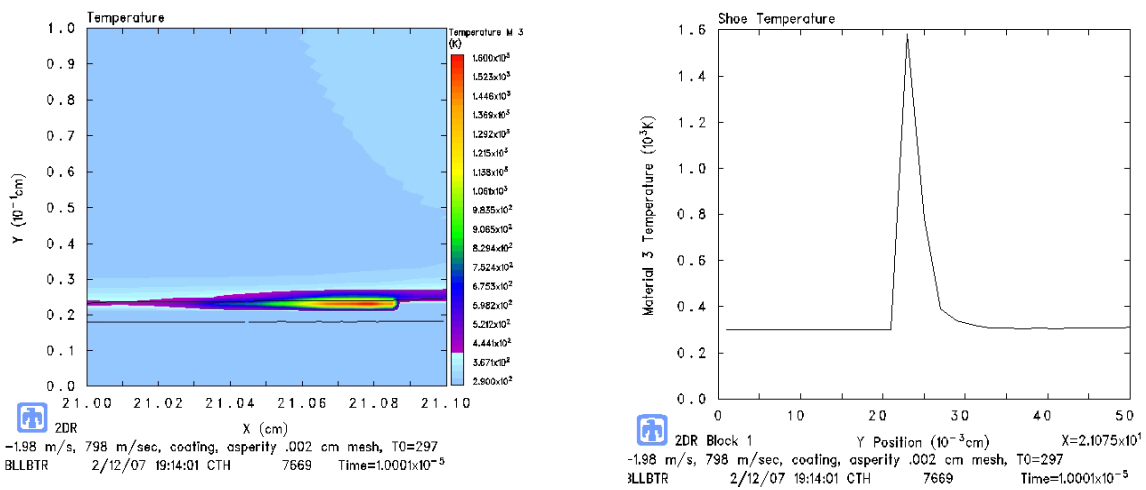
Figure 50 - Temperature for 798 m/s, Asperity, Coating, Initial Ambient

Temperature

74

Figure 51 shows the maximum principal stress for this case, and like the slower velocity, wear is also evident as the stress exceeds the fracture strength of the material. However this case reaches an even higher value than the slower velocity, 6.7 GPa versus 6.0 GPa. As a result the wear also increases by a thickness of 0.05 cm to 0.13 cm.
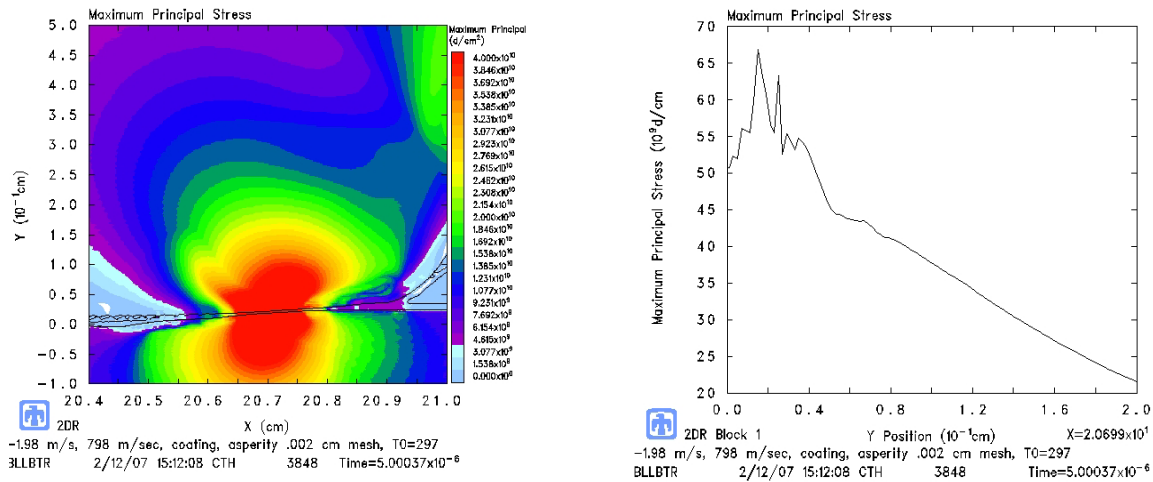
Figure 51 - Maximum Principal Stress for 798 m/s, Asperity, Coating, Initial

Ambient Temperature

The effect of using the frictional heat temperature profile is displayed in Figure 52 and Figure 53. The temperature and maximum value of the maximum principal stress were significantly reduced, however the wear thickness increased to 0.14 cm.
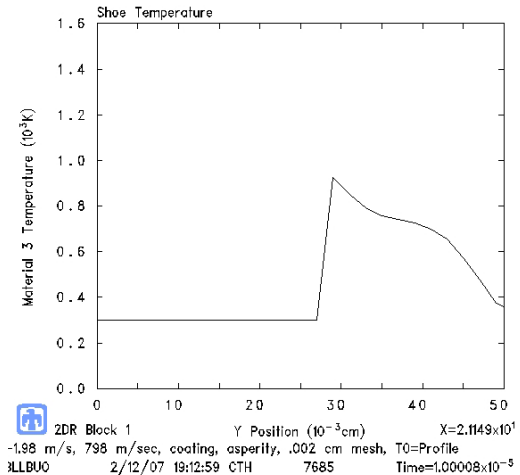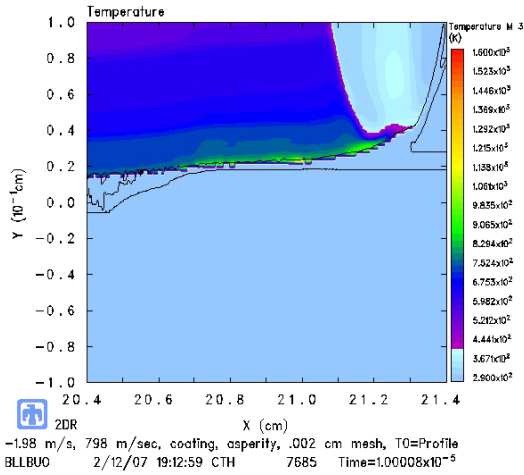
Figure 52 - Temperature for 798 m/s, Asperity, Coating, Initial Temperature Profile
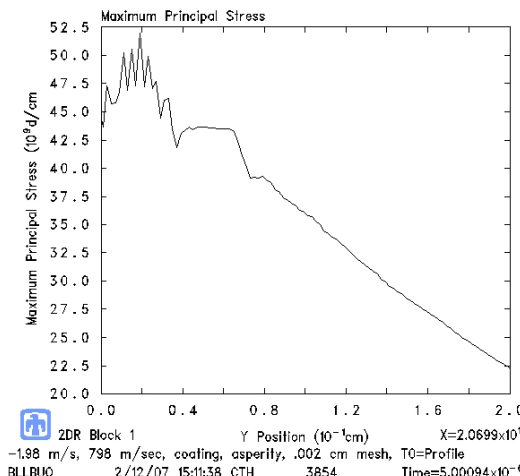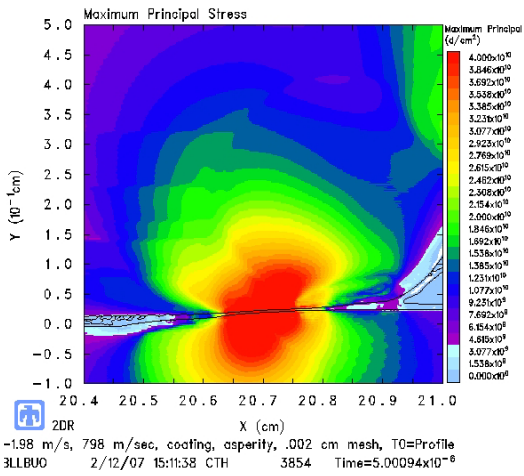
Figure 53 - Maximum Principal Stress for 798 m/s, Asperity, Coating, Initial

Temperature Profile

Asperity, 394 m/s, No Coating

This next case involves the slower speed of 394 m/s case with an asperity, however there is no epoxy coating. The results are shown in Figure 54 and Figure 55. Figure 54 indicates that the maximum temperature is approximately 1520 K, while Figure 55 shows a wear amount of 0.16 cm thick resulting from the maximum principal stress.

76

Just as in the case with this velocity with a coating, there is no appreciable difference at the boundary resulting from the initial temperature profile due to frictional heating. It can be seen in comparing Figure 54 with Figure 56 that the temperature away from the boundary is elevated due to the profile, but this appears to not affect the wear or maximum temperature.
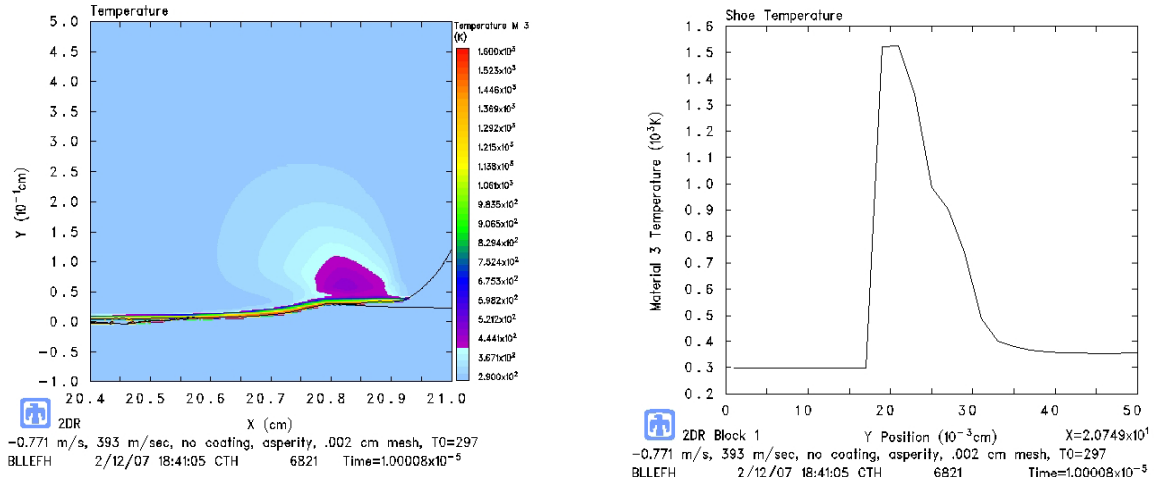
Figure 54 - Temperature for 394 m/s, Asperity, No Coating, Initial Ambient Temperature
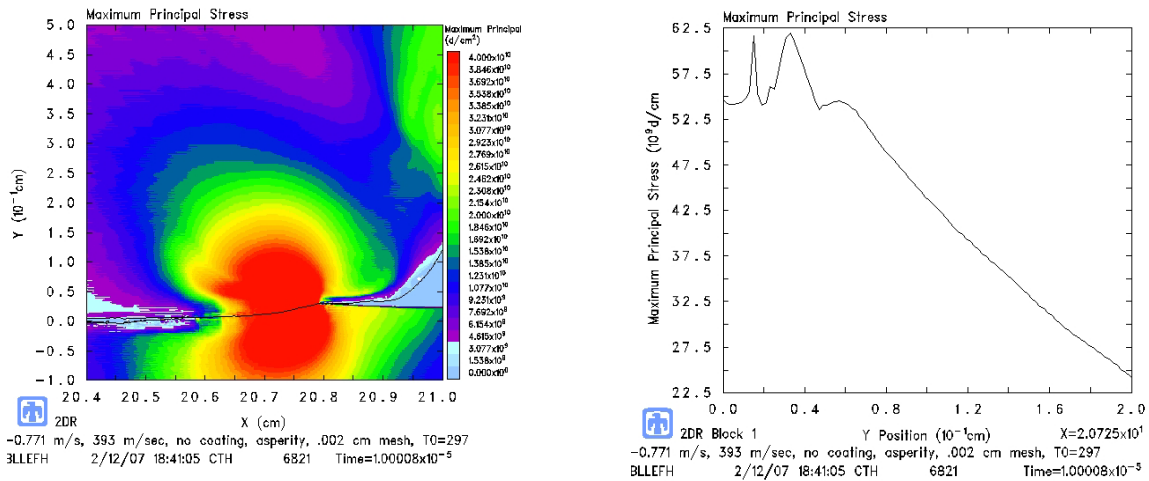
Figure 55 - Maximum Principal Stress for 394 m/s, Asperity, No Coating, Initial Ambient Temperature

77

Figure 56 and Figure 57 are the results for temperature and maximum principal stress when an initial temperature profile is used.
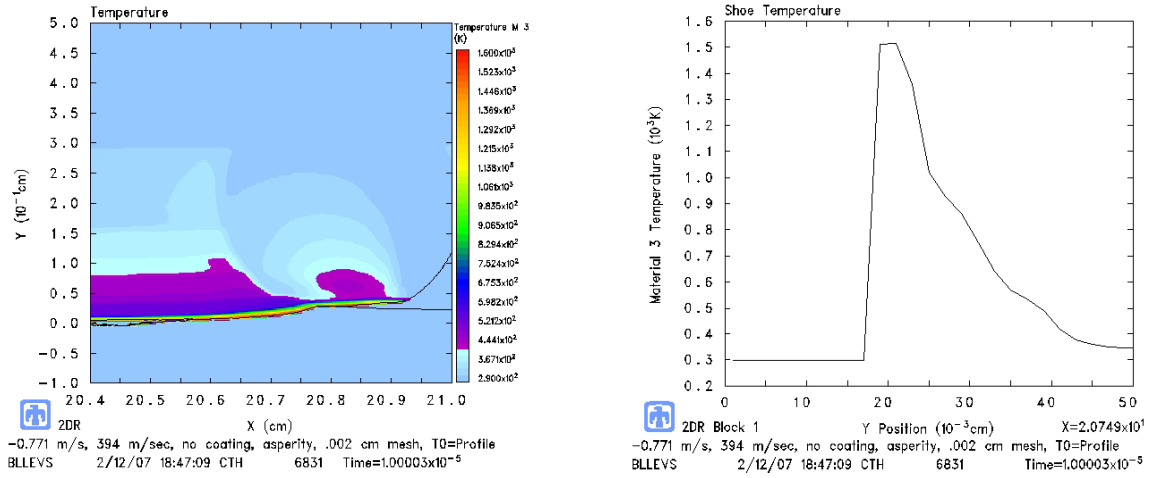
Figure 56 - Temperature for 394 m/s, Asperity, No Coating, Initial Temperature Profile
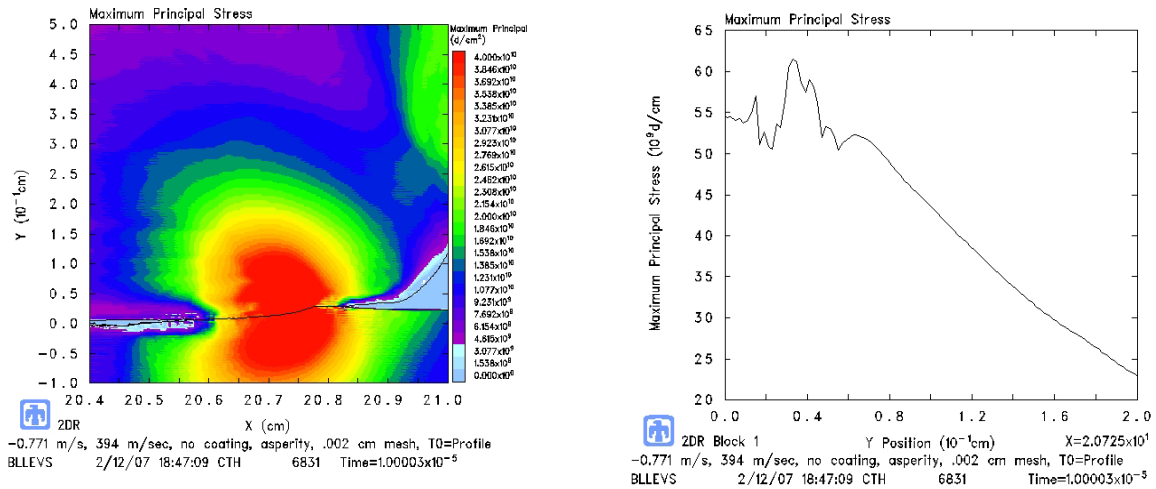
Figure 57 - Maximum Principal Stress for 394 m/s, Asperity, No Coating, Initial Temperature Profile

78

Asperity, 798 m/s, No Coating

The final case in this combination of scenarios is the 798 m/s case with the shoe running into an asperity to initiate wear and no coating on the rail. Figure 58 shows that the temperature reaches a value of approximately 1590 K, the highest temperature of all the scenarios. And the wear as indicated by the maximum principal stress being greater than the fracture stress shows a value of 0.23 cm (Figure 59).
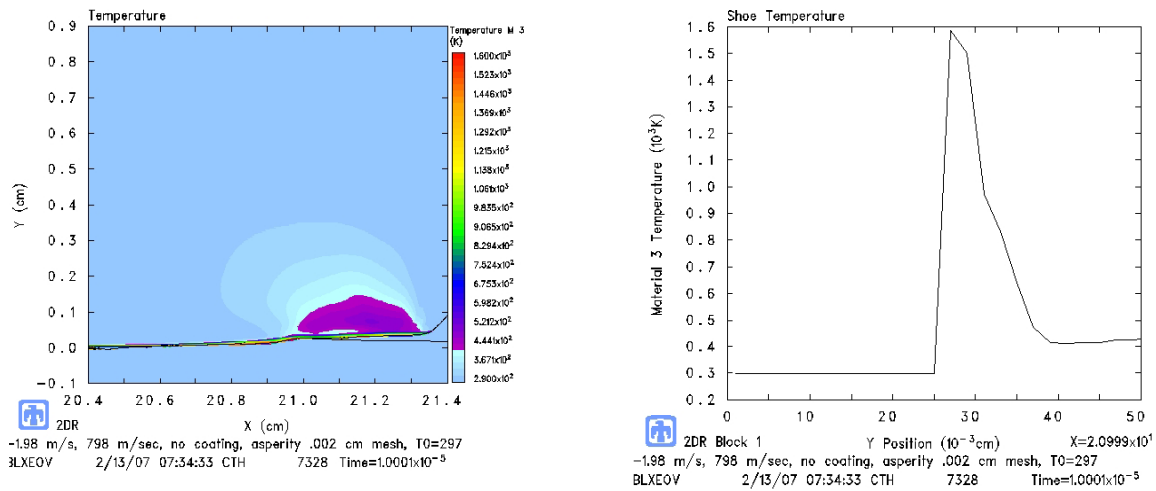
Figure 58 - Temperature for 798 m/s, Asperity, No Coating, Initial Ambient
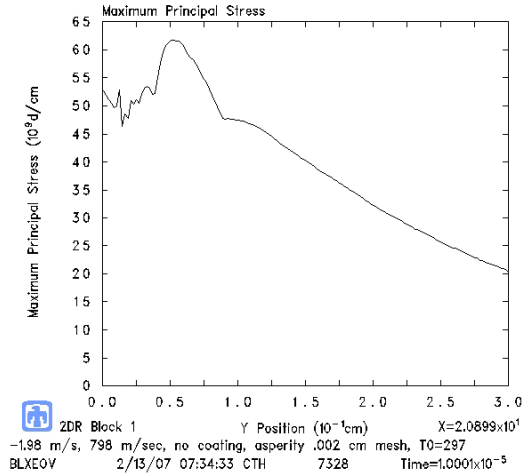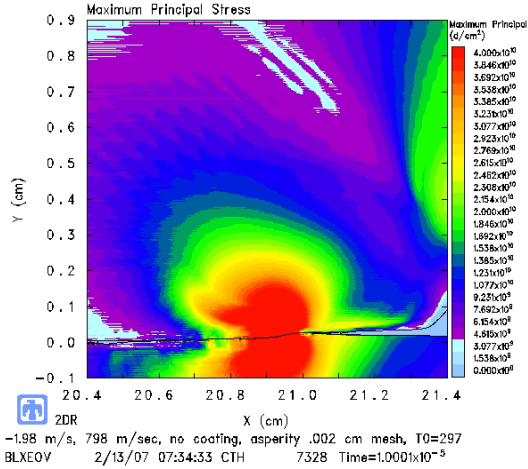
Temperature

Figure 59 - Maximum Principal Stress for 798 m/s, Asperity, No Coating, Initial Ambient Temperature

The temperature profile from frictional heating affected the maximum temperature by reducing it by approximately 100 K to 1500 K, yet it increased the maximum principal stress to 6.4 GPa and increased the wear to 0.24 cm. These effects can be seen in Figure 60 and Figure 61.
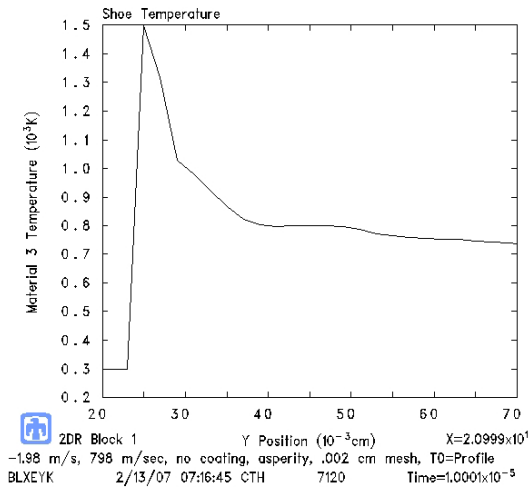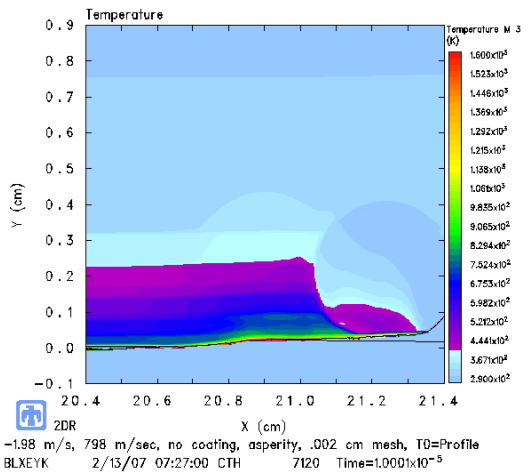
Figure 60 - Temperature for 798 m/s, Asperity, No Coating, Initial Temperature Profile

80
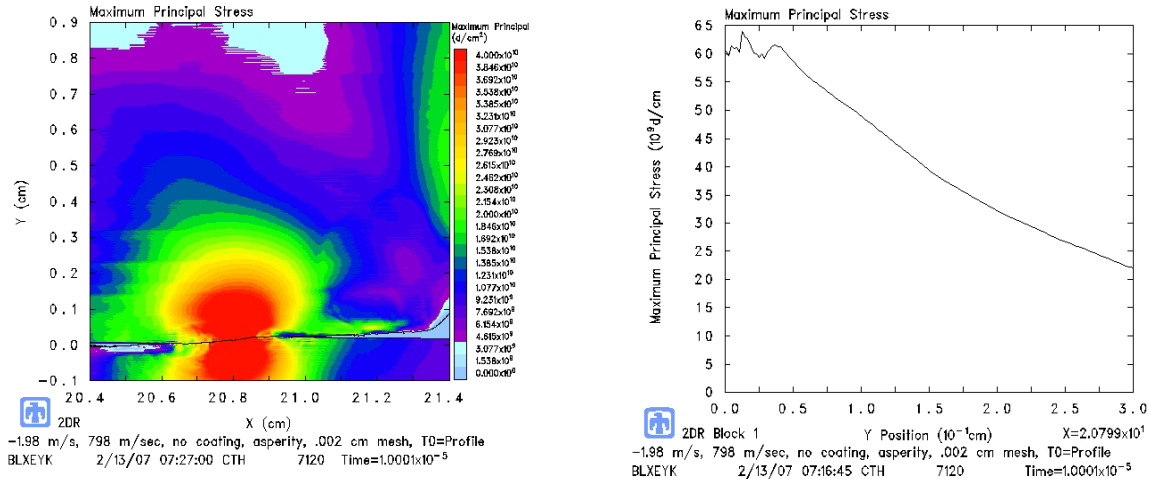
Figure 61 - Maximum Principal Stress for 798 m/s, Asperity, No Coating, Initial Temperature Profile

Asperity, 1,411 m/s, No Coating

One final case was conducted to determine if melt would occur if the horizontal velocity were increased. This case was simulated at ambient temperature only. Figure 62 and Figure 63 respectively show the results for temperature and maximum principal stress. The melt temperature was not reached; in fact the maximum temperature was 1540 K, which was less than the similar case run at 798 m/s. On the other hand, the depth into the shoe that the maximum principal stress exceeded the fracture strength was significantly higher than all of the preceding cases. That thickness was 0.37 cm. Figure 62 also shows behavior similar to gouging in that a mass of material is flowing toward the rear of the shoe, however there is no mixing with the rail that would indicate gouging. If the simulation were to continue, it would be expected that this mass would generate a wear particle.

81
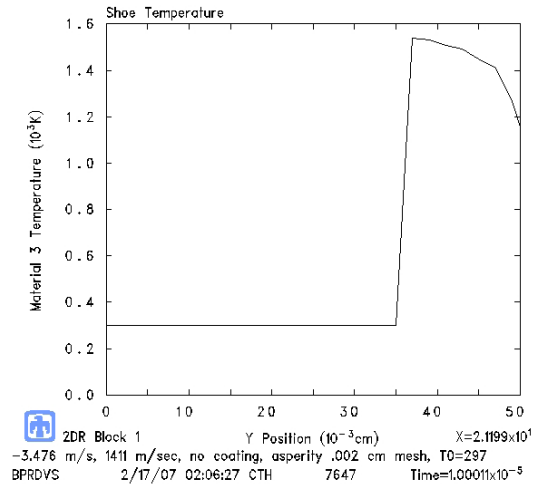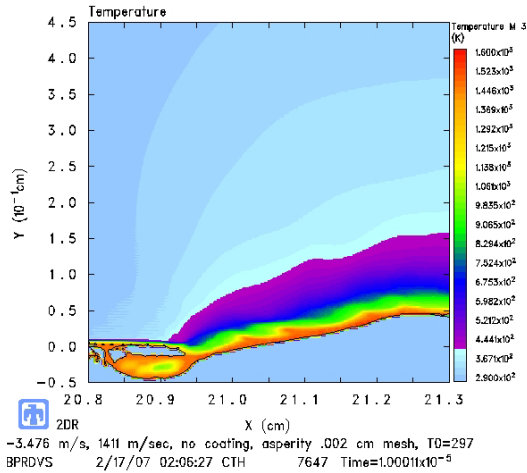
Figure 62 - Temperature for 1,411 m/s, Asperity, No Coating, Initial Ambient
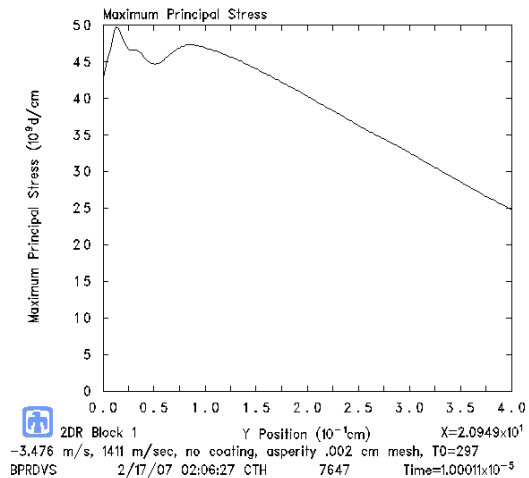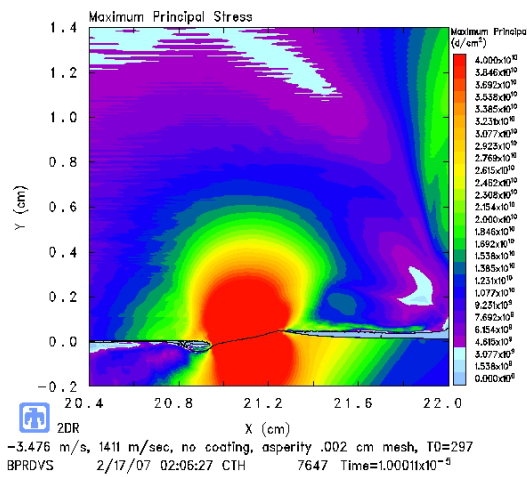
Temperature

Figure 63 - Maximum Principal Stress for 1,411 m/s, Asperity, No Coating, Initial

Ambient Temperature

Table 7 is a list of the results from the 17 numerical cases simulated in CTH. Listed are the maximum temperatures, maximum value for the maximum principal stresses and the corresponding wear amounts, if any occurred. It should be noted that the wear values listed in Table 7 are not material removal amounts. They simply characterized the depth at which the maximum principle stress exceeded the fracture

82

strength. Therefore, these values cannot be compared to the values in Table 6, which

represented a uniform amount of material removed from the bottom of the shoe.

Table 7 - Numerical Wear Results from CTH

				Max Temperature (K)	Melt Wear (cm)	Max Principal Stress (GPa)	Wear (cm)
Flat Rail	394 m/s	Coating	Ambient	329	–	1.4	–
			Profile	533	–	0.9	–
		No Coating	Ambient	1500	–	–	–
			Profile	1510	–	–	–
	798 m/s	Coating	Ambient	425	–	1.25	–
			Profile	775	–	1.25	–
		No Coating	Ambient	1520	–	–	–
			Profile	1500	–	–	–
Asperity	394 m/s	Coating	Ambient	1500	–	6.0	0.08
			Profile	1500	–	6.0	0.08
		No Coating	Ambient	1520	–	6.2	0.16
			Profile	1520	–	6.2	0.16
	798 m/s	Coating	Ambient	1580	–	6.7	0.13
			Profile	920	–	5.2	0.14
		No Coating	Ambient	1590	–	6.2	0.23
			Profile	1500	–	6.4	0.24
Asperity	1411 m/s	No Coating	Ambient	1500	–	5.0	0.37

83

IV. Conclusion

The first and most obvious conclusion is that melt wear, for the 17 cases studied, was never generated in CTH because the shoe material, VascoMax 300, never reached its melt temperature of 1685 K. It was originally thought that the application of a frictional heating would aid the shoe in reaching elevated temperatures when in fact it did very little at the interface. This is most likely due to the fact that the initial temperatures changed the shoe properties, i.e. thermal softening, enough so that less heat was generated due to plasticity. In other words, because the material was thermally softened at the beginning of the simulation, less energy was required to plastically deform the material, and therefore less energy in the form of heat was generated.

The second and also obvious conclusion is that the flat rail simulations neither generated melt wear nor did it generate wear in terms of material failure. In fact it might be fair to suggest that the values for maximum principal stress acquired from all of the simulations on the flat rail were of little use. In terms of CTH, sliding the shoe on the flat rail results in producing mostly shearing stresses. Looking back at Figure 36 and Figure 39 shows that the maximum principal stress values are not even at the interface. It is not until there is some type of impact, such as with an asperity, that reasonable values for principal stresses contribute to wear.

In reality, using an asperity in CTH is a matter of practicality. At the track there are rail seams approximately every 15 m (50 ft). One could statistically determine how many asperities a sled would encounter at a given speed if only 25% of these seams, for example, had a wear producing asperity (still yet to be determined). A technique that

84

estimates the number of these asperities encountered for a given run could be employed to determine the total wear for that run.

Previous research determined that gouging is initiated by asperities. Keeping the asperities below the critical values for gouging, as determined by Cinnamon, may not be enough to eliminate wear generation at those asperities as mentioned in the introduction.

The presence of the epoxy coating, especially in the cases without the asperity, significantly reduces the interface temperature. This occurs because the yield strength of the epoxy is lower than the yield strength of either the steel rail or the VascoMax 300 shoe. The cells at the interface are therefore weaker with the epoxy and require less energy to meet the no-slide criteria mentioned in chapter two. In effect, adding the epoxy lowered the coefficient of friction. In the case with the asperity, the coating also reduces the interface temperature but to a much lesser degree than the flat rail.

Finally, the values for wear that were achieved using the asperity, 0.03 cm in height and 10 degrees, are not consistent with wear values produced by the DADS analytical integration technique, nor are they realistic for a 10 microsecond period of time. However it is conceivable, with the use of the asperity, perhaps even a smaller one, that these simulations could encompass a larger duration of the run than the 10 microseconds in real time, in which case the wear in Table 7 would be more reasonable.

Additionally, these wear values were measured at one location near the front of the shoe, more specifically, at the contact point of the shoe and the asperity. This measurement of wear depth should be distributed over the entire length of the shoe, which would reduce the thickness to a more realistic value.

As demonstrated, CTH can be used to show wear due to material failure, however quantifying the wear in relation to real-time is difficult because the simulations run for such a short period of time. The author is confident that future research in this area can result in realistic and quantifiable wear values due to material failure as well as melting.

Future Research

It has been conveyed that wear is a complicated problem to understand and therefore difficult to model. Areas of future research should include attempting to correlate wear predicted by the analytical model and wear generated by CTH. It may be reasonable to adjusting the parameters studied here to a practical dimension, namely the asperity height, to find the values which produce wear in amounts that match the analytical model and even real track samples. By carefully choosing more scenarios in combinations of vertical and horizontal velocities (in accordance with DADS), asperity height and angle, initial temperature, and coating, it is conceivable that a function could be established to accurately determine wear for the entire sled run.

One of the big assumptions made in this research was with respect to the mass of the sled. For simplification, it was assumed that the entire sled mass could be evenly divided among the four shoes, and in addition, that mass would be constant through the run. In fact, the mass of the model used in CTH was never varied. All simulations, regardless of velocity, used one quarter of the entire sled mass. A quick check was performed, after the fact, to see if the change in momentum over time would be equal to the vertical force supplied by DADS using the equation

$$F_N = \frac{m(v_{v_2} - v_{v_1})}{t_2 - t_1} \qquad (28)$$

The results from this procedure were revealing. Orders of magnitude separate the two

normal force values in some intervals, while others correlated very well. In reality the

sled is pitching and rolling, and this calculation confirms it. These effects can actually be

seen in the DADS file if all four shoes are examined together. As the forces increase on

the front shoes, the forces on the rear shoes decrease indicating the sled might be pitching

forward. This suggests that the mass as well as the vertical and horizontal velocities need

to be unique input parameters for each CTH simulation.

Another area for future research concentration, as alluded to in the conclusions, is

attempting to statistically characterize the entire sled run in terms of shoe/rail contacts.

Figure 15 shows these contacts over a brief time period. If these events could be

examined for the entire run and categorized by force, duration/distance traveled and/or

velocity and quantified in a histogram of sorts, then selected CTH simulations could be

executed that adequately represent each category of contact. The results from that run

could then be multiplied by the number of contacts and summed for the entire run.

DADS does not currently perform such calculations, however an algorithm could be

easily generated in MATLAB.

With regard to the analytical model and the development of k_A from equation

(17), a refined range of k_A as a function of Pv should be examined. As mentioned, the

range of Pv for the shoe was 0 to 35 GPa m/s however almost 96% of the Pv values for

the shoe are less than 4.2 GPa m/s. The average Pv value for the entire run was 0.57 GPa

m/s which is not as telling considering all of the zero values (when there is not contact

87

between the shoe and the rail) included in this average. The emphasis however is on refining the range on which the k_A values were established. This would give a better approximation of the analytical wear. On the same note, the function for the coefficient of friction may need to be revisited to reduce its value in the lower Pv range (see Figure 20).

The models used for the DADS integration technique were based on the pin-on-disk geometry. These models may need to be modified and adapted to the shoe and rail system. More specifically, the pin radius, r_0, doesn't easily translate to the shoe. This research used a value of 5.08 cm (2 in), half the width of the shoe. A more appropriate value, based on the ratio of areas, would have been 8.10 cm (2.19 in). Also, as previously mentioned, a two dimensional heat transfer analysis may prove to be beneficial as well as considering the effects of using material properties that vary with changing temperature.

With regard to melt wear, additional work should be explored concerning the concept of flash temperatures at the interface of the shoe and the rail. This is the extreme temperature that occurs on the microstructure level where the surface asperities contact. The melt equation along with the α variable for heat distribution between the shoe and rail should be more closely examined and better understood.

For the cases studied, CTH did not produce temperatures above the melting point for VascoMax 300, suggesting that melt wear did not occur for the cases studied. Additionally, the heat transfer model did not achieve melting either, at least up to 1,411 m/s. On the other hand, the Lim and Ashby wear model produces melt wear for the entire sled run (see Figure 21) based on equation (11). This could be that both CTH and

88

the heat transfer models' cell sizes and finite differencing meshes are not small enough to detect these high flash temperatures that occur very close to the boundary.

Oxidation-dominated wear was briefly addressed in this paper. Recall that the values were unrealistically large when computed for the Montgomery data. This mechanism of wear may be a significant contributor to the overall amount of wear that takes place. In chapter two, an equation representing a model for oxidation wear was given for the pin-on-disk scenario, however it was neither explained nor examined beyond calculating oxidation wear for the DADS data.

Finally, wear, as mentioned several times, is complex. The scenario at Holloman adds to the complexity due to the speed and bouncing effects. This will not be a problem that is easily modeled in any fashion. Reliance on empirical techniques will, without a doubt, prove to be advantageous in this effort. In light of that, it may be beneficial to construct a test setup similar to the pin-on-disk and connect the pin to an actuator that can execute an input function that mimics a particular DADS file in terms of vertical velocities and forces.

```matlab
%%%%%%%%%%%%%%%%%%%%%%%%%%%%%%%%%%%%%%%%%%%%%%%%%%%%%%%%%%%%%%%%%%%%%%%%%
% Script Wear2.m
% Capt Greg Cameron
% Thesis - Winter 2007
% This script reads in the DADS file containing time(t), velocity(v),
% force(f) and vertical velocity(vv).  It also asks the user for a
% velocity to calculate frictional heating up to that input value.
% Then the script:
% - Calculates distance and acceleration and plots
%   along with velocity, vertical velocity, force (Thesis Figure 14-15)
% - Plots points vertical and horizontal velocities
%   vs time used in CTH runs                       (Thesis Figure 31)
% - Calculates coefficient of friction            (Thesis Figure 20)
% - Calculates wear from Lim and Ashby equations for
%   melt and "mechanical" wear from kA found in
%   montgomery.m script using Archard's equation   (Thesis Figure 21)
% - Calls Melt2.m to plot melt wear vs Lim and
%   Ashby model                                    (Thesis Figure 27-28)
% - Calculates the melt and mechanical wear thickness
%   by integrating as well as the heat flux        (Thesis Figure 22)
% - Calls Heat2.m to solve differential heat equation
%   to find temperature profile in the shoe from the
%   heat flux boundary condition                   (Thesis Figure 32-33)
%%%%%%%%%%%%%%%%%%%%%%%%%%%%%%%%%%%%%%%%%%%%%%%%%%%%%%%%%%%%%%%%%%%%%%%%%
%
clc
clear all
close all
warning off all
format long

% Prompt user to input ending velocity in m/s
velocity = input('Input Velocity in m/s:\n\n');

% Definition of Constants
Width = 4;               %Shoe Width                            in
Length = 8;              %Shoe Length                           in
An = Width*Length;       %Nominal Contact Area                  in^2
r0 = 2;                  %Radius of Nominal Contact Area        in
a = .006993; %.014105;   %Thermal Diffusivity  (Vascomax)       in^2/s
H = 1.45e5;              %VascoMax Hardness                     psi
beta = 6;                %Numerical Constant                    -
T0 = 535;    %522        %Sink Temperature (522 Lim/Ashby)      R
Tstar = 264;             %=aH/K                                 R
Tm = 3033;               %Melting Point for VascoMax (1685 K)   R
L = 3.05e5;              %Latent heat of melting for steel      psi
lb = .04;                %                                      in
KA_mild = 5e-5;          %Archard's Coefficient for mild wear   -
KA_severe = 5e-3;        %Archard's Coefficient for severe wear -
K = 0.5;                 %Fraction of heat transfer             -
mass_DADS = 1854/4;      %From Holloman on 18 Jan 07            lbm
```

```matlab
%file=['I:\My Documents\Thesis\DADS.txt'];
file=['z:\Greg\Work\Air Force\AFIT\Thesis\MATLAB\DADS3x.txt'];

% time(s),velocity(in/s),force(lbf),vertical velocity (in/s)
[t,v,f,vv] = textread(file,'%f %f %f %f');
% Convert v and vv to ft/s
v=v/12;
vv=vv/12;
n = size(t,1);

%Calculate the distance for each step by integrating the velocity
d(1)=0;
accel(1)=0;
for i=2:n
    d(i)=d(i-1)+(v(i)+v(i-1))*(t(i)-t(i-1))/2;          %In feet
    accel(i)=(v(i)-v(i-1))/(t(i)-t(i-1));
end

% Convert to SI units
d_SI=d*.30498;
v_SI=v*.30498;
vv_SI=vv*.30498;
accel_SI=accel*.30498;
f_SI=f*4.448;

%%%%%%%%%%%%%%%%%%%%%%%%%%%%%%%%%%%%%%%%%
% Plot dynamics of the entire sled run  %
%%%%%%%%%%%%%%%%%%%%%%%%%%%%%%%%%%%%%%%%%
figure(1)                                          %Thesis figure 14-15
set(gcf,'Color','w')
subplot(4,2,1);  plot(t,d_SI,'b');ylabel('Distance (m)');
                                xlabel('Time (s)');
                                xlim([0 2.5]);%ylim([4767 4844]);
subplot(4,2,2);  plot(t,v_SI,'b');ylabel('Velocity (m/s)');
                                xlabel('Time (s)');
                                xlim([0 2.5]);ylim([0 3000]);
                                %ylim([6292 6296]);
subplot(4,2,3:4);plot(t,accel_SI,'b');ylabel('Acceleration (m/s^2)');
                                     xlabel('Time (s)');
                                     xlim([0 2.5]);ylim([0 2438]);
subplot(4,2,5:6);plot(t,vv_SI,'b');ylabel('Vertical Velocity (m/s)');
                                 xlabel('Time (s)');
                                 xlim([0 2.5]);ylim([-3 3]);
                                 %xlim([.3 .32]);ylim([-1.5 3]);
subplot(4,2,7:8);plot(t,f_SI,'b');ylabel('Vertical Force (N)');
                                xlabel('Time (s)');
                                xlim([0 2.5]);
                                %xlim([.3 .32]);

%%%%%%%%%%%%%%%%%%%%%%%%%%%%%%%%%%%%%%%%%%%%%%%%%%%%%%%%%%%%%%%%%%%%%%%%%
% Plot Velocity and vertical velocity vs time showing points         %
% considered in CTH Modeling                                         %
%%%%%%%%%%%%%%%%%%%%%%%%%%%%%%%%%%%%%%%%%%%%%%%%%%%%%%%%%%%%%%%%%%%%%%%%%
figure(2)                                          %Thesis Figure 31
set(gcf,'Color','w')
```

91

```matlab
subplot(2,1,1);plot(t,v_SI,'b');ylabel('Down Track Velocity (m/s)');
                               xlabel('Time (s)');%xlim([.08 .2]);
hold on
plot(.31,394.0634,'ro');hold on
plot(.6298,797.5336,'ro');hold on
plot(1.1226,1410.8598,'ro')
text(.29,800,'A')
text(.61,1200,'B')
text(1.1,1816,'C')

subplot(2,1,2);plot(t,vv_SI,'b');ylabel('Vertical Velocity (m/s)');
                               xlabel('Time (s)');%xlim([.08 .2]);
hold on
plot(.31,-.7714,'ro');hold on
plot(.6298,-1.98330,'ro');hold on
plot(1.1226,-3.47610,'ro')
text(.32,-2,'A')
text(.66,-3.1,'B')
text(1.15,-4.45,'C')

% Calculate the pressure, pv, Ftil, vtil and pvtil for each step
p=f./An;                        %pressure (psi)
pv=p.*v*1e-6;                   %(psi*ft/s*1e-6)
pv_SI=pv/1e-6*.30498*6.895e-6;  %GPa m/s
Ftil=f./An./H;
vtil=v.*r0./a.*12;
pvtil=Ftil.*vtil;

% Calculate coefficient of friction and plot versus pv
mu=1.5704.*(pvtil).^-.2299;
C=min(mu)-0.02;
mu=mu-C;
Bravo=isnan(mu);
for z=1:n
    if Bravo(z)==1
     mu(z)=0;
    end
end

figure(3)                       %Thesis Figure 20
plot(pvtil,mu,'b.')
ylim([0 0.8])
set(get(gca,'XLabel'),'Interpreter','Latex')
xlabel('$\tilde{P}\tilde{v}$')
ylabel('Coefficient of Friction ( \it\mu\rm)')
set(gcf,'Color','w')

%alpha=1./(2+beta*(pi/8.*vtil).^(.5));
alpha=1./(2+lb*(pi/8/a/r0.*v*12).^(.5));

% Calculate Melt Wear
Wmelt=((Tm-T0)/Tstar*H/L/beta)./vtil.*(alpha.*mu.*Ftil.*vtil*...
      (Tstar*beta/(Tm-T0))-1)*An*12;
Wmelt_SI=Wmelt*53731.6; %in (mm^3/m)
Gamma=isnan(Wmelt);
```

```matlab
Phi=isnan(Wmelt_SI);
for z=1:n
    if Gamma(z)==1
        Wmelt(z)=0;
    end
    if Phi(z)==1
        Wmelt_SI(z)=0;
    end
end

% Calculate Mild and Severe Plastic Wear
Wplas_mild=KA_mild*Ftil*An*12;
Wplas_mild_SI=Wplas_mild*53731.6; %in (mm^3/m)
Wplas_severe=KA_severe*Ftil*An*12;
Wplas_severe_SI=Wplas_severe*53731.6; %in (mm^3/m)

% Determine kA based on experimental Montgomery Data
for j=1:n
    if pv(j)<2.00
            kA(j)=3.534e-3;
        elseif pv(j)>=2.00
        if pv(j)<=15.00
            kA(j)=8.160e-4;
          else
            kA(j)=1.303e-3;
        end
    end
end

kA=kA';
W=kA.*Ftil*An*12;
W_SI=W*53721.6;

figure(4)                                        %Thesis figure 21
set(gcf,'Color','w')
subplot(2,1,1);plot(d_SI,W_SI,'b',d_SI,Wmelt_SI,'r');
                ylabel('Wear Rate (mm^3/m)');xlabel('Distance (m)');
                legend('\itw_k_A\rm','\itw_m_e_l_t\rm');
                ylim([0 537.6]);xlim([0 3871])
subplot(2,1,2);plot(d_SI,W_SI,'b',d_SI,Wmelt_SI,'r');
                ylabel('Wear Rate (mm^3/m)');xlabel('Distance (m)');
                legend('\itw_k_A\rm','\itw_m_e_l_t\rm');
                ylim([0 268.8]);xlim([575 625])

figure(5)                %Deleted this figure from Thesis
set(gcf,'Color','w')
plot(v_SI,W_SI,'b',v_SI,Wmelt_SI,'r');
                            ylabel('Wear Rate (mm^3/m)');
                            xlabel('Velocity (m/s)');
                            legend('\itw_k_A\rm','\itw_m_e_l_t\rm')
                            ylim([0 100]);xlim([350 450])

Melt2                                    %figure(6) - Thesis figure 29-30

% Calculating the Wear Volume for the distance traveled by
```

93

```matlab
% integrating wear rate as a function of distance using the
% trapezoid rule

WearP(1)=0;                 %Total Plastic Wear at step 1 equals 0
WearM(1)=0;                 %Total Mechanical Wear at step 1 equals 0
Power(1)=0;                 %Power as a function of time
i=2;

% Calculate the melt and mechanical wear and heat flux up to the
% velocity specified by the user
while v(i) < velocity/.30498     %Convert input "velocity" to ft/s
    A=d(i-1);
        B=d(i);
        h=(B-A);                 %the distance between to data points
        WearP(i)=WearP(i-1)+(W(i-1)+W(i))*h/2;              %In in^3
        WearM(i)=WearM(i-1)+(Wmelt(i-1)+Wmelt(i))*h/2;
        if mu(i)==Inf
            mu(i)=0;
        end
        Power(i)=K*mu(i)*f(i)*v(i);  %In lbf*ft/s
        time(i)=t(i);               %For plotting purposes
        i=i+1;
end

Flux=Power/An*144;                %In lbf/s/ft

figure(7)                                %Thesis figure 22
set(gcf,'Color','w')
subplot(2,1,1)
Flux_SI=Flux*14.596;
plot(time,Flux_SI,'b')
xlabel('Time (s)')
ylabel('Flux (W/m^2)')
xlim([0 .3])
tf=t(i-1);              %Time were sled reaches input speed
hold on

% Calculate the temperature distribution in the shoe
Heat2(T0,Flux,a,tf,velocity)          %figure(8) - Thesis figure 32-33

fprintf('\nTotal Distance Traveled: %6.3f ft\n', d(i-1))
fprintf('                          or: %6.3f m\n', d(i-1)*.30498)
fprintf('This corresponds to a velocity of: %6.3f m/s\n',...
        v(i-1)*.30498)
fprintf('                          or: %6.3f ft/s\n',v(i-1))
fprintf('The vertical velocity for this speed is:  %6.3f m/s\n',...
        vv(i-1)*.30498)
fprintf('\nTotal Plastic Wear for This Distance is: %12.9f in^3',...
        WearP(i-1))
fprintf('\nThe Reduction in Shoe Height is: %12.9f in',WearP(i-1)/An)
fprintf('\n                          or: %12.9f cm\n',WearP(i-1)/...
        An*2.54)
fprintf('\nTotal Melt Wear for This Distance is: %12.9f in^3',...
        WearM(i-1))
fprintf('\nThe Reduction in Shoe Height is: %12.9f in', WearM(i-1)/An)
```

94

```
fprintf('\n                              or: %12.9f cm\n',...
        WearM(i-1)/An*2.54)
fprintf('\nThis Occurs at Time = %12.9f s\n\n', time(i-1))

return
```

```matlab
%%%%%%%%%%%%%%%%%%%%%%%%%%%%%%%%%%%%%%%%%%%%%%%%%%%%%%%%%%%%%%%%%%%%%%%%%%
% Script Melt2.m
% Capt Greg Cameron
% Thesis - Winter 2007
% This script is called from Wear2.m and does the following:
% - Creates a model for melt wear based on the Lim and Ashby model
%   plots the DADS data that was evaluated for melt wear in Wear2.m
%   and creates a video file to shoe in 3D (Thesis Figures 29-30)
%
%%%%%%%%%%%%%%%%%%%%%%%%%%%%%%%%%%%%%%%%%%%%%%%%%%%%%%%%%%%%%%%%%%%%%%%%%%
% Generating Data to plot contour lines for Lim and Ashby Model
%%%%%%%%%%%%%%%%%%%%%%%%%%%%%%%%%%%%%%%%%%%%%%%%%%%%%%%%%%%%%%%%%%%%%%%%
r0_model=2;
lb_model=.04;
beta_model=6;
An_model=pi*r0_model^2;
X=logspace(-2,8,100);   %This is Vtilde
Y=logspace(-5,5,100);   %This is Ftilde

[XI,YI] = meshgrid(X,Y);

vXY=XI*a*12/r0_model;
muXY=1.5704.*(XI.*YI).^(-.2299);
% C=min(min(muXY))-0.02;
% muXY=muXY-.02;
alphaXY=1./(2+lb_model*(pi/8/a/r0_model.*vXY*12).^(.5));
WmeltXY=((Tm-
T0)/Tstar*H/L/beta_model)./XI.*(alphaXY.*muXY.*YI.*XI*(Tstar*beta_model
/(Tm-T0))-1)*An_model*12;

V=[1e-9 1e-8 1e-7 1e-6 1e-5 1e-4 1e-3];
figure(6)                                   %Thesis Figure 29-30
contour3(XI,YI,WmeltXY,V)
set(gcf,'Color','w')

set(get(gca,'XLabel'),'Interpreter','Latex')
set(get(gca,'XLabel'),'String','$\tilde{v}$')
set(get(gca,'YLabel'),'Interpreter','Latex')
set(get(gca,'YLabel'),'String','$\tilde{F}$')
set(get(gca,'ZLabel'),'Interpreter','Latex')
set(get(gca,'ZLabel'),'String','$\tilde{w}$','FontSize',16,'Rotation',0
)
zlim([1e-9 1e-3])
hold on

plot3(vtil,Ftil,Wmelt,'b.')

set(gca,'ZScale','log')
set(gca,'XScale','log')
set(gca,'YScale','log')
set(gca,'XTick',[.01 .1 1 10 100 1000 10000 100000 1000000 10000000
100000000])
set(gca,'YTick',[.00000001 .0000001 .000001 .00001 .0001 .001 .01 .1 1
10 100 1000])
set(gca,'XMinorGrid','off','YMinorGrid','off','ZMinorGrid','off')
```

96

```matlab
set(gca,'XMinorTick','off','YMinorTick','off','ZMinorTick','off')
ylim([1e-7 1e3])

I=0;
J=90;
set(gca,'View',[I J])
%return
Az=0;
El=90;
KAz=0;       %Gain
KEl=1;       %Gain
mov = avifile('DADS_Melt.avi','FPS',20);
M(i) = getframe(gcf);
mov = addframe(mov,M(i));
for i=1:150
    Az=Az-KAz;
    El=El-KEl;
    if El<61
        KAz=1;
        KEl=0;
    end
    if Az<-109
        KAz=0;
        KEl=0;
    end

    Look=[Az El];
    set(gca,'View',Look);
    M(i) = getframe(gcf);
    mov = addframe(mov,M(i));
end
mov = close(mov);
```

97

```matlab
function []=Heat2(Tf,Flux,alpha,tf,velocity)
%%%%%%%%%%%%%%%%%%%%%%%%%%%%%%%%%%%%%%%%%%%%%%%%%%%%%%%%%%%%%%%%%%%%%%%%%%%%
% Capt Greg Cameron
% Thesis Winter - 2007
% This program solves the one-dimensional heat equation as called from
% Wear2.m and calls CTH_Profile.m to generate the points needed for
% creating the temperature profile in CTH
%%%%%%%%%%%%%%%%%%%%%%%%%%%%%%%%%%%%%%%%%%%%%%%%%%%%%%%%%%%%%%%%%%%%%%%%%%%%
% Tf = Sink Temperature of the sled in Rankin of the sled (Ambient)
% Flux = Flux at the Boundary as a function of time
% alpha = thermal diffusivity in in^2/s
% tf = time required to reach input velocity in seconds

Flux=Flux*.0014594;             %Convert from lbf/s/ft to W/cm^2
k=0.306582;                     %Thermal conductivity of Vmax in W/cm/K
alpha = alpha*2.54^2;           %Converting to cm^2/s - for CTH
Tf=(Tf-459.67-32)*5/9+273.15;   %Converting to Kelvin - for CTH

t0=0;                           %Time = 0
dt=.0001;                       %Time Step

depth=2.5;          %Depth of thermal profile into shoe (cm)
dy=.015;

% Check Stability as determined by ratio r
r=alpha*dt/dy^2;
fprintf('r = %6.3f\n',r)
if r>.5
    fprintf('r should be less than 0.5\n\n')
    return
end

%T(y,t) => Temperature as a function of position(y) and time(t)
t=t0:dt:tf;
N=size(t,2);

y=0:dy:depth;
M=size(y,2);

T(1:M,1)=Tf; %Temp just over the interface at time t=0 (Ambient)
T(M,1:N)=Tf; %Temp far away from the interface for all times (Ambient)

Tzero=T(2,1)+2*dy*Flux(1)/k;
for j=2:N                    %time(t)
    T(1,j)=T(1,j-1)+r*(T(2,j-1)-2*T(1,j-1)+Tzero);
    for i=2:M-1          %position(y)
        T(i,j)=T(i,j-1)+r*(T(i+1,j-1)-2*T(i,j-1)+T(i-1,j-1));
    end
    Tzero=T(2,j)+2*Flux(j)*dy/k;
end

% This goes through and plots the Temperature profile into the shoe as
% a function of time. Note that the last time step may not produce the
% hottest temperature at the boundary due to the changing flux.
figure(8)
```

```matlab
set(gcf,'Color','w')
for k=1:1:j
    Temp=T(:,k);
    plot(y',Temp)
end
hold on

T0=max(max(T));        %This is the maximum over all times - see above
xlim([0 .5]);
%ylim([Tf T0]);
ylim([250 800]);
YT=250:50:800;
set(gca,'YTick',YT)
xlabel('Vertical Distance into the Shoe (cm)')
ylabel('Temperature (K)')

figure(7)
subplot(2,1,2)
plot(t,T(1,:));
xlabel('Time (s)')
ylabel('Temperature (K)')
xlim([0 .33])

% Prepare data and call function to create the output temp profile
% for input into CTH
% Temp ends up being the last column in T(y,t)
CTH_Profile(y',Temp)                    %figure(8) -Thesis figure 32-33

fprintf('\nThe hottest temperature reached was:  %6.2f K\n', T0)
```

```matlab
function []=CTH_Profile(y,T)
%%%%%%%%%%%%%%%%%%%%%%%%%%%%%%%%%%%%%%%%%%%%%%%%%%%%%%%%%%%%%%%%%%%%%%%%%%%%%%
% Capt Greg Cameron
% Thesis - Winter 2007
% This file will analyze the last temperature vs y profile from Heat
% and select the best points for creating a temperature profile in CTH
%
% Inputs:  y is the y position
%          T is the temperature at that y position
% The temperature exponentially decays with y position so we only need
% to take points that change significantly

% first look at the total temperature difference from y=0 to y=endpoint

% y=0:100;
% T=200:-2:0;
K=11604.5;          %Constant for converting from Kelvin to eV for CTH
N=size(y,1);
T0=T(1);
Tf=T(N);
[C,I]=max(T);       %Find the Maximum temperature
DeltaT=C-Tf;        %it may not be at the boundary

% First Row of the Temperature Profile for CTH
CTH(1,:)=[y(1) T(1) T(1)/K];

Q=2;     %Now fill in the remaining rows until we get to Tf

% Take points at 1-Pct% of previous Temperature point.
Pct=0.93;   %Only need to change this variable
            %(.93 for 394.1 m/s and 798 m/s)
D=1-Pct;
Point=Pct*C;
for i=2:N
    if T(i)<Point
        CTH(Q,:)=[y(i) T(i) T(i)/K];
        Q=Q+1;
        Pct=Pct-D;
        Point=Pct*C;
        if Point<Tf+0.1
            while T(i)>Tf+0.1
                i=i+1;
            end
            CTH(Q,:)=[y(i) T(i) T(i)/K];
            break
        end
    end
end

figure(8)                               %Thesis figures 32 and 33
plot(CTH(:,1),CTH(:,2),'k.')
save CTH.out CTH -ASCII
```

100

```matlab
%%%%%%%%%%%%%%%%%%%%%%%%%%%%%%%%%%%%%%%%%%%%%%%%%%%%%%%%%%%%%%%%%%%%%%%
% Script Montgomery.m
% Capt Greg Cameron
% Thesis - Winter 2007
% This script reads in the data from the Montgomery pin-on-disk
% experimentation table 10.  Specifically it reads in velocity,
% pressure, mu, distance, wear.  Then the script:
% - Calculates wear from the Lim and Ashby equations for melt
%   wear and both mild and severe plastic wear.    (Thesis Figure 16)
% - Calculates kA for three discrete ranges of Pv   (Thesis Figure 17)
% - Recalculates "mechanical" wear from new kA      (Thesis Figure 18)
% - Plot experimental coefficient of friction with
%   curve fit and adjusts the curve to approach 0.02
%   for the Pv range                                (Thesis Figure 19)
%
% Values are provided in English as well as SI units.  Variables with
% SI units are denoted with the SI suffix in the name.
%%%%%%%%%%%%%%%%%%%%%%%%%%%%%%%%%%%%%%%%%%%%%%%%%%%%%%%%%%%%%%%%%%%%%%%

clc
clear all
close all

warning off all
format long

% Definition of Constants
An = .00502655;          %Nominal Contact Area                 in^2
r0 = .04;                %Radius of Nominal Contact Area       in
a = .014105;             %Thermal Diffusivity  (Steel)         in^2/s
H = 1.45e5;              %Steel Hardness                       psi
beta = 6;                %Numerical Constant                   -
T0 = 535;                %Sink Temperature (522 Lim/Ashby)     R
Tstar = 400;             %=aH/K                                R
Tm = 3240;               %Melting Point for Steel    (1800 K)  R
L = 3.05e5;              %Latent heat of melting for steel     psi
lb = .04;                %Linear diffusion distance into pin   in
KA_mild = 5e-5;          %Archard's Coefficient for mild wear  -
KA_severe = 5e-3;        %Archard's Coefficient for severe wear -

%file=['I:\My Documents\Thesis\DADS.txt'];
file=['z:\Greg\Work\Air Force\AFIT\Thesis\MATLAB\Mont5.txt'];

% velocity(ft/s),pressure(psi),(-),distance(ft),wear(in^3/ft*1e-7)
[v,p,mu,d,Wexp]=textread(file,'%f %f %f %f %f');
Wexp=Wexp*1e-7;
Wexp_SI=Wexp*53731.6;                 %Convert to SI units (mm^3/m)
n=size(v,1);

pv=p.*v*1e-6;                         %(psi*ft/s*1e-6)
pv_SI=pv/1e-6*.30498*6.895e-6;        %(GPA m/s)
Ftil=p/H;
vtil=v.*r0./a.*12;
Pvtil=Ftil.*vtil;
```

101

```matlab
% Calculate alpha for melt wear equation
%alpha=1./(2+beta*(pi/8.*vtil).^(.5));
alpha=1./(2+lb*(pi/8/a/r0.*v*12).^(.5));

% Calculate Melt Wear
Wmelt=((Tm-T0)/Tstar*H/L/beta)./vtil.*(alpha.*mu.*Ftil.*vtil*...
      (Tstar*beta/(Tm-T0))-1)*An*12;
Wmelt_SI=Wmelt*53731.6;

% Calculate Mild Plastic Wear
Wplas_mild=KA_mild*Ftil*An*12;
Wplas_mild_SI=Wplas_mild*53731.6;

% Calculate Severe Plastic Wear
Wplas_severe=KA_severe*Ftil*An*12;
Wplas_severe_SI=Wplas_severe*53731.6;

% Plot the 3 wear equations with experimental versus Pv
figure(1)                          % Thesis Figure 16
%plot(pv,Wexp,'b.',pv,Wplas_mild,'c.',pv,Wplas_severe,'g.',pv,...
%      Wmelt,'r.')
plot(pv_SI,Wexp_SI,'b.',pv_SI,Wplas_mild_SI,'c.',pv_SI,...
     Wplas_severe_SI,'g.',pv_SI,Wmelt_SI,'r.')
legend('Experimental','Mild Plastic','Severe Plastic','Melt')
%ylim([0 3e-5])
ylim([0 1.6])
%xlabel('\itPv\rm (psi ft/s x 10^-^6)')
xlabel('\itPv\rm (GPa m/s)')
%ylabel('Wear Rate (in^3/ft)')
ylabel('Wear Rate (mm^3/m)')
set(gcf,'Color','w')

%%%%%%%%%%%%%%%%%%%%%%%%%%%%%%%%%%%%%%%%%%%%%%%%%%%%%%%%%%%%%%%%%%%%%%%
% Solve for kA using empirical data
%%%%%%%%%%%%%%%%%%%%%%%%%%%%%%%%%%%%%%%%%%%%%%%%%%%%%%%%%%%%%%%%%%%%%%%
kA=H/An*(Wexp./p)/12;

% This is for kA_adjust3e.  If kA is out the limits set by Lim and
% Ashby, manually bring it back to the limit
for i=1:n
    kA_adj(i)=kA(i);
    if kA(i)>5e-3
        kA_adj(i)=5e-3;
    end
end

% This is for kA_averaged.  Define 3 arbitrary regions of Pv, average
% over the three regions.
kA_avg_1=0;
kA_avg_2=0;
kA_avg_3=0;
count1=0;
count2=0;
count3=0;
for j=1:n
```

102

```matlab
        if pv(j)<2.00
                kA_avg_1=kA_avg_1+kA_adj(j);
                count1=count1+1;
        elseif pv(j)>=2.00
            if pv(j)<=15.00
                kA_avg_2=kA_avg_2+kA_adj(j);
                count2=count2+1;
            else
                kA_avg_3=kA_avg_3+kA_adj(j);
                count3=count3+1;
            end
        end
end

% These are the 3 discrete values for kA as a function of Pv.
for m=1:n
    if pv(m)<2.00
            kA_avg(m)=kA_avg_1/count1;
    elseif pv(m)>=2.00
        if pv(m)<=15.00
            kA_avg(m)=kA_avg_2/count2;
        else
            kA_avg(m)=kA_avg_3/count3;
        end
    end
end

kA_of_Pv_1=kA_avg_1/count1;
kA_of_Pv_2=kA_avg_2/count2;
kA_of_Pv_3=kA_avg_3/count3;

% Plot the 3 series in solving for kA from experimental data
figure(2)                               % Thesis Figure 17
%plot(pv,kA,'b.',pv,kA_adj,'ro',pv,kA_avg,'g.')
plot(pv_SI,kA,'b.',pv_SI,kA_adj,'ro',pv_SI,kA_avg,'g.')
%xlabel('\itPv\rm (psi ft/s x 10^-^6)')
xlabel('\itPv\rm (GPa m/s)')
ylabel('\itk_A\rm')
legend('\itk_A\rm','\itk_A\rm adjusted','\itk_A\rm averaged')
set(gcf,'Color','w')

% Now recalculate the wear with the newly established kA_Average
Wnew=kA_avg'.*p*12*An./H;
Wnew_SI=Wnew*53731.6;
figure(3)                               % Thesis Figure 18
%plot(pv,Wexp,'b.',pv,Wnew,'g.')
plot(pv_SI,Wexp_SI,'b.',pv_SI,Wnew_SI,'g.')
%xlabel('\itPv\rm (psi ft/s x 10^-^6)')
xlabel('\itPv\rm (GPa m/s)')
%ylabel('Wear Rate (in^3/ft)')
ylabel('Wear Rate (mm^3/m)')
set(gcf,'Color','w')
legend('Experimental','New \itk_A\rm')

%%%%%%%%%%%%%%%%%%%%%%%%%%%%%%%%%%%%%%%%%%%%%%%%%%%%%%%%%%%%%%%%%%%%%%
```

103

```matlab
% Looking at the Coefficient of Friction
%%%%%%%%%%%%%%%%%%%%%%%%%%%%%%%%%%%%%%%%%%%%%%%%%%%%%%%%%%%%%%%%%%%%%%%%%%%
xdata=10:8000;
mu_func1=1.5704.*(xdata).^-.2299;
C=min(mu_func1)-0.02;
mu_func2=mu_func1-C;
figure(4)                                    % Thesis Figure 19
set(gcf,'Color','w')
plot(Pvtil,mu,'b.',xdata,mu_func1,'r',xdata,mu_func2,'g')
ylim([0 1.4])
set(get(gca,'XLabel'),'Interpreter','Latex')
xlabel('$\tilde{P}\tilde{v}$')
ylabel('Coefficient of Friction ( \it\mu\rm)')
legend('Montgomery','$\mu = f(\tilde{P}\tilde{v})$',...
       '$\mu = f(\tilde{P}\tilde{v})^*$')
set(legend,'Interpreter','Latex')

text('Interpreter','Latex','string',...
     '$\mu = 1.5704(\tilde{P}\tilde{v})^{-0.2299}$','position',...
     [4000,.5,])
```

104

```matlab
%%%%%%%%%%%%%%%%%%%%%%%%%%%%%%%%%%%%%%%%%%%%%%%%%%%%%%%%%%%%%%%%%%%%%%%%%
% Script Montgomery_Melt.m
% Capt Greg Cameron
% Thesis - Winter 2007
% This script reads in the Montgomery data from table 10 and
% reproduces the Lim and Ashby melt model and plots the Montgomery
% data on that model and then rotates in 3D  (Thesis Figure 28)
%
%%%%%%%%%%%%%%%%%%%%%%%%%%%%%%%%%%%%%%%%%%%%%%%%%%%%%%%%%%%%%%%%%%%%%%%%%
% lb = really affects how this data matches Lim and Ashby
%%%%%%%%%%%%%%%%%%%%%%%%%%%%%%%%%%%%%%%%%%%%%%%%%%%%%%%%%%%%%%%%%%%%%%%%%

clc
clear all
close all

warning off all
format long

%Definition of Constants common for both Lim and Ashby and Montgomery
a = .014105;          %Thermal Diffusivity (Steel)          in^2/s
H = 1.45e5;           %Steel Hardness                       psi
T0 = 527.4;           %Sink Temperature (20 C Lim/Ashby)    R
Tstar = 399.6;        %222 K Lim and Ashby                  R
Tm = 3240;            %Melting Point for Steel              R
L = 3.05e5;           %Latent heat of melting for steel
                      %(Lim and Ashby 2.1e9 J/m^3) - psi

%file=['z:\Greg\Work\Air Force\AFIT\Thesis\MATLAB\Mont5.txt'];
file='Mont5.txt';
%%%%%%%%%%%%%%%%%%%%%%%%%%%%%%%%%%%%%%%%%%%%%%%%%%%%%%%%%%%%%%%%%%%%%%%
% This is for the Montgomery Data
%%%%%%%%%%%%%%%%%%%%%%%%%%%%%%%%%%%%%%%%%%%%%%%%%%%%%%%%%%%%%%%%%%%%%%%
%velocity(ft/s),pressure(psi),(-),distance(ft),wear(in^3/ft*1e-7)
[v,p,mu,d,Wexp] = textread(file,'%f %f %f %f %f');
%Variables used by Montgomery
r0=0.040;
An=r0^2*pi;
lb=0.04;
beta=6;
Wexp=Wexp./An/12*1e-7;
Ftil=p/H;
vtil=v.*r0./a.*12;
%%%%%%%%%%%%%%%%%%%%%%%%%%%%%%%%%%%%%%%%%%%%%%%%%%%%%%%%%%%%%%%%%%%%%%%%%
% Calculate Melt wear from Montgomery using Lim and Asbhy equations
%%%%%%%%%%%%%%%%%%%%%%%%%%%%%%%%%%%%%%%%%%%%%%%%%%%%%%%%%%%%%%%%%%%%%%%%%
alpha=1./(2+lb*(pi/8/a/r0.*v*12).^(.5));
Wmelt=((Tm-T0)/Tstar*H/L/beta)./vtil.*(alpha.*mu.*Ftil.*vtil*...
      (Tstar*beta/(Tm-T0))-1)*An*12;
%%%%%%%%%%%%%%%%%%%%%%%%%%%%%%%%%%%%%%%%%%%%%%%%%%%%%%%%%%%%%%%%%%%%%%%
% Generating Data to plot contour lines for Lim and Ashby Model
%%%%%%%%%%%%%%%%%%%%%%%%%%%%%%%%%%%%%%%%%%%%%%%%%%%%%%%%%%%%%%%%%%%%%%%
r0_model=.04;         %Stated in Table 3 Lim and Ashby r0=1.5 mm
An_model=r0_model^2*pi;
lb_model=.004;
```

```matlab
beta_model=10;
X=logspace(-1,5,100);    %This is Vtilde
Y=logspace(-4,1,100);    %This is Ftilde

[XI,YI] = meshgrid(X,Y);

vXY=XI*a*12/r0_model;
muXY=0.78-0.13*log10(XI);   %Using Lim and Ashby's equation 9
alphaXY=1./(2+lb_model*(pi/8/a/r0_model.*vXY*12).^(.5));
WmeltXY=((Tm-T0)/Tstar*H/L/beta_model)./XI.*(alphaXY.*muXY.*YI.*...
        XI*(Tstar*beta_model/(Tm-T0))-1)*An_model*12;
%%%%%%%%%%%%%%%%%%%%%%%%%%%%%%%%%%%%%%%%%%%%%%%%%%%%%%%%%%%%%%%%%%%%%
% Generate Plot
%%%%%%%%%%%%%%%%%%%%%%%%%%%%%%%%%%%%%%%%%%%%%%%%%%%%%%%%%%%%%%%%%%%%%

s=[1e-7 1e-6 1e-5 1e-4 1e-3];
contour3(XI,YI,WmeltXY,s)

set(get(gca,'XLabel'),'Interpreter','Latex')
set(get(gca,'XLabel'),'String','$\tilde{v}$')
set(get(gca,'YLabel'),'Interpreter','Latex')
set(get(gca,'YLabel'),'String','$\tilde{F}$')
set(get(gca,'ZLabel'),'Interpreter','Latex')
set(get(gca,'ZLabel'),'String','$\tilde{w}$','FontSize',16,'Rotation',0
)

zlim([1e-7 1e-2])
set(gca,'XScale','log')
set(gca,'XTick',[1e-1 1e0 1e1 1e2 1e3 1e4 1e5])
set(gca,'YTick',[1e-4 1e-3 1e-2 1e-1 1e0 1e1])
set(gca,'YScale','log')
set(gca,'ZScale','log')
set(gca,'XMinorGrid','off','YMinorGrid','off','ZMinorGrid','off')
set(gca,'XMinorTick','off','YMinorTick','off','ZMinorTick','off')
set(gcf,'Color','w')
hold on

% Now plot experimental Montgomery Data as points
plot3(vtil,Ftil,Wexp,'b.')
hold on

I=0;
J=90;
set(gca,'View',[I J])

Az=1;
El=91;
KAz=.3;      %Gain
KEl=1;      %Gain
mov = avifile('Montgomery_Melt.avi','FPS',20);
for i=1:155
    Az=Az-KAz;
    El=El-KEl;
    if El<50
        KAz=1;
```

```matlab
        KEl=0;
    end
    if Az<-112
%         KAz=0;
        KEl=-1;
    end

    Look=[Az El];
    set(gca,'View',Look);
    M(i) = getframe(gcf);
    mov = addframe(mov,M(i));
end
mov = close(mov);
```

```
*
*eor* genin
*
*   cthgen input for wear simulation
*
*            _____
*           |        ----->  |
*           |        |       |
*           |        v       /
*    ----------------------------
*
*
*   vx=varies, vy=-1 m/s  V300 Steel Slider, 1080 Steel Rail, No Atm.
*   No Slide line. mix=1 frac=1 Rounded corner.
*   Added mass on top to simulate sled mass
*
```
-1.98 m/s, 798 m/sec, coating, asperity, .002 cm mesh, T0=Profile

```
control
  mmp3       * enable multiple material temps and pressures in each cell
  ep         * enable elastic-plastic computations
  vpsave     * save cell yield stress and plastic strain rate data
endcontrol


*_/_/_/_/_/_/_/_/_/_/_/_/_/_/_/_/_/_/_/_/_/_/_/
* MESH AND BLOCK DEFINITION SET
**********************************************
*   geom=2DR(rectangular x,y)
*   geom=2DC(cylindrical x=radius, y=axis)
*   geom=3DR(rectangular x,y,z)
*   type=e (Eulerian)
*   x#=coordinate range for plot
*   y#=coordinate range for plot
*   dxf=width of first cell in the region
*   dxl=width of last cell in the region
*   n=number of cells added in this region
*   w=total width of this region in centimeters
*   r=ratio of adjacent cell widths
*_/_/_/_/_/_/_/_/_/_/_/_/_/_/_/_/_/_/_/_/_/_/_/

mesh
  block 1  geom=2dr    type=e        * coord for 2D rect Eulerian mesh
    x0 = 0.0000
      x1 w = 15.00 dxf = 1.000 dxl = 0.1
      x2 w = 3.000 dxf = 0.100 dxl = 0.050
      x3 w = 2.400 dxf = 0.050 dxl = 0.002
      x4 w = 1.500 dxf = 0.002 dxl = 0.002
      x5 w = 3.000 dxf = 0.002 dxl = 0.100
      x6 w = 5.100 dxf = 0.100 dxl = 1.000
    endx
    y0 = -4.000
```

108

```
      y1 w = 2.200 dyf = 0.100 dyl = 0.050
      y3 w = 1.000 dyf = 0.050 dyl = 0.002
      y4 w = 1.600 dyf = 0.002 dyl = 0.002
      y5 w = 2.200 dyf = 0.002 dyl = 0.050
      y6 w = 5.000 dyf = 0.050 dyl = 0.100
      y7 w = 41.50 dyf = 0.100 dyl = 1.000
    endy
  endblock
endmesh

insertion of material
  block 1

package rail               * normal level rail height
      material 2
      numsub 100
        temperature = 2.55935e-2 * eV = 74.93F = 297 K
      xvel 0.0
      yvel 0.0
      insert box
         p1 0.0 0.0
        p2 50.0 -4.0
      endinsert
endpackage

package coating    * normal level rail coating
      material 1
      numsub 100
        temperature = 2.55935e-2 * eV = 74.93F = 297 K
        xvel 0.0
      yvel 0.0
      insert box
        p1 0.0 0.0
        p2 50.0 0.01
      endinsert
      delete triangle
        p1 20.46 0.0
        p2 24.0 0.0
        p3 20.63 0.03
      enddelete
endpackage

package coating2
      material 1
      numsub 100
      temperature = 2.55935e-2 * eV = 74.93F = 297 K
      xvel 0.0
      yvel 0.0
      insert triangle
        p1 20.46 0.01
        p2 24.0 0.01
         p3 20.63 0.04
      endinsert
      delete triangle
        p1 20.46 0.0
```

```
      p2 24.0 0.0
      p3 20.63 0.03
    enddelete
endpackage


*This part is for the asperity part of the rail
package rail2
    material 2
    numsub 100
    temperature = 2.55935e-2 * eV = 74.93F = 297 K
    xvel 0.0
    yvel 0.0
    insert triangle    *This should match the delete triangle above.
      p1 20.46 0.0
      p2 24.0 0.0
      p3 20.63 0.03
    endinsert
endpackage

package shoe1           * shoe on normal level rail
    material 3
    numsub 100
    temperature = 6.489e-2 * eV =  753.1 K
     xvel 7.98e+4
     yvel -1.98e+2
     insert box
      p1 0.300, 0.01
      p2 20.62, 0.03
    endinsert
    delete circle
      center 20.42, 0.21
      radius 0.2
    enddelete
    delete box
      p1 20.42, 0.21
      p2 20.62, .01
    enddelete
endpackage

package shoe2           * shoe on normal level rail
    material 3
    numsub 100
    temperature = 5.795e-2 * eV = 672.4 K
     xvel 7.98e+4
     yvel -1.98e+2
     insert box
      p1 0.300, 0.03
      p2 20.62, 0.045
    endinsert
    delete circle
      center 20.42, 0.21
      radius 0.2
    enddelete
    delete box
      p1 20.42, 0.21
```

110

```
        p2 20.62, .01
        enddelete
endpackage


package shoe3          * shoe on normal level rail
        material 3
        numsub 100
        temperature = 5.495e-2 * eV = 637.7 K
         xvel 7.98e+4
         yvel -1.98e+2
         insert box
          p1 0.300, 0.045
          p2 20.62, 0.075
        endinsert
        delete circle
          center 20.42, 0.21
          radius 0.2
        enddelete
        delete box
          p1 20.42, 0.21
          p2 20.62, .01
        enddelete
endpackage

package shoe4          * shoe on normal level rail
        material 3
        numsub 100
        temperature = 4.927e-2 * eV = 571.8.0 K
         xvel 7.98e+4
         yvel -1.98e+2
         insert box
          p1 0.300, 0.075
          p2 20.62, 0.09
        endinsert
        delete circle
          center 20.42, 0.21
          radius 0.2
        enddelete
        delete box
          p1 20.42, 0.21
          p2 20.62, .01
        enddelete
endpackage

package shoe5          * shoe on normal level rail
        material 3
        numsub 100
        temperature = 4.672e-2 * eV = 542.2 K
         xvel 7.98e+4
         yvel -1.98e+2
         insert box
          p1 0.300, 0.090
          p2 20.62, 0.135
        endinsert
```

```
          delete circle
            center 20.42, 0.21
            radius 0.2
          enddelete
          delete box
            p1 20.42, 0.21
            p2 20.62, .01
          enddelete
endpackage

package shoe6             * shoe on normal level rail
          material 3
          numsub 100
          temperature = 4.038e-2 * eV = 468.6 K
           xvel 7.98e+4
           yvel -1.98e+2
           insert box
            p1 0.300, 0.135
            p2 20.62, 0.165
          endinsert
          delete circle
            center 20.42, 0.21
            radius 0.2
          enddelete
          delete box
            p1 20.42, 0.21
            p2 20.62, .01
          enddelete
endpackage

package shoe7             * shoe on normal level rail
          material 3
          numsub 100
          temperature = 3.712e-2 * eV = 430.8 K
           xvel 7.98e+4
           yvel -1.98e+2
           insert box
            p1 0.300, 0.165
            p2 20.62, 0.225
          endinsert
          delete circle
            center 20.42, 0.21
            radius 0.2
          enddelete
          delete box
            p1 20.42, 0.21
            p2 20.62, .01
          enddelete
endpackage

package shoe8             * shoe on normal level rail
          material 3
          numsub 100
          temperature = 3.240e-2 * eV = 375.9 K
           xvel 7.98e+4
```

112

```
        yvel -1.98e+2
         insert box
          p1 0.300, 0.225
          p2 20.62, 0.315
        endinsert
        delete circle
          center 20.42, 0.21
          radius 0.2
        enddelete
        delete box
          p1 20.42, 0.21
          p2 20.62, .01
        enddelete
endpackage

package shoe9           * shoe on normal level rail
        material 3
        numsub 100
        temperature = 2.842e-2 * eV = 329.8 K
         xvel 7.98e+4
         yvel -1.98e+2
         insert box
          p1 0.300, 0.315
          p2 20.62, 0.750
        endinsert
        delete circle
          center 20.42, 0.21
          radius 0.2
        enddelete
        delete box
          p1 20.42, 0.21
          p2 20.62, .01
        enddelete
endpackage

package shoe10          * shoe on normal level rail
        material 3
        numsub 100
        temperature = 2.55935e-2 * eV = 297 K
         xvel 7.98e+4
         yvel -1.98e+2
         insert box
          p1 0.300, 0.750
          p2 20.62, 2.550
        endinsert
        delete circle
          center 20.42, 0.21
          radius 0.2
        enddelete
        delete box
          p1 20.42, 0.21
          p2 20.62, .01
        enddelete
endpackage
```

```
package shoetip
      material 3
      numsub 100
        temperature = 2.55935e-2 * eV = 74.93F = 297 K
      xvel 7.98e+4
      yvel -1.98e+2
      insert circle
         center 20.42 0.21
       radius 0.2
         endinsert
endpackage

package sledsim           * sled mass concentrated on top of shoe
      material 4
      numsub 100
      temperature = 2.55935e-2 * eV = 74.93F = 297 K
      xvel 7.98e+4
      yvel -1.98e+2
      insert box
        p1 0.300, 49.08
        p2 20.62, 2.55
      endinsert
endpackage

endblock
endinsertion

edit
  block 1
  expanded
  endblock
endedit

*_/_/_/_/_/_/_/_/_/_/_/_/
* TRACER DEFINITION SET
*_/_/_/_/_/_/_/_/_/_/_/_/
tracer  4x4 set of points in the bottom of the shoe
  *Bottom Row in shoe
     add 2.84, .010 to 18.08, .010 n=7
     add 2.84, .020 to 18.08, .020 n=7
  *2nd Row
     add 2.84, .060 to 18.08, .060 n=7
  *3rd Row
     add 2.84, .180 to 18.08, .180 n=7
  *4th Row
     Add 2.84, .540 to 18.08, .540 n=7
  *5th Row
     Add 2.84, 40.00 to 18.08, 40.00 n=7
endt

*_/_/_/_/_/_/_/_/_/_/_/_/_/_/_/_/
* EQUATION OF STATE DEFINITION SET
*_/_/_/_/_/_/_/_/_/_/_/_/_/_/_/_/_/

eos          * Sesame tabular option (primary MIG model)
```

114

```
*  MAT1 SES IRON
  MAT1 SES GREPXY1 *for epoxy
  MAT2 SES IRON
  MAT3 SES STEEL_V300
  MAT4 MGR PLATINUM
endeos

epdata            * elastic-plastic data
  vpsave    * cell yield stress and plastic strain rate data is saved
  lstrain   * compute and save Lagrangian strain tensor components
  mix = 3   * vol avg yield strength normalized by sum of vol fractions

  matep = 1         *Epoxy Glider Coating
    poisson 0.46
    yield 1.0e8

  matep = 2 ZE USER     * 1080 Steel rail
    aze = 0.825e10      * dynes/cm^2
    nze = 0.289
    c1ze = 4.0e10       * dynes/cm^2
    c2ze = 0.0
    c3ze = 160.0  * 1/eV
    c4ze = 12.0         * 1/eV
    c5ze = 0.266e10     * dynes/cm^2
    poisson 0.27

  matep = 3 ZE USER     * VascoMax 300 shoe
    aze = 1.42e10       * dynes/cm^2
    nze = 0.289
    c1ze = 4.0e10       * dynes/cm^2
    c2ze = 0.0
    c3ze = 79.0         * 1/eV
    c4ze = 3.0          * 1/ev
    c5ze = 0.266e10     * dynes/cm^2
    poisson 0.283

  matep = 4       * what is this for?
    poisson .2
    yield 10e10

*_____
*
* BL algorithm inputs
*_____
*  blint 1
*    soft 1
*    hard 3
*    csl 1.5
*    cbl 1.5
*    fric 0.3
*    corr
*    nofreeze
*  ende

ende        * end elastic-plastic data
```

```
*************************************************************
*eor* cthin
-1.0 m/s, 100.0 m/sec, coating, .002 cm mesh

*_/_/_/_/_/_/_/_/_/_/_/_/_/_/_/_/_/_/_/_/_/_/_/_/_/_/_/_/_/
*CONTROL DATA SET
*********************************************************
*  mmp enables multiple material temps
*  and pressures in mixed cells
*  frac=1 changes fracture default
*******************************
* CELL THERMODYNAMICS INPUT SET
*******************************
* cellthermo
*  dtmax = max temp difference allowed in mixed cells
*  mmp distributes volume and energy based on volume
*  fractions of material in the cell
*  mmp=default
*  mmp1=same as mmp except uses new logic
*       and distributes volume and energy
*       based on volume fraction cubed divided
*       by mass of material in the cell
*  mmp2=allocation of work done on the cell is
*       dependent on material compressibility
*       and allows pressure relaxation between materials
*       in a cell
* endc
*_/_/_/_/_/_/_/_/_/_/_/_/_/_/_/_/_/_/_/_/_/_/_/_/_/_/_/_/_/


control
  mmp3      * allocates PdV work done between materials of a mixed cell
  tstop = 10.00E-6      * stop criteria - total simulation time
  nscycle = 55000 * maximum number of cycles to be run
  rdumpf = 991800.      * time for back-ups of restart file updates
  cpshift = 600.  * time left when normal termination procedure begins
  ntbad = 99999999
  dtcourant = 0.6 * Courant condition multiplier
  ygravity=-980      * Acceleration due to gravity
endc

Convct                   * enable convection of internal energy
  convection = 1  * use int energy slope and mass density, discard KE
residual
  interface = high_resolution * scheme for interface tracker
endc

fracts                   * enable fracture data (dynes/cm^2)
*pfrac1 = -0.5e7        * fracture stress or pressure for nth material
pfrac1 = -1.0e8
pfrac2 = -2.0e10
pfrac3 = -2.5e10
pfrac4 = -1.2e10
pfmix = -1.20e10   * fract stress or pressure in a cell with no voids
```

```
pfvoid = -1.20e10 * fract stress or pressure in a cell with a voids
endfracts

edit
  shortta          * short edits based on time
    time = 0.0   , dt = 1.0e-6
  ends
  longt            * long edits based on time
    time = 0.0e0  , dt = 1.0
  endl
  plott            * plot dumps based on time
    time  0.0e-6  dtfrequency 0.5e-6
  endp
  histt            * tracer history based on time
    time  0.0e-6  dtfrequency 0.5e-6
    htracer all
  endhistt
ende

*_/_/_/_/_/_/_/_/_/_/_/_/_/_/_/_/_/_/_/_/_/_/_/_/_/_/_/_/_/
* Hydrodynamic Boundary Conditions
*********************************************************
* 0=symmetry
* 1=sound speed based absorbing
* 2=extrapolated pressure with no mass allowed to enter
* 3=extrapolated pressure but mass is allowed to enter
*_/_/_/_/_/_/_/_/_/_/_/_/_/_/_/_/_/_/_/_/_/_/_/_/_/_/_/_/_/

boundary                 * enable boundary condition data
  bhydro                 * enable hydrodynamic boundary conditions
    block 1
      bxbot = 1 , bxtop = 1   * x = xmin, x = xmax, 1 = sound speed
based absorbing (transmitting) b.c.
      bybot = 1 , bytop = 1   * y = ymin, y = ymax, 1 = sound speed
based absorbing (transmitting) b.c.
    endb
  endh
endb

*heatconduction          * enable heat conduction
*   MAT1 TABLE = 3       * condty tabls defined in DEFTABLE below
*   MAT2 TABLE = 1
*   MAT3 TABLE = 2
*endh

*   DEFTABLE=1           * 1080 STEEL
  *T(eV)    k(erg/s/eV/cm)
*  1.4684e-3 4.7700e10
*  1.0377e-2 4.8100e10
*  1.9090e-2 4.5200e10
*  2.7900e-2 4.1300e10
*  3.6711e-2 3.8100e10
*  4.5521e-2 3.5100e10
*  5.4332e-2 3.2700e10
*  6.3142e-2 3.0100e10
```

117

```
*   7.1953e-2 2.4400e10
*   8.9574e-2 2.6800e10
*   1.1111e-1 3.0100e10
*   endd

*   DEFTABLE=2              * VascoMax 300 Steel
   *T(eV)    k(erg/s/eV/cm)
*   3.6711e-3 2.4715e10
*   1.4684e-2 2.7424e10
*   2.9369e-2 2.9794e10
*   3.9158e-2 3.0132e10
*   endd

*   DEFTABLE=3              * Epoxy
   *T(eV)    k(erg/s/eV/cm)
*   3.6711e-3 6.5e8
*   1.4684e-2 6.5e8
*   2.9369e-2 6.5e8
*   3.9158e-2 6.5e8
*   endd


*vadd             * Added velocity to maintain gouging in view
*   block = 1
*   tadd = 0.0
*   xvel = -1.08333e+5
*endvadd

*mindt                   * minimum allowable time step in mesh
*   time = 0.0 dt = 1.e-12
*endm

maxdt              * maximum allowable time step in mesh
   time = 0.0 dt = .01
endm
```

Appendix C.   Calculation of Sled Mass for CTH

Evenly distribute the mass over four shoes and divide by the width to make it plane strain.

$$\text{mass} := \frac{1854}{4 \cdot (10.16)} \cdot lb$$

$$\text{mass} = 45.62 lb$$

Length of the Shoe:

$$\text{Length} := 8 \cdot in$$

Height and Density of the Respective Shoe (VascoMax) and the Mass (platinum):

$$\text{Height}_{vmax} := 2.54 \, cm \qquad\qquad \text{Height}_{platinum} := (49.07 - 2.54) \cdot cm$$

$$\rho_{vmax} := 8 \cdot \frac{gm}{cm^3} \qquad\qquad \rho_{platinum} := 21.45 \frac{gm}{cm^3}$$

Calculation of the volume for each material:

$$\text{Vol}_{vmax} := \text{Length} \cdot \text{Height}_{vmax} \cdot 1 \cdot cm \qquad\qquad \text{Vol}_{platinum} := \text{Length} \cdot \text{Height}_{platinum} \cdot 1 \cdot cm$$

$$\text{Vol}_{vmax} = 51.61 cm^3 \qquad\qquad \text{Vol}_{platinum} = 945.49 cm^3$$

Calculation of the mass for each material:

$$\text{Mass}_{vmax} := \rho_{vmax} \cdot \text{Vol}_{vmax} \qquad\qquad \text{Mass}_{platinum} := \rho_{platinum} \cdot \text{Vol}_{platinum}$$

$$\text{Mass}_{vmax} = 0.91 lb \qquad\qquad \text{Mass}_{platinum} = 44.71 lb$$

Total mass should equal the mass above:

$$\text{Mass} := \text{Mass}_{platinum} + \text{Mass}_{vmax}$$

$$\text{Mass} = 45.62 lb$$

Therefore the platinum mass in CTH should have a height of:

$$\text{Height}_{platinum} = 46.53 cm$$

t	v	F_N	v_v
(s)	(in/s)	(lbf)	(in/s)
0.0000	0.000	0.0	0.000
0.0001	0.000	0.0	-0.625
0.0002	0.000	0.0	-2.945
0.0003	0.006	0.0	-5.193
0.0004	0.125	0.0	-7.082
0.0005	1.079	0.0	-8.784
0.0006	5.450	0.0	-9.279
0.0007	18.651	0.0	-9.372
0.0008	46.947	0.0	-9.752
0.0009	91.282	0.0	-10.558
0.0010	141.067	0.0	-12.785
0.0011	175.615	0.0	-15.607
0.0012	176.052	0.0	-17.325
0.0013	140.216	0.0	-18.504
0.0014	87.804	0.0	-19.287
0.0015	49.531	0.0	-19.321
0.0016	46.915	0.0	-19.352
0.0017	77.466	0.0	-19.971
0.0018	116.671	0.0	-20.866
0.0019	135.712	0.0	-21.695
0.0020	121.851	0.0	-21.972
0.0021	86.434	0.0	-21.934
0.0022	55.443	0.0	-21.625
0.0023	50.871	0.0	-20.865
0.0024	76.668	0.0	-19.530
0.0025	117.567	0.0	-17.619
0.0026	149.551	0.0	-15.311
0.0027	154.558	0.0	-12.933
0.0028	131.215	0.0	-10.826
0.0029	95.965	0.0	-9.204
0.0030	73.676	0.0	-8.111
0.0031	82.509	0.0	-7.442
0.0032	121.923	0.0	-6.947
0.0033	171.855	0.0	-6.275
0.0034	204.855	0.0	-5.092
0.0035	204.214	0.0	-3.232
0.0036	175.786	0.0	-0.777
0.0037	144.323	0.0	1.954
0.0038	136.187	0.0	4.473
0.0039	161.043	0.0	6.273
0.0040	206.057	0.0	7.036
0.0041	246.029	0.0	4.628
0.0042	260.890	0.0	2.468
0.0043	247.897	0.0	3.191
0.0044	221.513	0.0	4.820
0.0045	203.067	0.0	6.973
0.0046	207.946	0.0	9.042
0.0047	237.799	0.0	10.431
0.0048	280.773	0.0	10.779
0.0049	318.210	0.0	5.841
0.0050	333.969	0.0	5.529
0.0051	322.464	0.0	6.584
0.0052	291.953	0.0	8.062
0.0053	260.661	0.0	9.328
0.0054	246.651	0.0	9.828
0.0055	257.018	0.0	5.575
0.0056	283.772	0.0	3.344
0.0057	309.638	0.0	4.333
0.0058	319.710	0.0	6.291
0.0059	310.713	0.0	8.685
0.0060	291.846	0.0	10.806
0.0061	277.594	0.0	12.075
0.0062	278.225	0.0	11.717
0.0063	294.278	0.0	6.525
0.0064	317.589	0.0	6.859
0.0065	336.832	0.0	8.146
0.0066	343.657	0.0	9.873
0.0067	336.577	0.0	11.354
0.0068	321.506	0.0	11.963
0.0069	308.690	0.0	6.987
0.0070	306.927	0.0	4.071
0.0071	317.990	0.0	4.993
0.0072	335.282	0.0	6.816
0.0073	348.463	0.0	8.967
0.0074	351.145	0.0	10.725
0.0075	345.849	0.0	11.437
0.0076	342.238	0.0	4.160
0.0077	349.871	0.0	1.037
0.0078	371.078	0.0	1.966
0.0079	399.384	0.0	3.436
0.0080	424.373	0.0	4.720
0.0081	438.761	0.0	5.179
0.0082	442.229	0.0	-1.609
0.0083	439.991	0.0	-3.721
0.0084	438.439	0.0	-2.983
0.0085	441.511	0.0	-2.057
0.0086	449.479	0.0	-1.645
0.0087	459.631	0.0	-7.772
0.0088	467.885	0.0	-9.850
0.0089	470.843	0.0	-8.994
0.0090	467.819	0.0	-7.752
0.0091	461.698	0.0	-6.791
0.0092	457.655	0.0	-7.898
0.0093	460.160	0.0	-16.952
0.0094	470.282	0.0	-17.284
0.0095	485.381	0.0	-16.158
0.0096	501.237	0.0	-14.731
0.0097	514.466	0.0	-13.626
0.0098	523.070	0.0	-13.544
0.0099	525.474	0.0	-19.808
0.0100	520.398	0.0	-20.530
0.0101	508.769	0.0	-19.718
0.0102	495.621	0.0	-18.721
0.0103	488.730	0.0	-18.089
0.0104	493.523	0.0	-20.347
0.0105	508.083	0.0	-25.198
0.0106	523.176	0.0	-24.978
0.0107	528.454	0.0	-24.445
0.0108	520.529	0.0	-24.104
0.0109	506.386	0.0	-26.083
0.0110	498.940	0.0	-28.857
0.0111	507.886	13.6	-28.315
0.0112	532.735	1199.9	-24.776
0.0113	563.032	2813.6	-13.821
0.0114	585.157	4050.4	-16.217
0.0115	590.708	6087.3	-14.299
0.0116	581.277	4032.5	2.319
0.0117	567.324	4791.9	-0.237
0.0118	562.175	3369.9	5.566
0.0119	574.274	2558.1	11.606
0.0120	601.699	2270.9	8.568
0.0121	632.432	1701.2	10.488
0.0122	651.183	1142.5	12.334
0.0123	649.405	881.2	9.213
0.0124	631.933	668.7	10.730
0.0125	614.756	416.6	11.194
0.0126	614.304	204.6	7.984
0.0127	635.519	45.7	8.184
0.0128	667.838	0.0	7.669
0.0129	692.652	0.0	3.501
0.0130	696.747	0.0	2.257
0.0131	681.517	0.0	1.872
0.0132	661.327	0.0	-1.909
0.0133	652.983	0.0	-3.738
0.0134	664.558	0.0	-3.852
0.0135	691.108	0.0	-6.220

Appendix E.   **Montgomery Data [19]**

v	P	μ	d	w
(ft/s)	(psi)	(-)	(ft)	(in^3/ft x 10^7)
50	11300	0.26	5.7	200
600	11900	0.27	7.2	6
900	11500	0.22	6.1	13
1200	10900	0.25	8.3	23
1200	10500	0.3	4.6	52
150	11700	0.35	1.5	250
900	11500	0.24	10.2	14
1200	11100	0.27	13.6	47
600	11800	0.24	6.1	18
600	11900	0.23	16.2	9
600	11900	0.23	3.7	13
600	11100	0.26	11.2	15
150	10900	0.42	3	250
900	10700	0.35	13	71
1200	10700	0.3	19.6	72
900	11900	-	24	48
900	11500	0.24	21.9	22
900	11900	-	18.4	19
1200	10900	0.29	26.6	75
900	11100	0.24	21	19
30	11900	0.48	0.36	86
60	10100	0.63	0.52	750
60	10900	0.54	0.64	920
10	12700	0.49	0.081	96
20	12500	0.35	0.22	110
150	6000	0.52	5.6	150
30	3900	1.3	5.7	160
30	3900	1.3	2.7	220
300	3900	0.5	29	8
300	3700	0.46	13.2	8
450	16900	0.32	9.8	79
600	12900	0.28	13.1	36
600	12000	0.28	14.2	27
600	5700	0.24	7.6	6
600	12100	0.3	14.5	26
600	12400	0.27	6.4	18
600	3600	0.28	27.2	5
600	3500	0.29	15.5	5
900	8300	0.3	20.7	25
1200	5400	0.37	26.5	27
1200	11400	0.3	32.2	83

v (ft/s)	P (psi)	μ (-)	d (ft)	w (in^3/ft x 10^7)
1200	19400	0.24	5.4	95
1200	18200	0.24	10.6	106
1200	18100	0.21	16.3	89
1200	19700	0.22	19.8	114
1200	18700	0.23	25.6	111
1200	23500	0.22	25.4	305
1200	4400	0.39	32.2	30
1500	17500	0.2	26.1	24
1500	3400	0.28	38.2	28
1800	4000	0.3	42.8	19
1800	4800	0.29	40	38
1800	17500	0.19	18.7	29

Appendix F.   Rail Undulation

This appendix documents an effort that was initially pursued in order to analyze the dynamics of the sled as it encounters the undulation in the rail. This information was not used due to the fact that DADS provides the vertical velocity. The analysis was simplified by considering a particle of constant mass traveling along a curved path. Figure 64 below is a depiction of a particle as it travels along a curved path from point *A* to point *B*. At point *A*, the particle has a velocity of v_A. Similarly, the particle has velocity v_B at point *B*.
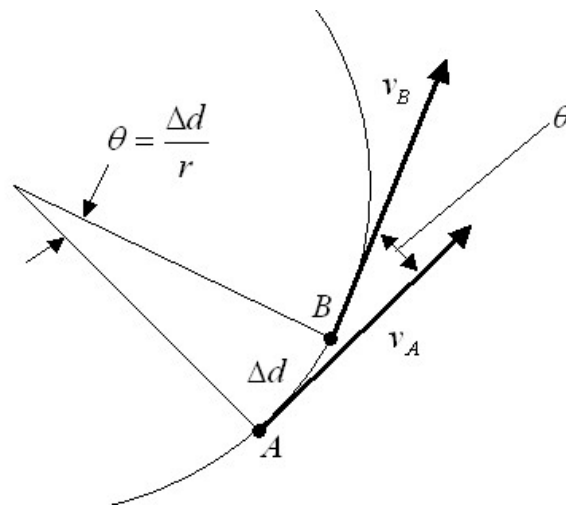

Figure 64 - Particle on a Curved Path

From dynamics, it is know that a particle traveling along a curved path experiences accelerations in the form of

$$\vec{a} = \vec{a}_t + \vec{a}_n = \frac{dv}{dt} + \frac{v^2}{r} \tag{29}$$

v is the tangential velocity provided by DADS. Therefore, the radius of the rail undulation can be solved for using Newton's Second Law as

123

$$r = \frac{mv^2}{F} \tag{30}$$

The geometric relations associated with a particle traveling on a curve path can be seen in Figure 64. This shows that the angle between the two points *A* and *B* can be solved for by

$$\theta = \frac{\Delta d}{r} \tag{31}$$

Δd is the distance the sled travels between time steps and is calculated be integrating the velocity time curve accomplished earlier. Points *A* and *B* can be any two successive points in the DADS data. With the angle *θ*, the vertical velocity can be calculated by assuming that the curved path is comprised of short line segments, and that the tangential velocity provided by DADS for the previous time step will be the velocity at which the sled encounters the next change in track slope. Resolving the components of this incoming velocity vector gives the geometric relations for the vertical velocity as depicted in Figure 65 and equation (32):
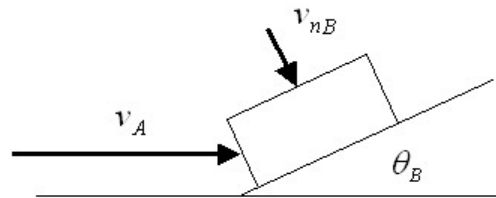

Figure 65 - Shoe as It Encounters the Next Segment of a Curved Rail

$$v_{nB} = v_A \sin \theta_B \tag{32}$$

This set of calculations can be performed for the entire set of DADS data in order to determine the vertical velocity for each time step. This was carried out and compared

124

with the DADS provided values for vertical velocity. This method resulted in vertical velocities less than what DADS calculates. This suggests that this technique over simplifies the problem in assuming that the mass is constant throughout the entire sled run in addition to neglecting other system forces such as springs and dampers used by DADS.

125

Bibliography

1. Ayers, G. (2007). *DADS File for Nike Sled 80X-A1*. Unpublished manuscript.

2. Bayer, R. G. (2004). *Mechanical Wear Fundamentals and Testing* (Second ed.). New York, NY: Marcel Dekker.

3. Beer, F. P., & Johnston, Russell E. Jr. (1988). *Vector Mechanics for Engineers: Dynamics* (Fifth ed.). New York, NY: McGraw-Hill.

4. Bhushan, B. (2002). *Introduction to Tribology*. New York: John Wiley and Sons.

5. Bowden, F. P., & Tabor, D. (1973). *Friction; An Introduction to Tribology*. Garden City, NY: Anchor Press.

6. Burden, R. L., & Faires, J. D. (2005). *Numerical Analysis* (Eighth ed.). Belmont, CA: Thomson Brooks/Cole.

7. Cinnamon, J. D. (June 2006). *Analysis and Simulation of Hypervelocity Gouging Impacts AFIT/DS/ENY/06-01*. Ph. D. Dissertation, Air Force Institute of Technology, Wright-Patterson, AFB, OH.

8. C-K Technologies (2006). *SBIR Phase I Final Report – Accurately Validated High-Speed Wear Prediction Code*, No. TR300. Ballwin, MO.

9. Holmberg, K., & Matthews, A. (2005). Tribology of Engineered Surfaces. In G. W. Stachowiak (Ed.), *Wear: Materials, Mechanisms and Practice*. Chichester, England: John Wiley and Sons.

10. Hooser, M. (2007). *Rail dimensions.* Unpublished manuscript.

11. Hooser, M. (2002). The Holloman High Speed Test Track Gone Soft: Recent Advances in Hypersonic Test Track Vibration Environment. *Aerodynamic Measurement Technology and Ground Testing Conference, 22nd,* St. Louis, MO, 24-26 Jun 2002. *, AIAA 2002-3035*

12. Hooser, M., & Schwing, A. (2000). Validation of Dynamic Simulation Techniques at the Holloman High speed Test Track. *Aerospace Sciences Meeting and Exhibit, 38th,* Reno, NV, 10-13 Jan 2000. , *AIAA 2000-0155*

13. Hutchings, I. M. (2005). The Challenge of Wear. In G. W. Stachowiak (Ed.), *Wear: Materials, Mechanisms and Practice*. Chichester, England: John Wiley and Sons.

14. Hutchings, I. M. (1992). *Tribology: Friction and Wear of Engineering Materials*. Boca Raton, FL: CRC Press.

15. Incropera, F. P., & DeWitt, D. P. (1990). *Fundamentals of Heat and Mass Transfer* (Third ed.)John Wiley and Sons.

16. Kato, K. (2005). Classification of Wear Mechanisms/Models. In G. W. Stachowiak (Ed.), *Wear: Materials, mechanisms and practice*. Chichester, England: John Wiley and Sons.

17. Laird, D. J. (March 2002). *The Investigation of Hypervelocity Gouging AFIT/DS/ENY/02-01*. Ph. D. Dissertation, Air Force Institute of Technology, Wright-Patterson, AFB, OH.

18. Lim, S. C., & Ashby, M. F. (1987). Overview no. 55 Wear-Mechanism Maps. *Acta Metallurgica, Vol. 35* (Issue 1)

19. Montgomery, R. S. (1976). Friction and Wear at High Sliding Speeds. *Wear, Vol. 36, 275-298*

20. Montgomery, R. S. (1976). Surface Melting of Rotating Bands. *Wear, Vol. 38, 235-243*

21. Rabinowicz, E. (1965). *Friction and Wear of Materials* (Second ed.). New York, NY: John Wiley and Sons.

22. Ryder, J. T., Wittenauer, J. P., & Mendez, D. J. (1996). *Physical Characterization of SiO$_2$ Aerogel Phase II Final Report Subcontract 565-9204*. Lockheed Martin Missiles & Space, Palo Alto, CA, *NASA-CR-201461*.

23. Stachowiak, G. W., & Batchelor, A. W. (2000). *Engineering Tribology* (Second ed.). Boston, MA: Butterworth-Heinemann.

24. Szmerekovsky, A. G. (September 2004). The Physical Understanding of the use of Coatings to Mitigate Hypervelocity Gouging Considering Real Test Sled Dimensions AFIT/DS/ENY/04-06. Ph. D. Dissertation, Air Force Institute of Technology, Wright-Patterson, AFB, OH.

127

1. REPORT DATE *(DD-MM-YYYY)* 22 Mar 07	2. REPORT TYPE Master's Thesis		3. DATES COVERED *(From – To)* Aug 2005 – Mar 2007
4. TITLE AND SUBTITLE An Evaluation of High Velocity Wear			**5a. CONTRACT NUMBER**
			5b. GRANT NUMBER
			5c. PROGRAM ELEMENT NUMBER
6. AUTHOR(S) Gregory J. Cameron, Captain, USAF			**5d. PROJECT NUMBER** ENY06-183
			5e. TASK NUMBER
			5f. WORK UNIT NUMBER
7. PERFORMING ORGANIZATION NAMES(S) AND ADDRESS(S) Air Force Institute of Technology Graduate School of Engineering and Management (AFIT/EN) 2950 Hobson Way WPAFB OH 45433-7765			**8. PERFORMING ORGANIZATION REPORT NUMBER** AFIT/GAE/ENY/07-M06
9. SPONSORING/MONITORING AGENCY NAME(S) AND ADDRESS(ES) Air Force Office of Scientific Research Attn: Dr. John Schmisseur 4015 Wilson Blvd, Rm 713 Arlington, VA 22203-1954			**10. SPONSOR/MONITOR'S ACRONYM(S)** AFOSR/NM
			11. SPONSOR/MONITOR'S REPORT NUMBER(S)

12. DISTRIBUTION/AVAILABILITY STATEMENT
APPROVED FOR PUBLIC RELEASE; DISTRIBUTION UNLIMITED.

13. SUPPLEMENTARY NOTES

14. ABSTRACT

The Holloman High Speed Test Track (HHSTT) is a rocket-powered sled track facility used for testing a variety of hypervelocity aerospace applications. The current speed record is 6,453 miles per hour. While this seems fast there are customers at the track that have requirements demanding even faster speeds. Significant research has been conducted in the area of rail gouging as it relates to the test track, and efforts are under way to reduce and even eliminate this phenomenon. Any steps taken in this effort may eliminate catastrophic sled failures caused by gouging, however wear is another damaging issue that needs to be understood. This research evaluates wear in two fashions. First, data from the Dynamic Analysis and Design System (DADS) software, used by the HHSTT to model sled loading and vibration, is evaluated in a theoretical model originating from "high-speed" pin-on-disk experimentation. The second method evaluates wear by conducting a series of simulations in which temperature, rail geometry in the form of an asperity, speed and rail coating are varied. These short duration simulations are performed with CTH, a hydrocode designed for analyzing hypervelocity impact problems. A validated CTH model, used in previous gouging research, was used to estimate wear by examining local areas of failure and melting. DADS provides forces related to frictional heating and vertical velocity information that will be incorporated as input into CTH.

15. SUBJECT TERMS
wear, high velocity, hypervelocity, pin-on-disk, CTH, VascoMax 300, Holloman High Speed Test Track (HHSTT), friction

16. SECURITY CLASSIFICATION OF:			17. LIMITATION OF ABSTRACT	18. NUMBER OF PAGES	19a. NAME OF RESPONSIBLE PERSON Dr. Anthony Palazotto
REPORT U	**ABSTRACT** U	**c. THIS PAGE** U	UU	143	19b. TELEPHONE NUMBER *(Include area code)* (937) 255-3636, ext 4599 anthony.palazotto@afit.edu

Standard Form 298 (Rev: 8-98)
Prescribed by ANSI Std. Z39-18